Coupling Impedances in Accelerator Rings

K.Y. Ng

Fermilab

November, 2009

Slides can be downloaded from
www-ap.fnal.gov/ng/lecture09.pdf
This file is frequently updated.

Contents

Introduction

- A particle interacts with the vacuum chamber produces EM fields.
- The motion of a particle following is perturbed.

$$(\vec{E},\vec{B})_{\substack{\text{seen by}\\ \text{particles}}} = (\vec{E},\vec{B})_{\substack{\text{external, from}\\ \text{magnets, rf, etc.}}} + (\vec{E},\vec{B})_{\substack{\text{wake}\\ \text{fields}}}$$

where

$$(\vec{E},\vec{B})_{\substack{\text{wake}\\ \text{fields}}} \begin{cases} \propto & \text{beam intensity} \\ \ll & (\vec{E},\vec{B})_{\text{external}} \end{cases}$$

Introduction

- A particle interacts with the vacuum chamber produces EM fields.
- The motion of a particle following is perturbed.

$$(\vec{E},\vec{B})_{\substack{\text{seen by}\\ \text{particles}}} = (\vec{E},\vec{B})_{\substack{\text{external, from}\\ \text{magnets, rf, etc.}}} + (\vec{E},\vec{B})_{\substack{\text{wake}\\ \text{fields}}}$$

where

$$(\vec{E},\vec{B})_{\substack{\text{wake}\\ \text{fields}}} \begin{cases} \propto & \text{beam intensity} \\ \ll & (\vec{E},\vec{B})_{\text{external}} \end{cases}$$

- Perturbation breaks down when potential-well distortion is large. Then, distortion has to be included into non-perturbative part.

Introduction

- A particle interacts with the vacuum chamber produces EM fields.
- The motion of a particle following is perturbed.

$$(\vec{E},\vec{B})_{\substack{\text{seen by}\\ \text{particles}}} = (\vec{E},\vec{B})_{\substack{\text{external, from}\\ \text{magnets, rf, etc.}}} + (\vec{E},\vec{B})_{\substack{\text{wake}\\ \text{fields}}}$$

where

$$(\vec{E},\vec{B})_{\substack{\text{wake}\\ \text{fields}}} \begin{cases} \propto & \text{beam intensity} \\ \ll & (\vec{E},\vec{B})_{\text{external}} \end{cases}$$

- Perturbation breaks down when potential-well distortion is large. Then, distortion has to be included into non-perturbative part.
- What we need to compute are the EM wake fields at a distance z behind the source particle.
- The computation of the wake fields is nontrivial.
- Two approximations lead to a lot of simplification.

1. Rigid-Bunch Approximation [1]

- Motion of beam not affected during traversal through discontinuities.

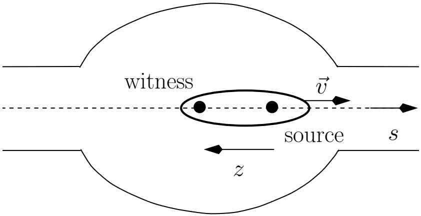

Source particle at $s = \beta ct$

Witness particle at $s = z + \beta ct$

$z < 0$ for particle following.

This does not imply

no synchrotron motion.

- Rigidity implies beam at high energies.

1. Rigid-Bunch Approximation [1]

- Motion of beam not affected during traversal through discontinuities.

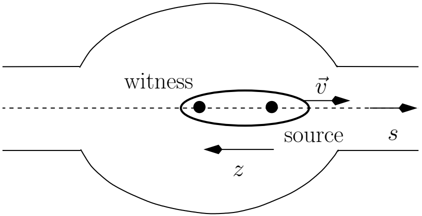

Source particle at $s = \beta ct$

Witness particle at $s = z + \beta ct$

$z < 0$ for particle following.

This does not imply

no synchrotron motion.

- Rigidity implies beam at high energies.

2. Impulse Approximation

- We do not care about the wake fields $\vec{E}$, $\vec{B}$, or the wake force $\vec{F}$.
- We only care about the impulse

$$\Delta\vec{p} = \int_{-\infty}^{\infty} dt\ \vec{F} = \int_{-\infty}^{\infty} dt\ q(\vec{E} + \vec{v} \times \vec{B})$$

- We will see how the simplification evolves.

Panofsky-Wenzel Theorem [2]

- Maxwell equation for witness particle at (x, y, s, t) with $s = z + \beta t$:

$$\vec{\nabla}\cdot\vec{E} = \frac{q\rho}{\epsilon_0} \qquad \text{Gauss's law for electric charge}$$

$$\vec{\nabla}\times\vec{B} - \frac{1}{c^2}\frac{\partial\vec{E}}{\partial t} = \mu_0 q\beta c\rho\hat{s} \qquad \text{Ampere's law}$$

$$\vec{\nabla}\cdot\vec{B} = 0 \qquad \text{Gauss's law for magnetic charge}$$

$$\vec{\nabla}\times\vec{E} + \frac{\partial\vec{B}}{\partial t} = 0 \qquad \text{Faraday's \& Lenz law}$$

- Want to write Maxwell equation for the impulse $\Delta\vec{p}$.

  First compute

with $\vec{F} = q(\vec{E} + \vec{v}\times\vec{B})$

$$\vec{\nabla}\cdot\vec{F} = \frac{q\rho}{\epsilon_0\gamma^2} - \frac{q\beta}{c}\frac{\partial E_s}{\partial t},$$

$$\vec{\nabla}\times\vec{F} = -q\left(\frac{\partial}{\partial t} + \beta c\frac{\partial}{\partial s}\right)\vec{B}.$$

$$\vec{\nabla} \times \Delta\vec{p}\,(x,y,z) = \int_{-\infty}^{\infty} dt \, \left[\vec{\nabla} \times \vec{F}(x,y,s,t) \right]_{s=z+\beta ct} .$$

$\uparrow$ this $\vec{\nabla}$ refers to x, y, z

$\uparrow$ this $\vec{\nabla}$ refers to x, y, s

$$\vec{\nabla}\times\Delta\vec{p}\,(x,y,z)=\int_{-\infty}^{\infty}dt\,\left[\vec{\nabla}\times\vec{F}(x,y,s,t)\right]_{s=z+\beta ct}.$$

$\uparrow$ this $\vec{\nabla}$ refers to x,y,z

$\uparrow$ this $\vec{\nabla}$ refers to x,y,s

We obtain

$$\begin{aligned}\vec{\nabla}\times\Delta\vec{p}&=-q\int_{-\infty}^{\infty}dt\,\left[\left(\frac{\partial}{\partial t}+\beta c\frac{\partial}{\partial s}\right)\vec{B}(x,y,s,t)\right]_{s=z+\beta ct}\\&=-q\int_{-\infty}^{\infty}dt\,\frac{d\vec{B}}{dt}=-q\vec{B}(x,y,z+\beta ct,t)\Big|_{t=-\infty}^{\infty}=0,\end{aligned}$$

$$\vec{\nabla}\times\Delta\vec{p}\,(x,y,z)=\int_{-\infty}^{\infty}dt\ \left[\vec{\nabla}\times\vec{F}(x,y,s,t)\right]_{s=z+\beta ct}.$$

$\uparrow$ this $\vec{\nabla}$ refers to x,y,z

$\uparrow$ this $\vec{\nabla}$ refers to x,y,s

We obtain

$$\vec{\nabla}\times\Delta\vec{p}=-q\int_{-\infty}^{\infty}dt\ \left[\left(\frac{\partial}{\partial t}+\beta c\frac{\partial}{\partial s}\right)\vec{B}(x,y,s,t)\right]_{s=z+\beta ct}$$

$$=-q\int_{-\infty}^{\infty}dt\ \frac{d\vec{B}}{dt}=-q\vec{B}(x,y,z+\beta ct,t)\Big|_{t=-\infty}^{\infty}=0,$$

- Dot product with $\hat{s}\Longrightarrow\vec{\nabla}\cdot(\hat{s}\times\Delta\vec{p})\Longrightarrow\dfrac{\partial\Delta p_x}{\partial y}=\dfrac{\partial\Delta p_y}{\partial x}$

$$\vec{\nabla}\times\Delta\vec{p}\,(x,y,z)=\int_{-\infty}^{\infty}dt\ \left[\vec{\nabla}\times\vec{F}(x,y,s,t)\right]_{s=z+\beta ct}.$$

$\uparrow$ this $\vec{\nabla}$ refers to x,y,z

$\uparrow$ this $\vec{\nabla}$ refers to x,y,s

We obtain

$$\vec{\nabla}\times\Delta\vec{p}=-q\int_{-\infty}^{\infty}dt\ \left[\left(\frac{\partial}{\partial t}+\beta c\frac{\partial}{\partial s}\right)\vec{B}(x,y,s,t)\right]_{s=z+\beta ct}$$

$$=-q\int_{-\infty}^{\infty}dt\ \frac{d\vec{B}}{dt}=-q\vec{B}(x,y,z+\beta ct,t)\Big|_{t=-\infty}^{\infty}=0,$$

- Dot product with $\hat{s}\Longrightarrow\vec{\nabla}\cdot(\hat{s}\times\Delta\vec{p})\Longrightarrow\dfrac{\partial\Delta p_x}{\partial y}=\dfrac{\partial\Delta p_y}{\partial x}$
- Cross product with $\hat{s}\Longrightarrow\dfrac{\partial}{\partial z}\Delta\vec{p}_\perp=\vec{\nabla}_\perp\Delta p_s.$ $\longleftarrow$ P-W Theorem

$$\vec{\nabla}\times\Delta\vec{p}\,(x,y,z)=\int_{-\infty}^{\infty}dt\;\Big[\vec{\nabla}\times\vec{F}(x,y,s,t)\Big]_{s=z+\beta ct}.$$

this $\vec{\nabla}$ refers to x, y, z

this $\vec{\nabla}$ refers to x, y, s

We obtain

$$\vec{\nabla}\times\Delta\vec{p}=-q\int_{-\infty}^{\infty}dt\;\left[\left(\frac{\partial}{\partial t}+\beta c\frac{\partial}{\partial s}\right)\vec{B}(x,y,s,t)\right]_{s=z+\beta ct}$$

$$=-q\int_{-\infty}^{\infty}dt\;\frac{d\vec{B}}{dt}=-q\vec{B}(x,y,z+\beta ct,t)\Big|_{t=-\infty}^{\infty}=0,$$

- Dot product with $\hat{s}\Longrightarrow\vec{\nabla}\cdot(\hat{s}\times\Delta\vec{p})\Longrightarrow\dfrac{\partial\Delta p_x}{\partial y}=\dfrac{\partial\Delta p_y}{\partial x}$
- Cross product with $\hat{s}\Longrightarrow\dfrac{\partial}{\partial z}\Delta\vec{p}_\perp=\vec{\nabla}_\perp\Delta p_s.$ $\longleftarrow$ P-W Theorem
- P-W theorem gives strong restriction between longitudinal and transverse.
- But it is very general. Does not depend on any boundary conditions. Even do not require $\beta=1$.

Supplement to Panofsky-Wenzel Theorem

$$\beta = 1 \implies \vec{\nabla}_\perp \cdot \Delta\vec{p}_\perp = 0.$$

Proof:

$$\vec{\nabla}\cdot\Delta\vec{p} = \int_{-\infty}^{\infty} dt \left[\vec{\nabla}\cdot\vec{F}(x,y,s,t)\right]_{s=z+ct} = q\int_{-\infty}^{\infty} dt \left[\frac{\rho}{\epsilon_0\gamma^2} - \frac{\beta}{c}\frac{\partial E_s}{\partial t}\right]_{s=z+ct}$$

$$\longrightarrow q\int_{-\infty}^{\infty} dt \left[\frac{\partial E_s}{\partial s}\right]_{s=z+ct} = \frac{\partial}{\partial z}\Delta p_s$$

Use has been made of

1. Space-charge term $\dfrac{q\rho}{\epsilon_0\gamma^2}$ omitted because $\beta \to 1$.
2. $\dfrac{\partial}{\partial t}E_s(s,t) = \dfrac{d}{dt}E_s(s,t) - \dfrac{ds}{dt}\dfrac{\partial}{\partial s}E_s(s,t).$

Maxwell equations now become

$$\vec{\nabla}\times\Delta\vec{p} = 0 \quad \text{and} \quad \vec{\nabla}\cdot\Delta\vec{p} = \frac{\partial}{\partial z}\Delta p_s$$ without any source terms.

Cylindrical Symmetric Vacuum Chamber

$$\begin{cases} \dfrac{\partial}{\partial r}(r\Delta p_\theta) = \dfrac{\partial}{\partial\theta}\Delta p_r \\ \dfrac{\partial}{\partial z}\Delta p_r = \dfrac{\partial}{\partial r}\Delta p_s \\ \dfrac{\partial}{\partial z}\Delta p_\theta = \dfrac{1}{r}\dfrac{\partial}{\partial\theta}\Delta p_s \\ \dfrac{\partial}{\partial r}(r\Delta p_r) = -\dfrac{\partial}{\partial\theta}\Delta p_\theta \quad (\beta = 1) \end{cases} \Longrightarrow \begin{cases} \dfrac{\partial}{\partial r}(r\Delta\tilde{p}_\theta) = -m\Delta\tilde{p}_r \\ \dfrac{\partial}{\partial z}\Delta\tilde{p}_r = \dfrac{\partial}{\partial r}\Delta\tilde{p}_s \\ \dfrac{\partial}{\partial z}\Delta\tilde{p}_\theta = -\dfrac{m}{r}\Delta\tilde{p}_s \\ \dfrac{\partial}{\partial r}(r\Delta\tilde{p}_r) = -m\Delta\tilde{p}_\theta \quad (\beta = 1) \end{cases}$$

- Cylindrical symmetry $\Longrightarrow$ expansion in terms of $\cos m\theta$ or $\sin m\theta$.

  We write $\Delta p_s = \Delta\tilde{p}_s \cos m\theta, \quad \Delta p_r = \Delta\tilde{p}_r \cos m\theta, \quad \Delta p_\theta = \Delta\tilde{p}_\theta \sin m\theta,$

  where $\Delta\tilde{p}_s$, $\Delta\tilde{p}_r$, and $\Delta\tilde{p}_\theta$ are θ-independent.

Cylindrical Symmetric Vacuum Chamber

$$
\begin{cases}
\dfrac{\partial}{\partial r}(r\Delta p_\theta) = \dfrac{\partial}{\partial\theta}\Delta p_r \\
\dfrac{\partial}{\partial z}\Delta p_r = \dfrac{\partial}{\partial r}\Delta p_s \\
\dfrac{\partial}{\partial z}\Delta p_\theta = \dfrac{1}{r}\dfrac{\partial}{\partial\theta}\Delta p_s \\
\dfrac{\partial}{\partial r}(r\Delta p_r) = -\dfrac{\partial}{\partial\theta}\Delta p_\theta \quad (\beta = 1)
\end{cases}
\Longrightarrow
\begin{cases}
\dfrac{\partial}{\partial r}(r\Delta\tilde{p}_\theta) = -m\Delta\tilde{p}_r \\
\dfrac{\partial}{\partial z}\Delta\tilde{p}_r = \dfrac{\partial}{\partial r}\Delta\tilde{p}_s \\
\dfrac{\partial}{\partial z}\Delta\tilde{p}_\theta = -\dfrac{m}{r}\Delta\tilde{p}_s \\
\dfrac{\partial}{\partial r}(r\Delta\tilde{p}_r) = -m\Delta\tilde{p}_\theta \quad (\beta = 1)
\end{cases}
$$

- Cylindrical symmetry $\Longrightarrow$ expansion in terms of $\cos m\theta$ or $\sin m\theta$.

  We write $\Delta p_s = \Delta\tilde{p}_s \cos m\theta$, $\Delta p_r = \Delta\tilde{p}_r \cos m\theta$, $\Delta p_\theta = \Delta\tilde{p}_\theta \sin m\theta$,

  where $\Delta\tilde{p}_s$, $\Delta\tilde{p}_r$, and $\Delta\tilde{p}_\theta$ are θ-independent.

- For $m = 0$, $\Delta\tilde{p}_r = \Delta\tilde{p}_\theta = 0$, otherwise they $\propto \dfrac{1}{r}$, singular at $r = 0$.

Cylindrical Symmetric Vacuum Chamber

$$\begin{cases} \dfrac{\partial}{\partial r}(r\Delta p_\theta) = \dfrac{\partial}{\partial \theta}\Delta p_r \\ \dfrac{\partial}{\partial z}\Delta p_r = \dfrac{\partial}{\partial r}\Delta p_s \\ \dfrac{\partial}{\partial z}\Delta p_\theta = \dfrac{1}{r}\dfrac{\partial}{\partial \theta}\Delta p_s \\ \dfrac{\partial}{\partial r}(r\Delta p_r) = -\dfrac{\partial}{\partial \theta}\Delta p_\theta \quad (\beta = 1) \end{cases} \Longrightarrow \begin{cases} \dfrac{\partial}{\partial r}(r\Delta \tilde{p}_\theta) = -m\Delta \tilde{p}_r \\ \dfrac{\partial}{\partial z}\Delta \tilde{p}_r = \dfrac{\partial}{\partial r}\Delta \tilde{p}_s \\ \dfrac{\partial}{\partial z}\Delta \tilde{p}_\theta = -\dfrac{m}{r}\Delta \tilde{p}_s \\ \dfrac{\partial}{\partial r}(r\Delta \tilde{p}_r) = -m\Delta \tilde{p}_\theta \quad (\beta = 1) \end{cases}$$

- Cylindrical symmetry $\Longrightarrow$ expansion in terms of $\cos m\theta$ or $\sin m\theta$.

  We write $\Delta p_s = \Delta \tilde{p}_s \cos m\theta$, $\Delta p_r = \Delta \tilde{p}_r \cos m\theta$, $\Delta p_\theta = \Delta \tilde{p}_\theta \sin m\theta$,

  where $\Delta \tilde{p}_s$, $\Delta \tilde{p}_r$, and $\Delta \tilde{p}_\theta$ are θ-independent.

- For $m = 0$, $\Delta \tilde{p}_r = \Delta \tilde{p}_\theta = 0$, otherwise they $\propto \dfrac{1}{r}$, singular at $r = 0$.

- For $m \neq 0$, $\dfrac{\partial}{\partial r}\left[r\dfrac{\partial}{\partial r}(r\Delta \tilde{p}_r)\right] = m^2\Delta \tilde{p}_r \Longrightarrow \Delta p_r(r,\theta,z) \sim mr^{m-1}\cos m\theta$.

Definition of Wake Functions

- Formal solution can be written as

$$\begin{cases} v\Delta\vec{p}_\perp = -q\mathcal{Q}_m W_m(z) m r^{m-1}\big(\hat{r}\cos m\theta - \hat{\theta}\sin m\theta\big), \\ v\Delta p_s = -q\mathcal{Q}_m W_m'(z) r^m \cos m\theta. \end{cases}$$

- Defn: $\begin{cases} W_m(z) \longrightarrow \text{transverse wake function of azimuthal } m \\ W_m'(z) \longrightarrow \text{longitudinal wake function of azimuthal } m \end{cases}$

Definition of Wake Functions

- Formal solution can be written as

$$\begin{cases} v\Delta\vec{p}_\perp = -q\mathcal{Q}_m W_m(z) m r^{m-1}\big(\hat{r}\cos m\theta - \hat{\theta}\sin m\theta\big), \\ v\Delta p_s = -q\mathcal{Q}_m W_m'(z) r^m \cos m\theta. \end{cases}$$

- Defn: $\begin{cases} W_m(z) \longrightarrow \text{transverse wake function of azimuthal } m \\ W_m'(z) \longrightarrow \text{longitudinal wake function of azimuthal } m \end{cases}$

  They are function of z only and dependent on boundary conditions. They are related because of P-W theorem.

Definition of Wake Functions

- Formal solution can be written as

$$\begin{cases} v\Delta\vec{p}_\perp = -q\mathcal{Q}_m W_m(z) m r^{m-1}\big(\hat{r}\cos m\theta - \hat{\theta}\sin m\theta\big), \\ v\Delta p_s = -q\mathcal{Q}_m W_m'(z) r^m \cos m\theta. \end{cases}$$

- Defn: $\begin{cases} W_m(z) & \longrightarrow \text{transverse wake function of azimuthal } m \\ W_m'(z) & \longrightarrow \text{longitudinal wake function of azimuthal } m \end{cases}$

  They are function of z only and dependent on boundary conditions. They are related because of P-W theorem.

- $\mathcal{Q}_m = ea^m$ is mth multipole of source particle of charge e. $W_m(z)$ has dimension V/Coulomb/m^{2m-1}.

Definition of Wake Functions

- Formal solution can be written as

$$\begin{cases} v\Delta\vec{p}_\perp = -q\mathcal{Q}_m W_m(z) m r^{m-1}\big(\hat{r}\cos m\theta - \hat{\theta}\sin m\theta\big), \\ v\Delta p_s = -q\mathcal{Q}_m W_m'(z) r^m \cos m\theta. \end{cases}$$

- Defn: $\begin{cases} W_m(z) & \longrightarrow \text{transverse wake function of azimuthal } m \\ W_m'(z) & \longrightarrow \text{longitudinal wake function of azimuthal } m \end{cases}$

  They are function of z only and dependent on boundary conditions. They are related because of P-W theorem.

- $\mathcal{Q}_m = ea^m$ is mth multipole of source particle of charge e.
  $W_m(z)$ has dimension V/Coulomb/m^{2m-1}.

- Recall that solution of $\vec{E}$ and $\vec{B}$ reduces to solution of $W_m(z)$ only. Simplification comes from P-W theorem or rigid-bunch and impulse approximations.

- negative sign in front is a convention to make $W_m'(z) > 0$, since witness particle loses energy from impulse.

Some Properties of Wake Functions

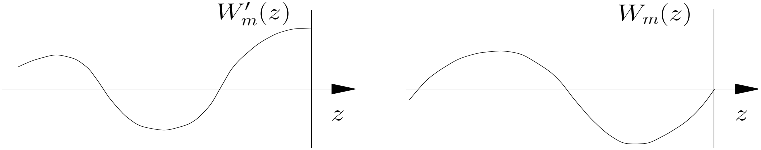

Some Properties of Wake Functions

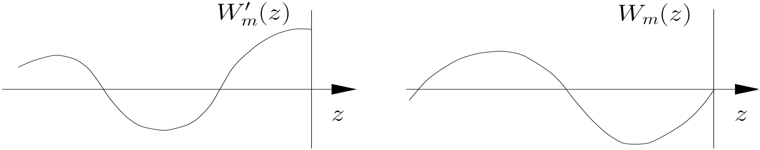

Fundamental Theorem of Beam Loading (P. Wilson)

A particle sees half of its wake, or $\frac{1}{2}W'_m(0_-)$.

Some Properties of Wake Functions

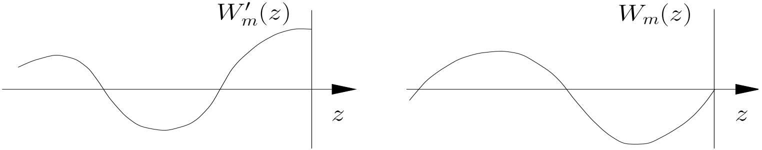

Fundamental Theorem of Beam Loading (P. Wilson)

A particle sees half of its wake, or $\frac{1}{2}W'_m(0_-)$.

Proof:

A particle of charge q passes a thin lossless cavity, excites cavity.

Energy gained $\Delta\mathcal{E}_1 = -fq^2W'_m(0_-)$, i.e., sees fraction f of own wake.

Some Properties of Wake Functions

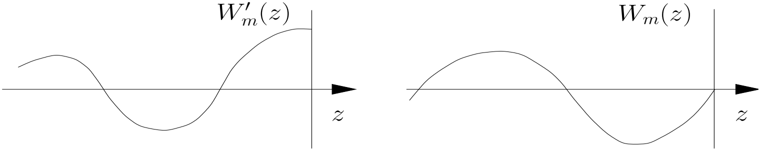

Fundamental Theorem of Beam Loading (P. Wilson)

A particle sees half of its wake, or $\frac{1}{2}W'_m(0_-)$.

Proof:

A particle of charge q passes a thin lossless cavity, excites cavity.

Energy gained $\Delta\mathcal{E}_1 = -fq^2 W'_m(0_-)$, i.e., sees fraction f of own wake.

Half cycle later, a 2nd particle of same charge passes the cavity.

Energy gained $\Delta\mathcal{E}_2 = -fq^2 W'_m(0_-) + q^2 W'_m(0_-)$.

Some Properties of Wake Functions

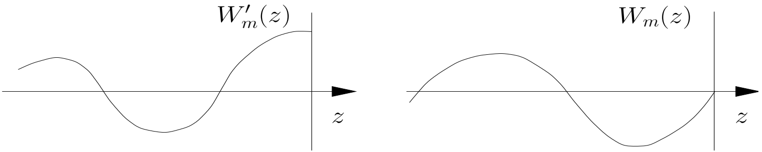

Fundamental Theorem of Beam Loading (P. Wilson)

A particle sees half of its wake, or $\frac{1}{2}W_m'(0_-)$.

Proof:

A particle of charge q passes a thin lossless cavity, excites cavity.

Energy gained $\Delta\mathcal{E}_1 = -fq^2 W_m'(0_-)$, i.e., sees fraction f of own wake.

Half cycle later, a 2nd particle of same charge passes the cavity.

Energy gained $\Delta\mathcal{E}_2 = -fq^2 W_m'(0_-) + q^2 W_m'(0_-)$.

Field inside cavity is completely cancelled.

$\Delta\mathcal{E}_1 + \Delta\mathcal{E}_2 = -2fq^2 W_m'(0_-) + q^2 W_m'(0_-) = 0 \Longrightarrow f = \frac{1}{2}$.

Properties of Wake Functions

- $W'_m(z) = 0$ for $z > 0$. (causality)
- $W'_m(0_-) \geq 0$ (energy conservation)

Properties of Wake Functions

- $W'_m(z) = 0$ for $z > 0$. (causality)
- $W'_m(0_-) \geq 0$ (energy conservation)
- $|W'_m(z)| \leq W'_m(0_-)$.

Properties of Wake Functions

- $W'_m(z) = 0$ for $z > 0$. (causality)
- $W'_m(0_-) \geq 0$ (energy conservation)
- $|W'_m(z)| \leq W'_m(0_-)$.

  1st particle of charge q loses energy $\frac{1}{2}q^2W'(0_-)$.

  2nd particle of charge q loses energy $\frac{1}{2}q^2W'(0_-) + q^2W'_0(z)$.

  Total loss $q^2W'(0_-) + q^2W'_0(z) \geq 0$. Or $W'_0(z) \geq -W'_0(0_-)$.

Properties of Wake Functions

- $W'_m(z) = 0$ for $z > 0$. (causality)
- $W'_m(0_-) \geq 0$ (energy conservation)
- $|W'_m(z)| \leq W'_m(0_-)$.

  1st particle of charge q loses energy $\frac{1}{2}q^2W'(0_-)$.

  2nd particle of charge q loses energy $\frac{1}{2}q^2W'(0_-) + q^2W'_0(z)$.

  Total loss $q^2W'(0_-) + q^2W'_0(z) \geq 0$. Or $W'_0(z) \geq -W'_0(0_-)$.

  2nd particle of charge $-q$ loses energy $\frac{1}{2}q^2W'(0_-) - q^2W'_0(z)$.

  Total loss $q^2W'(0_-) - q^2W'_0(z) \geq 0$. Or $W'_0(z) \leq W'_0(0_-)$.

Properties of Wake Functions

- $W'_m(z) = 0$ for $z > 0$. (causality)
- $W'_m(0_-) \geq 0$ (energy conservation)
- $|W'_m(z)| \leq W'_m(0_-)$.

  1st particle of charge q loses energy $\frac{1}{2}q^2 W'(0_-)$.

  2nd particle of charge q loses energy $\frac{1}{2}q^2 W'(0_-) + q^2 W'_0(z)$.

  Total loss $q^2 W'(0_-) + q^2 W'_0(z) \geq 0$. Or $W'_0(z) \geq -W'_0(0_-)$.

  2nd particle of charge $-q$ loses energy $\frac{1}{2}q^2 W'(0_-) - q^2 W'_0(z)$.

  Total loss $q^2 W'(0_-) - q^2 W'_0(z) \geq 0$. Or $W'_0(z) \leq W'_0(0_-)$.
- $W'_m(-D) = W'_m(0_-)$ for some $D > 0 \implies$ wake is of period D.

Properties of Wake Functions

- $W'_m(z) = 0$ for $z > 0$. (causality)
- $W'_m(0_-) \geq 0$ (energy conservation)
- $|W'_m(z)| \leq W'_m(0_-)$.

  1st particle of charge q loses energy $\frac{1}{2}q^2 W'(0_-)$.

  2nd particle of charge q loses energy $\frac{1}{2}q^2 W'(0_-) + q^2 W'_0(z)$.

  Total loss $q^2 W'(0_-) + q^2 W'_0(z) \geq 0$. Or $W'_0(z) \geq -W'_0(0_-)$.

  2nd particle of charge $-q$ loses energy $\frac{1}{2}q^2 W'(0_-) - q^2 W'_0(z)$.

  Total loss $q^2 W'(0_-) - q^2 W'_0(z) \geq 0$. Or $W'_0(z) \leq W'_0(0_-)$.
- $W'_m(-D) = W'_m(0_-)$ for some $D > 0 \Longrightarrow$ wake is of period D.

  Energy loss:

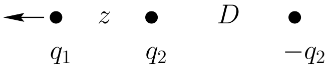

  1. $\frac{1}{2}q_1^2 W'_0(0_-)$.
  2. $\frac{1}{2}q_2^2 W'_0(0_-) + q_1 q_2 W'_0(-z)$.
  3. $\frac{1}{2}q_2^2 W'_0(0_-) - q_1 q_2 W'_0(-z-D) - q_2^2 W'_0(-D)$.

  Since total must be ≥ 0 and q_1 arbitrary, $W'_0(-z) \geq W'_0(-z-D)$.

  Change 3 charges to $(q_1, -q_2, q_2)$ to get $W'_0(-z) \leq W'_0(-z-D)$.

- Area under $W'_m(z)$ is non-negative.

- Area under $W_m'(z)$ is non-negative.

  Consider a dc beam current I.

  For a particle of charge q in the beam, energy loss is $q \int W_0'(z)\, I \frac{dz}{v} \geq 0$.

- Area under $W'_m(z)$ is non-negative.

  Consider a dc beam current I.

  For a particle of charge q in the beam, energy loss is $q\int W'_0(z)\, I\,\frac{dz}{v} \geq 0$.

- For longitudinal, lowest azimuthal is $m = 0$ or $W'_0(z)$.
- For transverse, lowest azimuthal is $m = 1$ or $W_1(z)$.
- Higher azimuthals can be important for large transverse beam size compared with pipe radius.

- Area under $W'_m(z)$ is non-negative.

  Consider a dc beam current I.

  For a particle of charge q in the beam, energy loss is $q\int W'_0(z)\, I\,\dfrac{dz}{v} \ge 0$.

- For longitudinal, lowest azimuthal is $m=0$ or $W'_0(z)$.
- For transverse, lowest azimuthal is $m=1$ or $W_1(z)$.
- Higher azimuthals can be important for large transverse beam size compared with pipe radius.

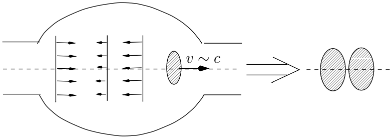

Particles in same vertical slice see same impulse. Can lead to longitudinal micro-bunching or microwave instability.

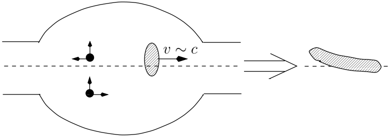

Particles in same vertical slice receive same vertical impulse independent of vertical position. Can lead to beam breakup.

Coupling Impedances

- Beam particles form current. Component with freq. ω is $I(s,t)=\hat{I}e^{-i\omega(t-s/v)}$.

- A test particle crossing a narrow discontinuity at s_1 gains energy from wake left by particles $-z$ in front ($z<0$). Voltage gained is

$$
\begin{aligned}
V(s_1,t) &= -\int_{-\infty}^{\infty}[W_0'(z)]_1\hat{I}e^{-i\omega[(t+z/v)-s_1/v]}\frac{dz}{v} \\
&= -I(s_1,t)\int_{-\infty}^{\infty}[W_0'(z)]_1 e^{-i\omega z/v}\frac{dz}{v} \equiv -I(s_1,t)\left[Z_0^{\parallel}(\omega)\right]_1
\end{aligned}
$$

- **Defn:** $Z_0^{\parallel}(\omega)=\int_{-\infty}^{\infty}W_0'(z)e^{-i\omega z/v}\frac{dz}{v}$ (summing over all continuities)

Coupling Impedances

- Beam particles form current. Component with freq. ω is $I(s,t)=\hat{I}e^{-i\omega(t-s/v)}$.

- A test particle crossing a narrow discontinuity at s_1 gains energy from wake left by particles $-z$ in front ($z<0$). Voltage gained is

$$V(s_1,t)=-\int_{-\infty}^{\infty}[W_0'(z)]_1\hat{I}e^{-i\omega[(t+z/v)-s_1/v]}\frac{dz}{v}$$
$$=-I(s_1,t)\int_{-\infty}^{\infty}[W_0'(z)]_1 e^{-i\omega z/v}\frac{dz}{v}\equiv -I(s_1,t)\left[Z_0^{\|}(\omega)\right]_1$$

- **Defn:** $Z_0^{\|}(\omega)=\int_{-\infty}^{\infty}W_0'(z)e^{-i\omega z/v}\frac{dz}{v}$ (summing over all continuities)

- Unlike a current in a circuit, a beam has transverse dimension and therefore higher multipoles.

- When the beam is off-center by amount a, the current mth multipole is $\mathcal{P}_m(s,t)=I(s,t)a^m=\hat{\mathcal{P}}_m e^{-i\omega(t-s/v)}$.

Higher Azimuthal Impedances

- At location i, test particle density is $\rho = q\dfrac{\delta(r-a)}{a}\delta(\theta)\delta(s-s_i)$.

  Subject to the mth multipole element $\mathcal{P}(s_i, t+z/v)dz$ passes location i $-z$ earlier, voltage gained is

$$
\begin{aligned}
V(s_i,t) &= -\int \frac{dz}{v}\mathcal{P}_m(s_i,t+z/v)[W_m'(z)]_i \int r dr d\theta\, r^m \cos m\theta \frac{\delta(r-a)\delta(\theta)}{a} \\
&= -\int \frac{dz}{v}\hat{\mathcal{P}}_m e^{-i\omega[(t+z/v)-s/v]}[W_m'(z)]_i a^m \\
&= -\frac{\mathcal{Q}_m}{q}\mathcal{P}_m(s_i,t)\int_{-\infty}^{0}\frac{dz}{v}\,[W_m'(z)]_i\, e^{-i\omega z/v} \qquad [\mathcal{Q}_m = qa^m]
\end{aligned}
$$

Higher Azimuthal Impedances

- At location i, test particle density is $\rho = q\dfrac{\delta(r-a)}{a}\delta(\theta)\delta(s-s_i)$.

  Subject to the mth multipole element $\mathcal{P}(s_i, t+z/v)dz$ passes location i $-z$ earlier, voltage gained is

$$V(s_i,t) = -\int \frac{dz}{v}\mathcal{P}_m(s_i,t+z/v)[W_m'(z)]_i \int r dr d\theta\, r^m \cos m\theta \frac{\delta(r-a)\delta(\theta)}{a}$$

$$= -\int \frac{dz}{v}\hat{\mathcal{P}}_m e^{-i\omega[(t+z/v)-s/v]}[W_m'(z)]_i a^m$$

$$= -\frac{\mathcal{Q}_m}{q}\mathcal{P}_m(s_i,t)\int_{-\infty}^{0}\frac{dz}{v}\,[W_m'(z)]_i\, e^{-i\omega z/v} \qquad [\mathcal{Q}_m = qa^m]$$

- Identify mth multipole longitudinal impedance across location i as

$$\left[Z_m^{\|}(\omega)\right]_i = -\frac{q\hat{V}}{\mathcal{Q}_m\hat{\mathcal{P}}_m} = \int_{-\infty}^{\infty}\frac{dz}{v}\,[W_m'(z)]_i\, e^{-i\omega z/v}.$$

- Summing up around the vacuum chamber: $Z_m^{\|}(\omega) = \sum_i \left[Z_m^{\|}(\omega)\right]_i$.

Transverse Impedances

- General defn. for long. imp.: $Z_m^{\|}(\omega) = \displaystyle\int_{-\infty}^{\infty} \frac{dz}{v} W_m'(z) e^{-i\omega z/v}$.
- If we replace W_m' by W_m, we obtain transverse impedances

Defn. $Z_m^{\perp}(\omega) = \dfrac{i}{\beta} \displaystyle\int_{-\infty}^{\infty} \frac{dz}{v} W_m(z) e^{-i\omega z/v}$ $\qquad [W_m(z) = 0 \text{ when } z > 0]$

- Long. and transverse imp. are then related by $Z_m^{\|}(\omega) = \dfrac{\omega}{c} Z_m^{\perp}(\omega)$,

  so that both $\mathcal{R}e\, Z_m^{\|}$ and $\mathcal{R}e\, Z_m^{\perp}$ represent energy loss or gain.
- Transverse force, $F_\perp \propto -W_m$, must lag $\mathcal{P}_m$ by $\dfrac{\pi}{2}$ in order for $\mathcal{R}e\, Z_m^{\perp}$ to dissipate energy. Hence the factor i.
- The factor β is to cancel β in Lorenz force, just a convention.

Direct Computation of Impedances

- $Z_1^{\perp}$ can also be derived directly from the transverse force $F_1^{\perp}$ without going through $Z_1^{\parallel}$.

Direct Computation of Impedances

- $Z_1^\perp$ can also be derived directly from the transverse force $F_1^\perp$ without going through $Z_1^\parallel$.
- When current $I(s,t)=\hat{I}e^{-i\omega(t-s/v)}$ is displaced by a transversely from axis of symmetry, deflecting force acting on a test particle is

$$\begin{aligned}\langle F_1^\perp(s,t)\rangle &= -q\int_{-\infty}^{\infty} W_1(z)a\hat{I}e^{-i\omega[(t+z/v)-s/v]}\frac{dz}{v}\\ &= -qaI(s,t)\int_{-\infty}^{\infty} W_1(z)e^{-i\omega z/v}\frac{dz}{v}=\frac{i\beta qI(s,t)a}{L}Z_1^\perp(\omega).\end{aligned}$$

- $\langle\cdots\rangle$ implies averaged over all preceding particles.

Direct Computation of Impedances

- $Z_1^\perp$ can also be derived directly from the transverse force $F_1^\perp$ without going through $Z_1^\parallel$.
- When current $I(s,t)=\hat{I}e^{-i\omega(t-s/v)}$ is displaced by a transversely from axis of symmetry, deflecting force acting on a test particle is

$$\langle F_1^\perp(s,t)\rangle = -q\int_{-\infty}^{\infty} W_1(z)a\hat{I}e^{-i\omega[(t+z/v)-s/v]}\frac{dz}{v}$$
$$= -qaI(s,t)\int_{-\infty}^{\infty} W_1(z)e^{-i\omega z/v}\frac{dz}{v} = \frac{i\beta qI(s,t)a}{L}Z_1^\perp(\omega).$$

- $\langle\cdots\rangle$ implies averaged over all preceding particles.
- For transverse: $Z_1^\perp(\omega) = -\dfrac{i}{q\hat{I}a\beta}\langle\hat{F}_1^\perp\rangle.$
- For longitudinal: $Z_0^\parallel(\omega) = -\dfrac{1}{q\hat{I}}\langle\hat{F}_0^\parallel\rangle.$
- Other than from wake fcns, these are formulas employed to compute imp. directly from the long. and trans. forces seen by test particle.

Some Properties of Impedances

1. $Z_m^{\parallel}(\omega) = \frac{\omega}{c} Z_m^{\perp}(\omega)$ (P-W theorem).

Some Properties of Impedances

1. $Z_m^{\parallel}(\omega) = \dfrac{\omega}{c} Z_m^{\perp}(\omega)$ (P-W theorem).
2. $Z_m^{\parallel}(-\omega) = \left[Z_m^{\parallel}(\omega)\right]^*$ and $Z_m^{\perp}(-\omega) = -\left[Z_m^{\perp}(\omega)\right]^*$ $\big[W_m(z)$ is real$\big]$

Some Properties of Impedances

1. $Z_m^{\parallel}(\omega) = \frac{\omega}{c} Z_m^{\perp}(\omega)$ (P-W theorem).
2. $Z_m^{\parallel}(-\omega) = \left[Z_m^{\parallel}(\omega)\right]^*$ and $Z_m^{\perp}(-\omega) = -\left[Z_m^{\perp}(\omega)\right]^*$ $\left[W_m(z) \text{ is real}\right]$
3. $Z_m^{\parallel}(\omega)$ and $Z_m^{\perp}(\omega)$ are analytic, poles only in lower half ω-plane.

$$W_m(z) = -\frac{i\beta}{2\pi}\int_{-\infty}^{\infty} Z_m^{\perp}(\omega) e^{i\omega z/v} d\omega$$

$$W_m'(z) = \frac{1}{2\pi}\int_{-\infty}^{\infty} Z_m^{\parallel}(\omega) e^{i\omega z/v} d\omega$$

Causality: $W_m(z) = W_m'(z) = 0$ when $z > 0$.

Singularities cannot occur in upper ω-plane.

Some Properties of Impedances

1. $Z_m^{\parallel}(\omega) = \frac{\omega}{c} Z_m^{\perp}(\omega)$ (P-W theorem).
2. $Z_m^{\parallel}(-\omega) = \left[Z_m^{\parallel}(\omega)\right]^*$ and $Z_m^{\perp}(-\omega) = -\left[Z_m^{\perp}(\omega)\right]^*$ $\left[W_m(z) \text{ is real}\right]$
3. $Z_m^{\parallel}(\omega)$ and $Z_m^{\perp}(\omega)$ are analytic, poles only in lower half ω-plane.

$$W_m(z) = -\frac{i\beta}{2\pi}\int_{-\infty}^{\infty} Z_m^{\perp}(\omega) e^{i\omega z/v} d\omega$$

$$W_m'(z) = \frac{1}{2\pi}\int_{-\infty}^{\infty} Z_m^{\parallel}(\omega) e^{i\omega z/v} d\omega$$

Causality: $W_m(z) = W_m'(z) = 0$ when $z > 0$.
Singularities cannot occur in upper ω-plane.

$$\mathcal{R}e\, Z_m^{\parallel}(\omega) = \frac{1}{\pi}\wp\int_{-\infty}^{\infty} d\omega' \frac{\mathcal{I}m\, Z_m^{\parallel}(\omega')}{\omega' - \omega}, \quad \mathcal{I}m\, Z_m^{\parallel}(\omega) = -\frac{1}{\pi}\wp\int_{-\infty}^{\infty} d\omega' \frac{\mathcal{R}e\, Z_m^{\parallel}(\omega')}{\omega' - \omega}.$$

Some Properties of Impedances

1. $Z_m^{\parallel}(\omega) = \dfrac{\omega}{c} Z_m^{\perp}(\omega)$ (P-W theorem).

2. $Z_m^{\parallel}(-\omega) = \left[Z_m^{\parallel}(\omega)\right]^*$ and $Z_m^{\perp}(-\omega) = -\left[Z_m^{\perp}(\omega)\right]^*$ $\left[W_m(z) \text{ is real}\right]$

3. $Z_m^{\parallel}(\omega)$ and $Z_m^{\perp}(\omega)$ are analytic, poles only in lower half ω-plane.

$$W_m(z) = -\frac{i\beta}{2\pi}\int_{-\infty}^{\infty} Z_m^{\perp}(\omega) e^{i\omega z/v} d\omega$$

$$W_m'(z) = \frac{1}{2\pi}\int_{-\infty}^{\infty} Z_m^{\parallel}(\omega) e^{i\omega z/v} d\omega$$

Causality: $W_m(z) = W_m'(z) = 0$ when $z > 0$.
Singularities cannot occur in upper ω-plane.

$$\mathcal{R}e\, Z_m^{\parallel}(\omega) = \frac{1}{\pi}\wp\int_{-\infty}^{\infty} d\omega' \frac{\mathcal{I}m\, Z_m^{\parallel}(\omega')}{\omega' - \omega}, \qquad \mathcal{I}m\, Z_m^{\parallel}(\omega) = -\frac{1}{\pi}\wp\int_{-\infty}^{\infty} d\omega' \frac{\mathcal{R}e\, Z_m^{\parallel}(\omega')}{\omega' - \omega}.$$

4. $\mathcal{R}e\, Z_m^{\parallel}(\omega) \geq 0$ and $\mathcal{R}e\, Z_m^{\perp}(\omega) \geq 0$ when $\omega > 0$, if beam pipe has same entrance and exit cross section. (no accelerating forces)

Some Properties of Impedances

1. $Z_m^\parallel(\omega) = \frac{\omega}{c} Z_m^\perp(\omega)$ (P-W theorem).

2. $Z_m^\parallel(-\omega) = \left[Z_m^\parallel(\omega)\right]^*$ and $Z_m^\perp(-\omega) = -\left[Z_m^\perp(\omega)\right]^*$ $\left[W_m(z)\text{ is real}\right]$

3. $Z_m^\parallel(\omega)$ and $Z_m^\perp(\omega)$ are analytic, poles only in lower half ω-plane.

$$W_m(z) = -\frac{i\beta}{2\pi}\int_{-\infty}^{\infty} Z_m^\perp(\omega) e^{i\omega z/v} d\omega$$

$$W_m'(z) = \frac{1}{2\pi}\int_{-\infty}^{\infty} Z_m^\parallel(\omega) e^{i\omega z/v} d\omega$$

Causality: $W_m(z) = W_m'(z) = 0$ when $z > 0$.
Singularities cannot occur in upper ω-plane.

$$\mathcal{R}e\, Z_m^\parallel(\omega) = \frac{1}{\pi}\wp\int_{-\infty}^{\infty} d\omega' \frac{\mathcal{I}m\, Z_m^\parallel(\omega')}{\omega' - \omega}, \quad \mathcal{I}m\, Z_m^\parallel(\omega) = -\frac{1}{\pi}\wp\int_{-\infty}^{\infty} d\omega' \frac{\mathcal{R}e\, Z_m^\parallel(\omega')}{\omega' - \omega}.$$

4. $\mathcal{R}e\, Z_m^\parallel(\omega) \ge 0$ and $\mathcal{R}e\, Z_m^\perp(\omega) \ge 0$ when $\omega > 0$, if beam pipe has same entrance and exit cross section. (no accelerating forces)

5. $\int_0^\infty d\omega\, \mathcal{I}m\, Z_m^\perp(\omega) = 0$ and $\int_0^\infty d\omega \frac{\mathcal{I}m\, Z_m^\parallel(\omega)}{\omega} = 0.$

General Comments

- $W_m(z)=0$, $W'_m(z)=0$ when $z>0$ because of causality.
- It is awkward to deal with negative z. Some like to use $z>0$ for particle following. Then $W_m(z)=0$, $W'_m(z)=0$ when $z<0$.

General Comments

- $W_m(z)=0$, $W'_m(z)=0$ when $z>0$ because of causality.
- It is awkward to deal with negative z. Some like to use $z>0$ for particle following. Then $W_m(z)=0$, $W'_m(z)=0$ when $z<0$.
- Then instead of

$$Z_m^{\parallel}(\omega)=\int_{-\infty}^{\infty}e^{-i\omega z/v}W'_m(z)\frac{dz}{v},\quad W_m(z)=-\frac{i\beta}{2\pi}\int_{-\infty}^{\infty}Z_m^{\perp}(\omega)e^{i\omega z/v}d\omega$$

we have

$$Z_m^{\parallel}(\omega)=\int_{-\infty}^{\infty}e^{i\omega z/v}W'_m(z)\frac{dz}{v},\quad W_m(z)=-\frac{i\beta}{2\pi}\int_{-\infty}^{\infty}Z_m^{\perp}(\omega)e^{-i\omega z/v}d\omega$$

and $W'_m(z)=-\dfrac{dW_m(z)}{dz}$. $\longleftarrow$ note negative sign

General Comments

- $W_m(z)=0$, $W'_m(z)=0$ when $z>0$ because of causality.
- It is awkward to deal with negative z. Some like to use $z>0$ for particle following. Then $W_m(z)=0$, $W'_m(z)=0$ when $z<0$.
- Then instead of

$$Z_m^{\parallel}(\omega)=\int_{-\infty}^{\infty}e^{-i\omega z/v}W'_m(z)\frac{dz}{v},\quad W_m(z)=-\frac{i\beta}{2\pi}\int_{-\infty}^{\infty}Z_m^{\perp}(\omega)e^{i\omega z/v}d\omega$$

we have

$$Z_m^{\parallel}(\omega)=\int_{-\infty}^{\infty}e^{i\omega z/v}W'_m(z)\frac{dz}{v},\quad W_m(z)=-\frac{i\beta}{2\pi}\int_{-\infty}^{\infty}Z_m^{\perp}(\omega)e^{-i\omega z/v}d\omega$$

and $W'_m(z)=-\dfrac{dW_m(z)}{dz}$. $\longleftarrow$ note negative sign

- All properties of the impedances remain unchanged, including no singularity in upper half ω-plane.

General Comments

- $W_m(z) = 0$, $W'_m(z) = 0$ when $z > 0$ because of causality.
- It is awkward to deal with negative z. Some like to use $z > 0$ for particle following. Then $W_m(z) = 0$, $W'_m(z) = 0$ when $z < 0$.
- Then instead of
$$Z_m^{\parallel}(\omega) = \int_{-\infty}^{\infty} e^{-i\omega z/v} W'_m(z) \frac{dz}{v}, \quad W_m(z) = -\frac{i\beta}{2\pi} \int_{-\infty}^{\infty} Z_m^{\perp}(\omega) e^{i\omega z/v} d\omega$$
we have
$$Z_m^{\parallel}(\omega) = \int_{-\infty}^{\infty} e^{i\omega z/v} W'_m(z) \frac{dz}{v}, \quad W_m(z) = -\frac{i\beta}{2\pi} \int_{-\infty}^{\infty} Z_m^{\perp}(\omega) e^{-i\omega z/v} d\omega$$
and $W'_m(z) = -\dfrac{dW_m(z)}{dz}$. $\longleftarrow$ note negative sign
- All properties of the impedances remain unchanged, including no singularity in upper half ω-plane.
- Some may like to use j instead of i to denote imaginary value. Most of the time $j = -i$. Then $Z_m^{\parallel}$ and $Z_m^{\perp}$ have no singularity in lower half ω-plane instead.

Space-Charge Impedances

- Sp-ch imp. come from EM fields of beam even when beam pipe is smooth and perfectly conducting.
- Want to compute E_s due to variation of linear density $\lambda(s - vt)$. Assume small variation of trans. dist.

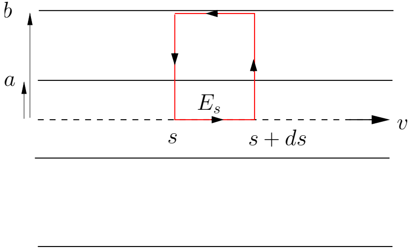

Space-Charge Impedances

- Sp-ch imp. come from EM fields of beam even when beam pipe is smooth and perfectly conducting.
- Want to compute E_s due to variation of linear density $\lambda(s-vt)$. Assume small variation of trans. dist.

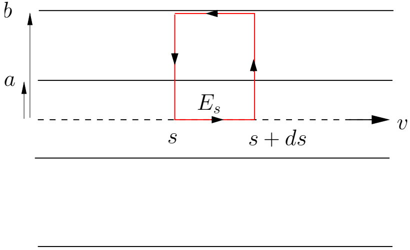

- Faraday law: $$\oint \vec{E}\cdot\overrightarrow{d\ell} = -\frac{\partial}{\partial t}\int \vec{B}\cdot d\vec{A}.$$

uniform dist. assumed

$$\oint \vec{E}\cdot\overrightarrow{d\ell} = E_s ds - \frac{e\lambda(s-vt)}{2\pi\epsilon_0}\left[\int_a^b \frac{dr}{r} + \int_0^a \frac{rdr}{a^2}\right] + \left\{s \to s+ds\right\}$$

- Geometric factor $g_0 = 2\left[\int_a^b \frac{dr}{r} + \int_0^a \frac{rdr}{a^2}\right] = 1 + 2\ln\frac{b}{a}.$

- Electric field or left side: $\oint \vec{E}\cdot\overrightarrow{d\ell} = E_s ds + \dfrac{eg_0}{4\pi\epsilon_0}\dfrac{\partial\lambda}{\partial s}\,ds.$
- Magnetic field or right side:

$$-\frac{\partial}{\partial t}\int \vec{B}\cdot d\vec{A} = -\frac{\partial}{\partial t}\frac{\mu_0 e\lambda(s-vt)v}{2\pi}\left[\int_0^a \frac{rdr}{a^2} + \int_a^b \frac{dr}{r}\right]ds = v^2\frac{e\mu_0 g_0}{4\pi}\frac{\partial\lambda}{\partial s}ds.$$

- Long. field seen by particles on-axis: $E_s = -\dfrac{eg_0}{4\pi\epsilon_0\gamma^2}\dfrac{\partial\lambda}{\partial s}.$

- Electric field or left side: $\oint \vec{E}\cdot\overrightarrow{d\ell} = E_s ds + \dfrac{eg_0}{4\pi\epsilon_0}\dfrac{\partial\lambda}{\partial s}\, ds.$

- Magnetic field or right side:

$$-\frac{\partial}{\partial t}\int \vec{B}\cdot d\vec{A} = -\frac{\partial}{\partial t}\frac{\mu_0 e\lambda(s-vt)v}{2\pi}\left[\int_0^a \frac{rdr}{a^2} + \int_a^b \frac{dr}{r}\right] ds = v^2\frac{e\mu_0 g_0}{4\pi}\frac{\partial\lambda}{\partial s} ds.$$

- Long. field seen by particles on-axis: $E_s = -\dfrac{eg_0}{4\pi\epsilon_0\gamma^2}\dfrac{\partial\lambda}{\partial s}.$

- Consider a long. harmonic wave $\lambda_1(s;t) \propto e^{i(ns/R-\Omega t)}$ perturbing a coasting beam of uniform linear density λ_0.

- Voltage drop per turn is $V = E_s 2\pi R = \dfrac{ineZ_0 cg_0}{2\gamma^2}\lambda_1 = \dfrac{inZ_0 g_0}{2\gamma^2\beta} I_1.$

- The wave constitutes a perturbing current of $I_1 = e\lambda_1 v.$

- Imp. is $\left.\dfrac{Z_0^{\|}}{n}\right|_{\rm sp\ ch} = \dfrac{iZ_0 g_0}{2\gamma^2\beta}$ with $g_0 = 1 + 2\ln\dfrac{b}{a}.$ $\left[Z_0 = \sqrt{\dfrac{\mu_0}{\epsilon_0}} = \dfrac{1}{\epsilon_0 c} = \mu_0 c\right]$

Comments

- $\left.\frac{Z_0^{\parallel}}{n}\right|_{\rm sp\ ch} = i\frac{Z_0 g_0}{2\beta\gamma^2}$ is independent of freq., but rolls off when $\omega \gtrsim \frac{\gamma c}{b}$.
- $\left.Z_0^{\parallel}\right|_{\rm sp\ ch} \propto \omega$, resembling a neg. inductive imp. rather than a cap. imp.
- For a freq.-independent reactive imp. $\left.\frac{Z_0^{\parallel}}{n}\right|_{\rm sp\ ch}$, corr. wake is

$$W_0'(z) = \delta'(z)\left[-iRc\beta\frac{Z_0^{\parallel}}{n}\right]_{\rm reactive} = \delta'(z)\frac{Z_0 cRg_0}{2\gamma^2}.$$

Comments

- $\left.\frac{Z_0^\parallel}{n}\right|_{\rm sp\ ch} = i\frac{Z_0 g_0}{2\beta\gamma^2}$ is independent of freq., but rolls off when $\omega \gtrsim \frac{\gamma c}{b}$.
- $\left. Z_0^\parallel\right|_{\rm sp\ ch} \propto \omega$, resembling a neg. inductive imp. rather than a cap. imp.
- For a freq.-independent reactive imp. $\left.\frac{Z_0^\parallel}{n}\right|_{\rm sp\ ch}$, corr. wake is

  $$W_0'(z) = \delta'(z)\left[-iRc\beta\frac{Z_0^\parallel}{n}\right]_{\rm reactive} = \delta'(z)\frac{Z_0 cRg_0}{2\gamma^2}.$$
- Longitudinal reactive impedance results from a longitudinal reactive force $F_0^\parallel(s,t) = \frac{ie^2v}{2\pi}\left.\frac{Z_0^\parallel}{n}\right|_{\rm reactive}\frac{\partial\lambda(s,t)}{\partial s}$.
- This force modifies the bunch shape, called *potential-well distortion.* Below/above transition, capacitive force lengthens/shortens the bunch.
- Below/above transition, inductive/capacitive force can generate micro-bunching and eventual microwave instabilities.

Space-Charge Compensation at PSR [3]

- Since $Z_0^{\parallel}|_{\rm sp\ ch}$ is just a negative inductance, an inductance can cancel the space-charge force. As an example, ferrite rings are placed in Los Alamos PSR to cancel space-charge force so as to shorten the bunch.

Space-Charge Compensation at PSR [3]

- Since $Z_0^{\|}|_{\rm sp\ ch}$ is just a negative inductance, an inductance can cancel the space-charge force. As an example, ferrite rings are placed in Los Alamos PSR to cancel space-charge force so as to shorten the bunch.

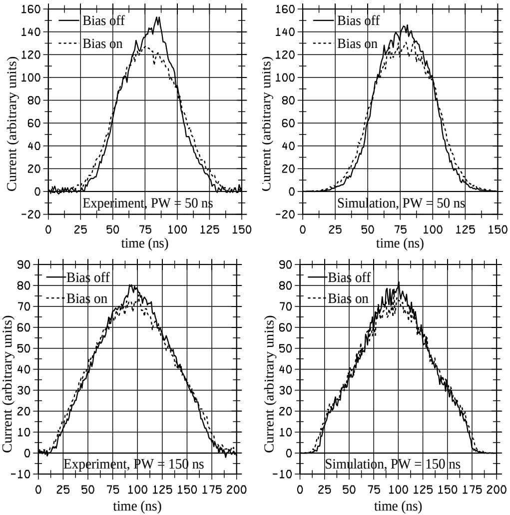

When 900-A bias is on, μ' of ferrite rings is reduced by 34%.

Bunches become longer when bias is on.

- However, resistive part of the ferrite, if too high, can generate microwave instabilities.

$\sim 500\ \mu$s into PSR storage with 3 ferrite tuners.

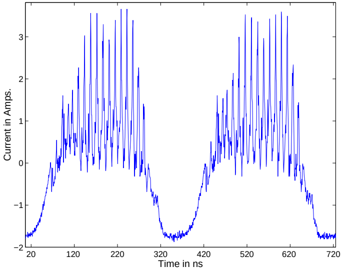

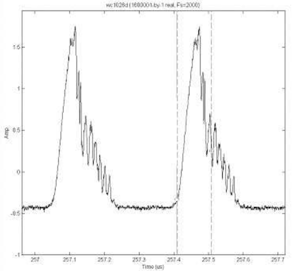

- However, resistive part of the ferrite, if too high, can generate microwave instabilities.

$\sim 500\ \mu$s into PSR storage with 3 ferrite tuners.

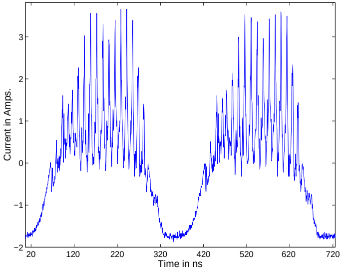

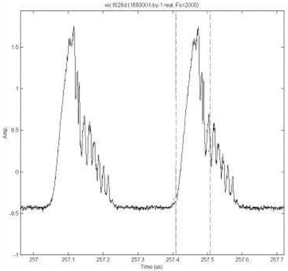

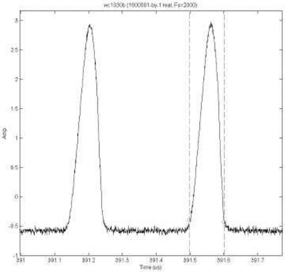

Heating ferrite increases μ' and decreases μ''.
Using 2 instead of 3 of ferrite tuners and heating to 130° C alleviates the instabilities.

-

Other Transverse Beam Distribution [4]

- The former geometric factor g_0 was computed according to uniform transverse distribution.
- It is easy to compute g_0 for any transverse distributions.
- We can also retain the form of g_0 for uniform distribution by introducing an effective beam radius $a_{\rm eff}$ such that $g_0 = 1 + 2\ln(b/a_{\rm eff})$.

Other Transverse Beam Distribution [4]

- The former geometric factor g_0 was computed according to uniform transverse distribution.
- It is easy to compute g_0 for any transverse distributions.
- We can also retain the form of g_0 for uniform distribution by introducing an effective beam radius $a_{\rm eff}$ such that $g_0 = 1 + 2\ln(b/a_{\rm eff})$.

	Phase space distribution	g_0	$a_{\rm eff}$
Uniform	$\dfrac{1}{\pi\hat r^2}H(\hat r - r)$	$1+2\ln\dfrac{b}{\hat r}$	$\hat r$
Elliptical	$\dfrac{3}{2\pi\hat r}\left(1-\dfrac{r^2}{\hat r^2}\right)^{1/2}H(\hat r - r)$	$\dfrac{8}{3}-2\ln 2+2\ln\dfrac{b}{\hat r}$	$0.8692\hat r$
Parabolic	$\dfrac{1}{2\pi\hat r^2}\left(1-\dfrac{r^2}{\hat r^2}\right)H(\hat r - r)$	$\dfrac{3}{2}+2\ln\dfrac{b}{\hat r}$	$0.7788\hat r$
Cosine-square	$\dfrac{2\pi}{\pi^2-4}\cos^2\dfrac{\pi r}{2\hat r}H(\hat r - r)$	$1.9212+2\ln\dfrac{b}{\hat r}$	$0.6309\hat r$
Bi-Gaussian	$\dfrac{1}{2\pi\sigma_r^2}e^{-r^2/(2\sigma_r^2)}$	$\gamma_e+2\ln\dfrac{b}{\sqrt{2}\sigma_r}$	$1.747\sigma_r$

Transverse Impedance from Self-Field

- A uniformly distributed beam is shifted by Δ in x-direction. There is a horizontal opposing force. Hence the imp.
- Beam density

  $$\rho(r) = \frac{e\lambda}{\pi a^2} H(a - r).$$

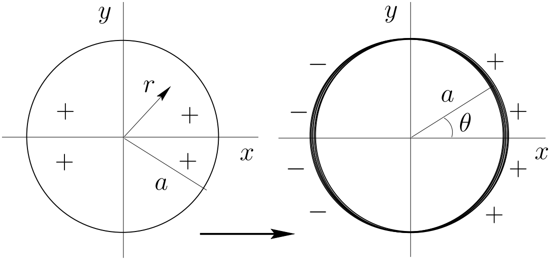

Shift to the right by $\Delta \to 0$

Transverse Impedance from Self-Field

- A uniformly distributed beam is shifted by Δ in x-direction. There is a horizontal opposing force. Hence the imp.

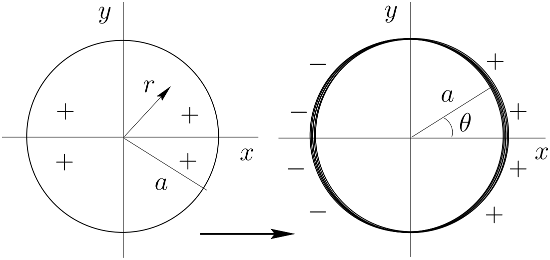

Shift to the right by $\Delta \to 0$

- Beam density

$$\rho(r) = \frac{e\lambda}{\pi a^2} H(a-r).$$

- Dipole density

$$\Delta\rho(r) = -\frac{\partial\rho(\vec{r})}{\partial x}\Delta = \frac{e\lambda\Delta\cos\theta}{\pi a^2}\delta(a-r).$$

- Dipole sees opposing electric force

$$F_{\rm elec} = \int_0^{2\pi} d\theta \int_0^{\infty} rdr \frac{e^2\lambda\Delta\cos\theta}{\pi a^2}\delta(a-r)\frac{\cos\theta}{2\pi\epsilon_0 r} = \frac{e^2\lambda\Delta Z_0 c}{2\pi a^2}.$$

- The shifted beam current $I = e\lambda\beta$ also generates a dipole current $\Delta I = e\beta\dfrac{\partial\lambda}{\partial x}\Delta$, and therefore a magnetic horizontal $F_x^{\rm mag}$.
- $F_x^{\rm mag} = -\beta F_x^{\rm elect}$. Total is $1-\beta^2 = 1/\gamma^2$,
  Total self-force $\displaystyle\int_0^C F_{\rm self}\,ds = \frac{e^2\lambda\Delta Z_0 cR}{\gamma^2 a^2}$.
- With beam current $I = e\lambda\beta$, trans. imp. is
  $$Z_1^\perp\Big|_{\rm self} = \frac{i}{\beta e I\Delta}\int_0^C F_{\rm self}\,ds = i\frac{Z_0 R}{\gamma^2\beta^2 a^2}.$$

- The shifted beam current $I = e\lambda\beta$ also generates a dipole current $\Delta I = e\beta \dfrac{\partial\lambda}{\partial x}\Delta$, and therefore a magnetic horizontal $F_x^{\rm mag}$.
- $F_x^{\rm mag} = -\beta F_x^{\rm elect}$. Total is $1-\beta^2 = 1/\gamma^2$,

  Total self-force $\displaystyle\int_0^C F_{\rm self}\, ds = \frac{e^2\lambda\Delta Z_0 cR}{\gamma^2 a^2}$.
- With beam current $I = e\lambda\beta$, trans. imp. is

$$Z_1^\perp\Big|_{\rm self} = \frac{i}{\beta e I\Delta}\int_0^C F_{\rm self}\, ds = i\frac{Z_0 R}{\gamma^2\beta^2 a^2}.$$

- Particle beam generates static charges and image current on beam pipe. So there is a similar trans. force but in opposite direction.
- Total is sp-ch imp.: $\displaystyle Z_1^\perp\Big|_{\rm sp\,ch} = i\frac{Z_0 R}{\gamma^2\beta^2}\left(\frac{1}{a^2}-\frac{1}{b^2}\right)$.

- The shifted beam current $I = e\lambda\beta$ also generates a dipole current $\Delta I = e\beta\dfrac{\partial\lambda}{\partial x}\Delta$, and therefore a magnetic horizontal $F_x^{\rm mag}$.
- $F_x^{\rm mag} = -\beta F_x^{\rm elect}$. Total is $1-\beta^2 = 1/\gamma^2$,
  Total self-force $\displaystyle\int_0^C F_{\rm self}\, ds = \frac{e^2\lambda\Delta Z_0 cR}{\gamma^2 a^2}$.
- With beam current $I = e\lambda\beta$, trans. imp. is
  $$Z_1^\perp\Big|_{\rm self} = \frac{i}{\beta e I\Delta}\int_0^C F_{\rm self}\, ds = i\frac{Z_0 R}{\gamma^2\beta^2 a^2}.$$
- Particle beam generates static charges and image current on beam pipe. So there is a similar trans. force but in opposite direction.
- Total is sp-ch imp.: $Z_1^\perp\Big|_{\rm sp\,ch} = i\dfrac{Z_0 R}{\gamma^2\beta^2}\left(\dfrac{1}{a^2} - \dfrac{1}{b^2}\right)$.
- The dependence on a^{-2} appears to resemble the incoherent self-field tune shift $\Delta\nu_{\rm self}$.
- Actually $Z_1^\perp\Big|_{\rm self}$ and $\Delta\nu_{\rm self}$ are even proportional to each other.

Coherent, Incoherent, and Impedance Forces

- Vertical force on a beam particle $\dfrac{d^2y}{ds^2}+\dfrac{\nu_{0y}^2}{R^2}\,y=\dfrac{F(y,\bar{y})}{\gamma m v^2}.$

Coherent, Incoherent, and Impedance Forces

- Vertical force on a beam particle $\dfrac{d^2y}{ds^2} + \dfrac{\nu_{0y}^2}{R^2}\, y = \dfrac{F(y,\bar{y})}{\gamma m v^2}$.
- For small offsets, $\dfrac{d^2y}{ds^2} + \dfrac{\nu_{0y}^2}{R^2} y = \dfrac{1}{\gamma m v^2}\left(\left.\dfrac{\partial F}{\partial y}\right|_{\bar{y}=0} y + \left.\dfrac{\partial F}{\partial \bar{y}}\right|_{y=0} \bar{y} \right)$.

Coherent, Incoherent, and Impedance Forces

- Vertical force on a beam particle $\dfrac{d^2y}{ds^2}+\dfrac{\nu_{0y}^2}{R^2}\,y=\dfrac{F(y,\bar{y})}{\gamma mv^2}$.
- For small offsets, $\dfrac{d^2y}{ds^2}+\dfrac{\nu_{0y}^2}{R^2}y=\dfrac{1}{\gamma mv^2}\left(\left.\dfrac{\partial F}{\partial y}\right|_{\bar{y}=0}y+\left.\dfrac{\partial F}{\partial \bar{y}}\right|_{y=0}\bar{y}\right)$.
- For center of mass, $\dfrac{d^2\bar{y}}{ds^2}+\dfrac{\nu_{0y}^2}{R^2}\bar{y}=\dfrac{1}{\gamma mv^2}\left(\left.\dfrac{\partial F}{\partial y}\right|_{\bar{y}=0}+\left.\dfrac{\partial F}{\partial \bar{y}}\right|_{y=0}\right)\bar{y}$.

Coherent, Incoherent, and Impedance Forces

- Vertical force on a beam particle $\dfrac{d^2y}{ds^2}+\dfrac{\nu_{0y}^2}{R^2}\,y=\dfrac{F(y,\bar{y})}{\gamma mv^2}$.
- For small offsets, $\dfrac{d^2y}{ds^2}+\dfrac{\nu_{0y}^2}{R^2}y=\dfrac{1}{\gamma mv^2}\left(\left.\dfrac{\partial F}{\partial y}\right|_{\bar{y}=0}y+\left.\dfrac{\partial F}{\partial \bar{y}}\right|_{y=0}\bar{y}\right)$.
- For center of mass, $\dfrac{d^2\bar{y}}{ds^2}+\dfrac{\nu_{0y}^2}{R^2}\bar{y}=\dfrac{1}{\gamma mv^2}\left(\left.\dfrac{\partial F}{\partial y}\right|_{\bar{y}=0}+\left.\dfrac{\partial F}{\partial \bar{y}}\right|_{y=0}\right)\bar{y}$.
- Thus $\Delta\nu_{y\,\mathrm{inc}}\propto\left.\dfrac{\partial F}{\partial y}\right|_{\bar{y}=0}$

  $\Delta\nu_{y\,\mathrm{coh}}\propto\left.\dfrac{\partial F}{\partial y}\right|_{\bar{y}=0}+\left.\dfrac{\partial F}{\partial \bar{y}}\right|_{y=0}$

Coherent, Incoherent, and Impedance Forces

- Vertical force on a beam particle $\dfrac{d^2y}{ds^2}+\dfrac{\nu_{0y}^2}{R^2}\,y=\dfrac{F(y,\bar{y})}{\gamma mv^2}.$

- For small offsets, $\dfrac{d^2y}{ds^2}+\dfrac{\nu_{0y}^2}{R^2}y=\dfrac{1}{\gamma mv^2}\left(\dfrac{\partial F}{\partial y}\bigg|_{\bar{y}=0}y+\dfrac{\partial F}{\partial \bar{y}}\bigg|_{y=0}\bar{y}\right).$

- For center of mass, $\dfrac{d^2\bar{y}}{ds^2}+\dfrac{\nu_{0y}^2}{R^2}\bar{y}=\dfrac{1}{\gamma mv^2}\left(\dfrac{\partial F}{\partial y}\bigg|_{\bar{y}=0}+\dfrac{\partial F}{\partial \bar{y}}\bigg|_{y=0}\right)\bar{y}.$

- Thus $\Delta\nu_{y\,\mathrm{inc}}\propto\dfrac{\partial F}{\partial y}\bigg|_{\bar{y}=0}$

$$\Delta\nu_{y\,\mathrm{coh}}\propto\frac{\partial F}{\partial y}\bigg|_{\bar{y}=0}+\frac{\partial F}{\partial \bar{y}}\bigg|_{y=0}$$

- But $Z_1^\perp\propto\dfrac{\partial F}{\partial \bar{y}}\bigg|_{y=0},$

- $\therefore$ Impedance Shift $=$ Coherent Shift $-$ Incoherent Shift.

- $\Delta\nu_{y\,\mathrm{coh}}$: result of all forces acting on center of beam at $\bar{y}$.
- $Z_1^{\perp}$: force generated by center motion of beam on individual particle.

- $\Delta\nu_{y\,\mathrm{coh}}$: result of all forces acting on center of beam at $\bar{y}$.
- $Z_1^\perp$: force generated by center motion of beam on individual particle.
- Example: a beam between two infinite horizontal conducting planes.
- Horizontal translational invariance $\Longrightarrow$ horizontal image force acting at center of beam vanishes independent of whether beam is oscillating horizontally or vertically. $\therefore\ \Delta\nu_{x\,\mathrm{coh}} = 0$.

- $\Delta\nu_{y\,\mathrm{coh}}$: result of all forces acting on center of beam at $\bar{y}$.
- $Z_1^{\perp}$: force generated by center motion of beam on individual particle.
- Example: a beam between two infinite horizontal conducting planes.
- Horizontal translational invariance $\Longrightarrow$ horizontal image force acting at center of beam vanishes independent of whether beam is oscillating horizontally or vertically. $\therefore\ \Delta\nu_{x\,\mathrm{coh}} = 0$.
- Single bunch tune shift measurement at CERN SPS. [5]

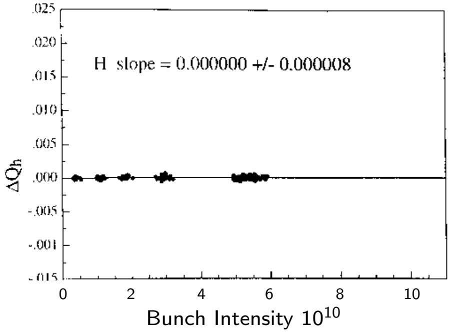

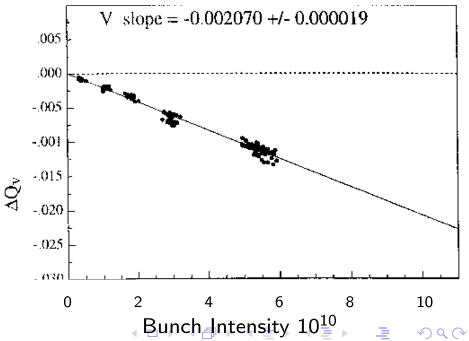

- Now let us come back to the self-field imp.
- Beam center moves with beam, does not see self-force, $\therefore \Delta\nu_{y\,\rm coh}^{\rm self} = 0$.
- Thus $\Delta\nu_y^{\rm imp} \propto -\Delta\nu_{y\,\rm incoh}^{\rm self}$.

  Or $Z_1^{\perp}\Big|_{\rm self}^{y,x} = -i\dfrac{2\pi Z_0 \gamma \nu_{0y,x}}{N r_0}\Delta\nu_{y,x\,\rm incoh}^{\rm self}$,

  where N is the number of beam particles, r_0 is classical radius.

- Now let us come back to the self-field imp.
- Beam center moves with beam, does not see self-force, $\therefore \Delta\nu_{y\,\mathrm{coh}}^{\mathrm{self}} = 0$.
- Thus $\Delta\nu_y^{\mathrm{imp}} \propto -\Delta\nu_{y\,\mathrm{incoh}}^{\mathrm{self}}$.

  Or $Z_1^{\perp}\Big|_{\mathrm{self}}^{y,x} = -i\dfrac{2\pi Z_0\gamma\nu_{0y,x}}{Nr_0}\Delta\nu_{y,x\,\mathrm{incoh}}^{\mathrm{self}}$,

  where N is the number of beam particles, r_0 is classical radius.
- As for the EM field inside the vacuum chamber,

  $Z_1^{y,x} = -i\dfrac{2Z_0R}{\gamma^2\beta^2}\dfrac{\xi_{1y,x} - \epsilon_{1y,x}}{h^2}$,

  where $\xi_{1y,x}/\epsilon_{1y,x}$ is *Laslett coherent/incoherent electric image coeff.*,

  h is vertical half gap in vacuum chamber.
- For circular beam pipe of radius b, $h = b$, $\xi_{1y,x} = \frac{1}{2}$, $\epsilon_{1y,x} = 0$.

  then $Z_1^{y,x} = -i\dfrac{Z_0R}{\gamma^2\beta^2b^2}$ is just vacuum chamber contribution to

  the trans. sp-ch imp.

Self-Field Impedance with Other Distributions [6]

- Shifted dipole density is $\Delta\rho(r) = -\dfrac{\partial\rho(r)}{\partial y}\,\Delta = -\dfrac{d\rho(r)}{dr}\,\cos\theta\,\Delta.$

- Dipole electric force in the horizontal direction can be written more generally as

$$F_{\rm elec} = -\Delta\int_0^{2\pi} d\theta \int_0^{\infty} r dr \left[-e^2\frac{d\rho(r)}{dr}\right]\frac{\cos^2\theta}{2\pi\epsilon_0 r} = -\frac{e^2\rho(0)\Delta}{2\epsilon_0}.$$

- Self-field imp. $Z_1^{\perp}\Big|_{\rm self} = i\,\dfrac{Z_0 R}{\gamma^2\beta^2}\,\dfrac{\pi\rho(0)}{\lambda}.$ $\left[\text{uniform dist. } \rho(0) = \dfrac{e\lambda}{\pi a^2}\right]$

Self-Field Impedance with Other Distributions [6]

- Shifted dipole density is $\Delta\rho(r) = -\dfrac{\partial\rho(r)}{\partial y}\,\Delta = -\dfrac{d\rho(r)}{dr}\,\cos\theta\,\Delta.$
- Dipole electric force in the horizontal direction can be written more generally as

$$F_{\rm elec} = -\Delta\int_0^{2\pi} d\theta \int_0^{\infty} rdr\left[-e^2\frac{d\rho(r)}{dr}\right]\frac{\cos^2\theta}{2\pi\epsilon_0 r} = -\frac{e^2\rho(0)\Delta}{2\epsilon_0}.$$

- Self-field imp. $Z_1^\perp\Big|_{\rm self} = i\dfrac{Z_0R}{\gamma^2\beta^2}\dfrac{\pi\rho(0)}{\lambda}.$ $\left[\text{uniform dist. } \rho(0) = \dfrac{e\lambda}{\pi a^2}\right]$
- If we write $Z_1^\perp\Big|_{\rm self} = i\dfrac{Z_0R}{\gamma^2\beta^2 a_{\rm eff}^2}$, same form as uniform distribution, equivalent beam radius is $a_{\rm eff} = \sqrt{\dfrac{\lambda}{\pi\rho(0)}}.$

  λ is linear density, $\rho(0)$ is volume density at beam center.

	Phase space distribution	$a_{\rm eff}$
Uniform	$\dfrac{1}{\pi\hat r^2}H(\hat r-r)$	$\hat r$
Elliptical	$\dfrac{3}{2\pi\hat r}\left(1-\dfrac{r^2}{\hat r^2}\right)^{1/2}H(\hat r-r)$	$\sqrt{\dfrac{2}{3}}\hat r$
Parabolic	$\dfrac{1}{2\pi\hat r^2}\left(1-\dfrac{r^2}{\hat r^2}\right)H(\hat r-r)$	$\frac{1}{\sqrt{2}}\hat r$
Cosine-square	$\dfrac{2\pi}{\pi^2-4}\cos^2\dfrac{\pi r}{2\hat r}H(\hat r-r)$	$\dfrac{\sqrt{\pi^2-4}}{\sqrt{2}\pi}\hat r$
Bi-Gaussian	$\dfrac{1}{2\pi\sigma_r^2}e^{-r^2/(2\sigma_r^2)}$	$\sqrt{2}\sigma_r$

Resistive Wall Impedance

- Consider a particle beam of current I in a cylindrical beam pipe of radius b.
- Want to compute resistive-wall impedance.
- Proper method: solve Maxwell equation in 2 media: vacuum and metal.
- We use here a simple model.

  At freq. ω, skin depth: $\delta_c = \sqrt{\dfrac{2}{\sigma_c \mu_c \omega}}$.

  Assume image current flows uniformly in one skin depth only;

  i.e., within $b < r < b + \delta_c$

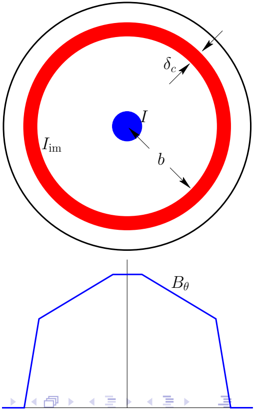

- $\mathcal{R}e\, Z_0^{\parallel}\Big|_{\rm RW} = \dfrac{2\pi R}{2\pi b \delta_c \sigma_c} = \dfrac{R}{b\delta_c\sigma_c}$.

- Now the image current generates magnetic flux.

  We have taken care of those inside the beam pipe as sp-ch imp.

  Need to take care of mag. flux inside beam pipe wall.

- Inside one skin depth of the pipe wall $B_{\theta\,\mathrm{av}} = \frac{1}{2}\left[\frac{\mu_c I}{2\pi b}\right]$.

  Factor $\frac{1}{2}$ occurs because B_θ decays linearly from $r = b$ to $b + \delta_c$.

- Total flux $\Phi = B_{\theta\,\mathrm{av}} 2\pi R\delta_c = \dfrac{\mu_c R\delta_c I}{2b}$.

- Inductive imp. is $\qquad \downarrow \delta_c^2 \qquad \downarrow$ same as $\mathcal{R}e\, Z_0^{\parallel}\Big|_{\mathrm{RW}}$

$$\mathcal{I}m\, Z_0^{\parallel}\Big|_{\mathrm{RW}} = -i\omega\frac{\mu_c R\delta_c}{2b} = -i\frac{\omega\mu_c R}{2b\delta_c}\left[\frac{2}{\sigma_c\mu_c\omega}\right] = -i\frac{R}{b\delta_c\sigma_c}.$$

- We can now write

$$Z_0^{\parallel}\Big|_{\mathrm{RW}} = [1 - i\,\mathrm{sgn}(\omega)]\frac{R}{b\delta_c\sigma_c} = [1 - i\,\mathrm{sgn}(\omega)]\sqrt{\frac{\omega\mu_c}{2\sigma_c}}\frac{R}{b}.$$

Comments

- We can now write $Z_0^{\parallel}\Big|_{\rm RW} = \big[1 - i\,{\rm sgn}(\omega)\big]\dfrac{R}{b\delta_c\sigma_c} = \mathcal{R}\dfrac{2\pi R}{2\pi b}$.

  where *surface impedance* is defined as $\mathcal{R} = \dfrac{1 - i\,{\rm sgn}(\omega)}{\delta_c\sigma_c}$.

- $Z_0^{\parallel}\Big|_{\rm RW} = \mathcal{R}\dfrac{\rm long.\,length}{\rm width}$. More accurate defn. $\mathcal{R} = \dfrac{E_s}{H_\perp}\Big|_{\rm surface}$.

Comments

- We can now write $Z_0^{\parallel}\Big|_{\rm RW} = \big[1 - i\,{\rm sgn}(\omega)\big]\dfrac{R}{b\delta_c\sigma_c} = \mathcal{R}\dfrac{2\pi R}{2\pi b}$.

  where *surface impedance* is defined as $\mathcal{R} = \dfrac{1 - i\,{\rm sgn}(\omega)}{\delta_c\sigma_c}$.

- $Z_0^{\parallel}\Big|_{\rm RW} = \mathcal{R}\dfrac{\rm long.\,length}{\rm width}$. More accurate defn. $\mathcal{R} = \dfrac{E_s}{H_\perp}\bigg|_{\rm surface}$.

- One may wonder why $\mathcal{R}e\, Z_0^{\parallel}\Big|_{\rm RW} \to 0$ when $\omega \to 0$.

  One may expect a dc beam still sees the resistivity of the pipe wall.

- $\omega = 0$ implies no time dependency of $\vec{B}$ and $\vec{E}$.

  Then $\vec{B}$ and $\vec{E}$ are not related because there is no more Faraday's law.

  $\vec{B}$ created by the dc current cannot generate $\vec{E}$ on surface or inside wall of beam pipe.

- Thus is no resistive loss at $\omega = 0$ and $\mathcal{R}e\, Z_m^{\parallel}\Big|_{\rm RW} \to 0$ for all $m \geq 0$.

Transverse Resistive Wall Impedance

- Compute image current distribution for an off-set beam.

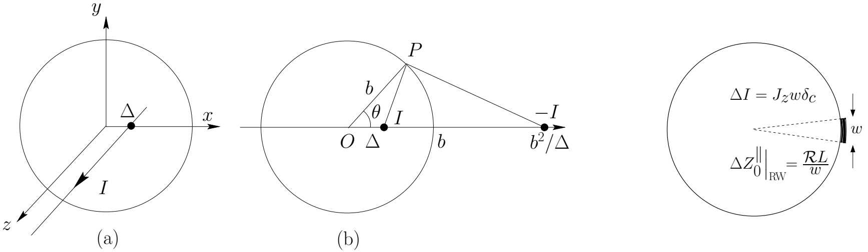

- Dipole image current density ↓ monopole

$$\Delta J_z(\theta) = -\frac{I\Delta}{2\pi b}\left[\frac{2\Delta(b\cos\theta-\Delta)}{b^2+\Delta^2-2b\Delta\cos\theta}-1\right] \approx -\frac{I\Delta}{\pi b^2}\cos\theta.$$

Transverse Resistive Wall Impedance

- Compute image current distribution for an off-set beam.

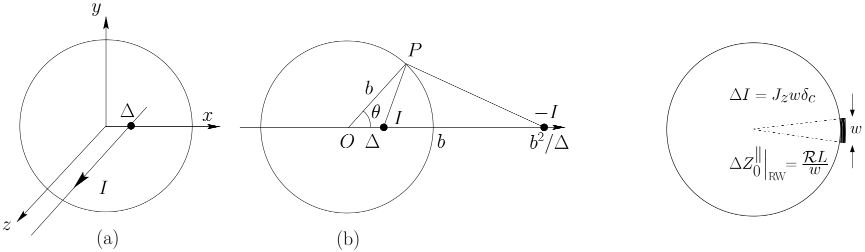

- Dipole image current density $\downarrow$ monopole

$$\Delta J_z(\theta) = -\frac{I\Delta}{2\pi b}\left[\frac{2\Delta(b\cos\theta - \Delta)}{b^2+\Delta^2-2b\Delta\cos\theta} - 1\right] \approx -\frac{I\Delta}{\pi b^2}\cos\theta .$$

- Voltage generated by image current element for length L at $\theta = 0$ is

$$V = \delta I\, \delta Z_0^{\|}\Big|_{\rm RW} = \left[-\frac{I\Delta}{\pi b^2}w\right]\left[Z_0^{\|}\Big|_{\rm RW}\frac{2\pi b}{w}\right] = -\frac{2I\Delta}{b}Z_0^{\|}\Big|_{\rm RW} = E_{z0}L,$$

where $E_{z0} = -\dfrac{2I\Delta Z_0^{\|}\Big|_{\rm RW}}{bL}$ is E_z on surface of beam pipe at $\theta = 0$.

- Because this is generated by a dipole beam, $E_z(x) = E_{z0}\dfrac{x}{b}$,

  Faraday law gives $i\omega B_y = -\dfrac{\partial E_z}{\partial x} \implies B_y = -\dfrac{iE_{z0}}{\omega b}$.
- B_y clinging the dipole current loop, creating a horizontal opposing force.
- $Z_1^x = \dfrac{i}{\beta I\Delta}\displaystyle\int_0^C \left[\vec{E} + \vec{v}\times\vec{B}\right]_x ds = \dfrac{2c}{b^2}\dfrac{Z_0^\parallel\Big|_{\rm RW}}{\omega}$.

- Because this is generated by a dipole beam, $E_z(x) = E_{z0}\dfrac{x}{b}$,

  Faraday law gives $i\omega B_y = -\dfrac{\partial E_z}{\partial x} \implies B_y = -\dfrac{iE_{z0}}{\omega b}$.

- B_y clinging the dipole current loop, creating a horizontal opposing force.

- $Z_1^x = \dfrac{i}{\beta I \Delta}\displaystyle\int_0^C \left[\vec{E} + \vec{v}\times\vec{B}\right]_x ds = \dfrac{2c}{b^2}\dfrac{Z_0^\parallel\Big|_{\rm RW}}{\omega}$.

- Note that $Z_1^\perp = \dfrac{2c}{b^2\omega_0}\dfrac{Z_0^\parallel\Big|_{\rm RW}}{n}$ [not P-W relation!!!!]

  $Z_1^\perp$ and $\dfrac{Z_0^\parallel\Big|_{\rm RW}}{n}$ are proportional for all frequencies.

- But as we will see below, this is not true at low frequencies.

Instabilities from Resistive-Wall Impedances

- For a coasting beam, all betatron sidebands are independent modes. Thus $Z_1^{\parallel}\Big|_{\rm RW}$ excites all modes.

Instabilities from Resistive-Wall Impedances

- For a coasting beam, all betatron sidebands are independent modes. Thus $Z_1^{\|}\Big|_{\rm RW}$ excites all modes.
- $Z_1^{\|}\Big|_{sp\,ch}$ shifts incoherent tune spread away from coherent tune lines and large chromaticities are often required for Landau damping.

Instabilities from Resistive-Wall Impedances

- For a coasting beam, all betatron sidebands are independent modes. Thus $Z_1^{\parallel}\Big|_{\rm RW}$ excites all modes.
- $Z_1^{\parallel}\Big|_{sp\ ch}$ shifts incoherent tune spread away from coherent tune lines and large chromaticities are often required for Landau damping.

Examples in Recycler [7, 8]

Long $\bar{p}$ beam
$\tau = 3.5\ \mu$s
$N_b = 28 \times 10^{10}$
$\epsilon_{x,y95\%} = 3 \times 10^{-6}\ \pi$m
$\xi_y = -2 \rightarrow 0.$

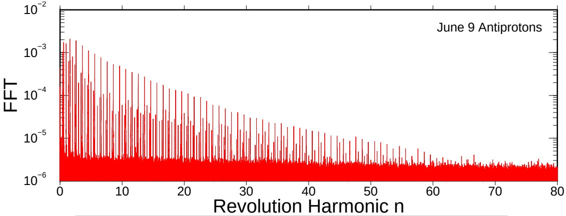

p beam unbunched
$N_b = 43.9 \times 10^{10}$
$\epsilon_{x,y95\%} = 6 \times 10^{-6}\ \pi$m
$\xi_y = -2 \rightarrow 0.$

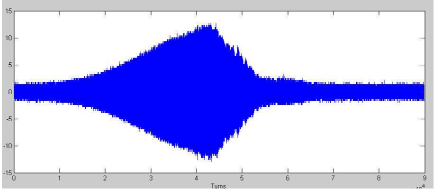

time

- All modes become stable in the presence of $\Delta\nu_y^{\rm sp\,ch}$ when chromaticity $\xi_y = -2.53$.

$$\Delta\nu_y^{\rm sp\,ch}\Big|_{av} = 14.2\times10^{-4}$$
$\xi_y = -2.53$ produces
$$\sigma_{\Delta\nu_y} = 8.59\times10^{-4}.$$

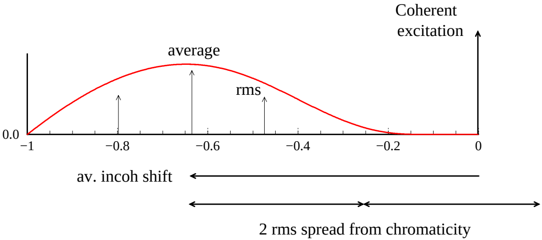

For higher $\bar{p}$ intensity, higher ξ_y is required.

Eventually a transverse kicker was built instead.

- All modes become stable in the presence of $\Delta\nu_y^{\rm sp\,ch}$ when chromaticity $\xi_y = -2.53$.

$\Delta\nu_y^{\rm sp\,ch}\Big|_{av} = 14.2\times10^{-4}$
$\xi_y = -2.53$ produces
$\sigma_{\Delta\nu_y} = 8.59 \times 10^{-4}$.

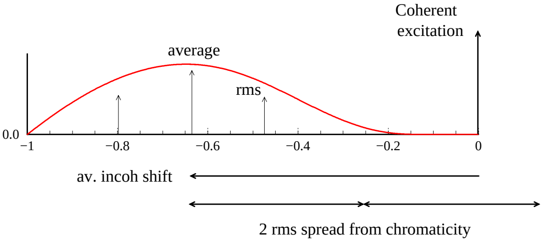

For higher $\bar{p}$ intensity, higher ξ_y is required.

Eventually a transverse kicker was built instead.

- Situation is different when beam is bunched. Driving impedance is

$$\mathcal{Z}_y = \sum_{p=-\infty}^{\infty} Z_1^y(\Omega + p\omega_0)h(\Omega + p\omega_0)$$

where h is bunch power spectrum and $\Omega = \omega_{y0} + \Delta\omega_{y\,\rm coh}$.

- Growth of many lower sidebands are cancelled by damping of upper sidebands, net growth will be much milder than for unbunched beam.

Transverse Coupled Bunch Instabilities

- For the Tevatron in target mode, if there are $M = 1113$ equally spaced bunches, there can be M modes of coupled motion.
- Each mode is driven by the imp. $\mathcal{Z}_{y\,m\mu} = \sum_q Z_1^y(\Omega + \omega_q) h_m(\omega_q - \chi/\tau_L)$, with $\omega_q = (qM + \mu)\omega_0 + \omega_\beta + m\omega_s$.

For each coupled mode μ, not all betatron sidebands contribute, but every Mth sideband contribute.

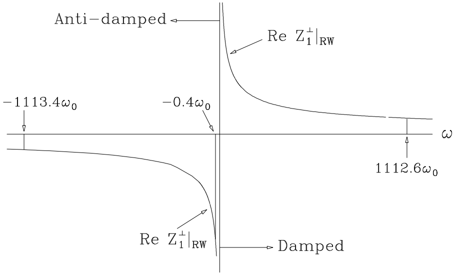

- Thus upper sidebands can no longer cancel growth from lower sidebands. Strongest drive is the sideband at negative freq. closest to $\omega = 0$, or at $\omega = -(1 - [\nu_y]_{\rm res})\omega_0$. It acts like a narrow resonance.

Remedy

- Change shape of bunch of power spectrum, like longer bunch, does not help much, because driving force is at very low freq.
- There are a few ways to minimize or avoid the instability:
- Chromaticity will certainly help by
  1. Widening tune spread to provide more Landau damping.
  2. Shifting driving betatron sideband to freq. with smaller power spectrum.
  3. Tevatron: $\eta = 0.0028$, $\tau_L = 5$ns, $f_0 = 47.7$ kHz.
     $\xi = +10$ shifts power spectrum by $\chi = \omega_\xi \tau_L = 2\pi f_0 \xi \tau_L/\eta = 5.4$.
  4. Power spectrum reduces by > 4 folds, and so is instability growth rate.
  5. But driving sideband hits $m = 1$ when $\omega_\xi \tau_L/\pi = 1.7$.
     Or high azimuthal modes become unstable.
- Octupole tune spread provide Landau damping.
- Coat beam pipe with copper to reduce resistive-wall impedance.
- Install wideband transverse kicker.

Scaling Law

- Apply to bunches that go from one accelerator ring to another, like the Booster, Main Injector, and Tevatron.
- Weiren Chou [9] shows that this transverse coupled bunch instability growth rate is the same for all the rings, provided that
  1. same rf bucket width with all bucket filled,
  2. same beam pipe, meaning same radius b and wall conductivity σ_c
  3. same residual betatron tune.

  Roughly, beam current the same for completely filled ring,
  $\omega_0 \propto 1/R$, $E \propto R$, $\nu_\beta \propto \sqrt{R} \implies$ same growth rate
- Typical growth time is a few or few tens ms.

Scaling Law

- Apply to bunches that go from one accelerator ring to another, like the Booster, Main Injector, and Tevatron.
- Weiren Chou [9] shows that this transverse coupled bunch instability growth rate is the same for all the rings, provided that
  1. same rf bucket width with all bucket filled,
  2. same beam pipe, meaning same radius b and wall conductivity σ_c
  3. same residual betatron tune.

  Roughly, beam current the same for completely filled ring, $\omega_0 \propto 1/R$, $E \propto R$, $\nu_\beta \propto \sqrt{R} \implies$ same growth rate
- Typical growth time is a few or few tens ms.
- **Problem:** Booster bunches see laminated magnets, resistive impedance must be much larger.
- Transverse coupled bunch instability is very milder in Booster, where there is no dedicated transverse damper.
- Something must be wrong with the expressions for resistive-wall impedance, especially at small frequencies.

Problems with $Z_1^{\perp}$

- Recall that we derived $Z_1^{\perp}(\omega) = \dfrac{2c}{b^2}\dfrac{Z_0^{\parallel}}{\omega}$ and $Z_1^{\perp} \to \dfrac{1}{\sqrt{\omega}}$ as $\omega \to 0$.
- Skin depth δ_c increases as $\omega^{-1/2}$. When $\delta_c > t$, wall thickness, must replace $\delta_c \to t$. Thus $Z_1^{\perp} \to \dfrac{1}{\omega}$ faster than $\dfrac{1}{\sqrt{\omega}}$.

Problems with $Z_1^\perp$

- Recall that we derived $Z_1^\perp(\omega) = \dfrac{2c}{b^2}\dfrac{Z_0^\parallel}{\omega}$ and $Z_1^\perp \to \dfrac{1}{\sqrt{\omega}}$ as $\omega \to 0$.
- Skin depth δ_c increases as $\omega^{-1/2}$. When $\delta_c > t$, wall thickness, must replace $\delta_c \to t$. Thus $Z_1^\perp \to \dfrac{1}{\omega}$ faster than $\dfrac{1}{\sqrt{\omega}}$.
- Both $Z_0^\parallel(\omega)$ and $Z_1^\perp(\omega)$ are analytic, because they are derived from causal wake functions $W_0'(z)$ and $W_1(z)$.
- We know that $Z_0^\parallel(\omega)$ is more well behaved, but $Z_1^\perp(\omega)$ is not.

Problems with $Z_1^{\perp}$

- Recall that we derived $Z_1^{\perp}(\omega)=\dfrac{2c}{b^2}\dfrac{Z_0^{\parallel}}{\omega}$ and $Z_1^{\perp} \to \dfrac{1}{\sqrt{\omega}}$ as $\omega \to 0$.
- Skin depth δ_c increases as $\omega^{-1/2}$. When $\delta_c > t$, wall thickness, must replace $\delta_c \to t$. Thus $Z_1^{\perp} \to \dfrac{1}{\omega}$ faster than $\dfrac{1}{\sqrt{\omega}}$.
- Both $Z_0^{\parallel}(\omega)$ and $Z_1^{\perp}(\omega)$ are analytic, because they are derived from causal wake functions $W_0'(z)$ and $W_1(z)$.
- We know that $Z_0^{\parallel}(\omega)$ is more well behaved, but $Z_1^{\perp}(\omega)$ is not.
- We also showed that there is no resistive loss at $\omega = 0$. So we should expect $\mathcal{R}e\, Z_m^{\perp}(0) = 0$.
- $\mathcal{R}e\, Z_1^{\perp}(\omega)$ must bend back to zero.
- $\mathcal{I}m\, Z_1^{\perp}(\omega)$ will approach a fixed value instead of infinity as $\omega \to 0$.

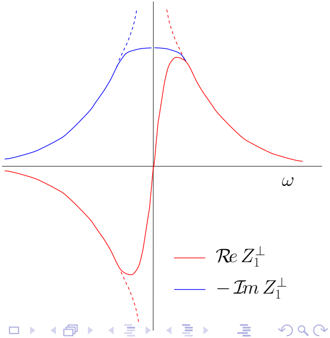

$Z_1^\perp$ near $\omega = 0$

- Best method is to solve Maxwell equation carefully, will get $\mathcal{R}e\, Z_m^\perp = 0$ and $\mathcal{I}m\, Z_m^\perp = \texttt{constant}$ as expected.
- Here, we follow an easier intuitive approach by Vos (CERN). [10]

$Z_1^\perp$ near $\omega = 0$

- Best method is to solve Maxwell equation carefully, will get $\mathcal{R}e\, Z_m^\perp = 0$ and $\mathcal{I}m\, Z_m^\perp = \texttt{constant}$ as expected.
- Here, we follow an easier intuitive approach by Vos (CERN). [10]
- Dipole surface current on pipe wall is $\Delta K_z(\theta) = \dfrac{I_{\rm im}\Delta}{\pi b^2}\cos\theta$. ($\Delta =$ offset)
- Total image current on each side: $I_d = \displaystyle\int_{-\pi/2}^{\pi/2} \Delta K_z(\theta) b d\theta = \frac{2iI_{\rm im}\Delta}{\pi b}$.
- Want to compute inductance seen by $\pm I_d$ loop.

$Z_1^\perp$ near $\omega = 0$

- Best method is to solve Maxwell equation carefully, will get $\mathcal{R}e\, Z_m^\perp = 0$ and $\mathcal{I}m\, Z_m^\perp = \texttt{constant}$ as expected.
- Here, we follow an easier intuitive approach by Vos (CERN). [10]
- Dipole surface current on pipe wall is $\Delta K_z(\theta) = \dfrac{I_{\rm im}\Delta}{\pi b^2}\cos\theta$. ($\Delta =$ offset)
- Total image current on each side: $I_d = \displaystyle\int_{-\pi/2}^{\pi/2} \Delta K_z(\theta) b d\theta = \frac{2iI_{\rm im}\Delta}{\pi b}$.
- Want to compute inductance seen by $\pm I_d$ loop.
- Mag. field from $\pm I_d$ on x-axis: $H_y(x) = -\dfrac{i_{\rm im}\Delta}{2\pi b^2}$. $(I_{\rm im} = -I)$
- Flux is $\Phi_y = \displaystyle\int_{-b}^{b} B_y dx = 2bB_y = -\frac{\mu_0 I_{\rm im}\Delta}{\pi b} = -\frac{\mu_0}{2} I_d$.
- Inductance seen by $\pm I_d$ loop is $\mathcal{L} = \dfrac{\mu_0}{2}$.

$Z_1^\perp$ near $\omega = 0$

- Best method is to solve Maxwell equation carefully, will get $\mathcal{R}e\, Z_m^\perp = 0$ and $\mathcal{I}m\, Z_m^\perp = \texttt{constant}$ as expected.
- Here, we follow an easier intuitive approach by Vos (CERN). [10]
- Dipole surface current on pipe wall is $\Delta K_z(\theta) = \dfrac{I_{\rm im}\Delta}{\pi b^2}\cos\theta$. ($\Delta =$ offset)
- Total image current on each side: $I_d = \displaystyle\int_{-\pi/2}^{\pi/2} \Delta K_z(\theta) b d\theta = \frac{2iI_{\rm im}\Delta}{\pi b}$.
- Want to compute inductance seen by $\pm I_d$ loop.
- Mag. field from $\pm I_d$ on x-axis: $H_y(x) = -\dfrac{i_{\rm im}\Delta}{2\pi b^2}$. ($I_{\rm im} = -I$)
- Flux is $\Phi_y = \displaystyle\int_{-b}^{b} B_y dx = 2bB_y = -\frac{\mu_0 I_{\rm im}\Delta}{\pi b} = -\frac{\mu_0}{2} I_d$.
- Inductance seen by $\pm I_d$ loop is $\mathcal{L} = \dfrac{\mu_0}{2}$.
- But inductance seen by beam current I is different.

  There is some sort of transformer effect as a result of the shift Δ.

Transformer Ratio

- Introduce mutual inductance $\mathcal{M}$: $-i\omega\mathcal{M}(I_{\rm im}-I_d)=-i\omega(\mathcal{L}-\mathcal{M})I_d$,
- Get $\dfrac{\mathcal{M}}{\mathcal{L}}=\dfrac{I_d}{I_{\rm im}}=\dfrac{2\Delta}{\pi b}$,
  This is a geometric relation.
- Force at beam: $F_x=e(E_x-\beta cB_y)$.
  Imp.: $\dfrac{Z_1^\perp}{L}=\dfrac{(F_x/e)_{\rm mag}}{i\beta I\Delta}=-\dfrac{cB_y}{iI\Delta}=\dfrac{c\mu_0 I_d}{i4\Delta b\,I}=i\dfrac{Z_0}{2\pi b^2}$.
  capacitive $\uparrow$

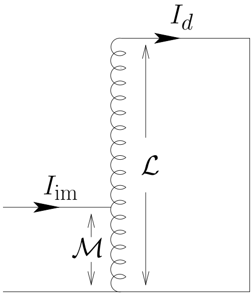

Transformer Ratio

- Introduce mutual inductance $\mathcal{M}$: $-i\omega\mathcal{M}(I_{\rm im}-I_d)=-i\omega(\mathcal{L}-\mathcal{M})I_d$,
- Get $\dfrac{\mathcal{M}}{\mathcal{L}}=\dfrac{I_d}{I_{\rm im}}=\dfrac{2\Delta}{\pi b}$,
  This is a geometric relation.
- Force at beam: $F_x=e(E_x-\beta cB_y)$.
  Imp.: $\dfrac{Z_1^\perp}{L}=\dfrac{(F_x/e)_{\rm mag}}{i\beta I\Delta}=-\dfrac{cB_y}{iI\Delta}=\dfrac{c\mu_0 I_d}{i4\Delta b I}=i\dfrac{Z_0}{2\pi b^2}$.
  capacitive ↑

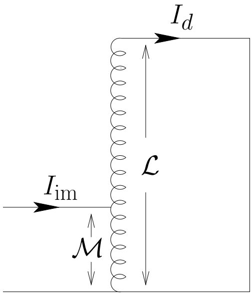

- This is the familiar imp. from magnetic image.
  Electric image gives similar, total $\dfrac{Z_1^\perp}{L}=-i\dfrac{1}{\gamma^2\beta^2}\dfrac{Z_0}{2\pi b^2}$. ← sp ch imp.

Transformer Ratio

- Introduce mutual inductance $\mathcal{M}$: $-i\omega\mathcal{M}(I_{\rm im}-I_d)=-i\omega(\mathcal{L}-\mathcal{M})I_d$,
- Get $\dfrac{\mathcal{M}}{\mathcal{L}}=\dfrac{I_d}{I_{\rm im}}=\dfrac{2\Delta}{\pi b}$,

  This is a geometric relation.
- Force at beam: $F_x=e(E_x-\beta cB_y)$.

  Imp.: $\dfrac{Z_1^\perp}{L}=\dfrac{(F_x/e)_{\rm mag}}{i\beta I\Delta}=-\dfrac{cB_y}{iI\Delta}=\dfrac{c\mu_0 I_d}{i4\Delta b\, I}=i\dfrac{Z_0}{2\pi b^2}$.

  capacitive ↑

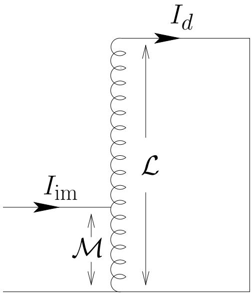

- This is the familiar imp. from magnetic image.

  Electric image gives similar, total $\dfrac{Z_1^\perp}{L}=-i\dfrac{1}{\gamma^2\beta^2}\dfrac{Z_0}{2\pi b^2}$. ← sp ch imp.
- Here we wish to emphasize that task of above is two-fold:
  1. contributes to sp ch imp.
  2. contributes to transformer ratio.

Inclusion of Resistivity

- Recall $\dfrac{Z_0^{\parallel}\big|_{\rm RW}}{L}=\dfrac{\mathcal{R}}{2\pi b}$, $\mathcal{R}$ is surface imp.
- For a length L, voltage generated:

$$V(\theta)=2\left[\frac{\mathcal{R}L}{w}\right]\Big[w\Delta K_z(\theta)\Big]=\frac{\mathcal{R}LI_d}{b}\cos\theta.$$

- $\dfrac{\hat{V}}{L}=\dfrac{\mathcal{R}I_d}{b}=2\pi\dfrac{Z_0^{\parallel}\big|_{\rm RW}}{L}I_d=\mathcal{Z}I_d.$

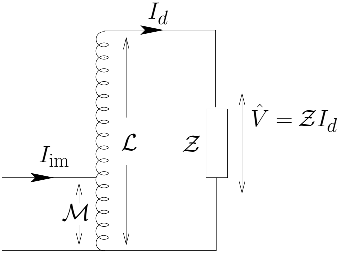

Inclusion of Resistivity

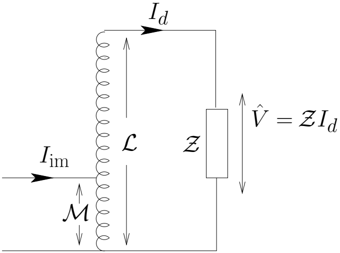

- Recall $\dfrac{Z_0^{\parallel}\big|_{\rm RW}}{L} = \dfrac{\mathcal{R}}{2\pi b}$, $\mathcal{R}$ is surface imp.
- For a length L, voltage generated:

$$V(\theta) = 2\left[\frac{\mathcal{R}L}{w}\right]\left[w\Delta K_z(\theta)\right] = \frac{\mathcal{R}LI_d}{b}\cos\theta.$$

- $\dfrac{\hat{V}}{L} = \dfrac{\mathcal{R}I_d}{b} = 2\pi\dfrac{Z_0^{\parallel}\big|_{\rm RW}}{L} I_d = \mathcal{Z} I_d.$
- On pipe wall surface $\hat{E}_z = \frac{1}{2}\dfrac{\hat{V}}{L} = \frac{1}{2}\mathcal{Z} I_d.$ (Note factor $\frac{1}{2}$)
- Now compute impedance: $\dfrac{F_x}{e} = E_x - vB_y = \dfrac{v}{i\omega}\dfrac{\partial E_z}{\partial x} = \dfrac{v\mathcal{Z}I_d}{i2\omega b}.$

$$\frac{Z_1^{H}\big|_{\rm RW}}{L} = \frac{F_x/e}{i\beta I\Delta} = -\frac{c\mathcal{Z}I_d}{2\omega bI\Delta} = -\frac{c\pi}{\omega b}\frac{I_d}{I\Delta}\frac{Z_0^{\parallel}\big|_{\rm RW}}{L}.$$

Inclusion of Resistivity

- Recall $\dfrac{Z_0^{\parallel}\big|_{\rm RW}}{L} = \dfrac{\mathcal{R}}{2\pi b}$, $\mathcal{R}$ is surface imp.
- For a length L, voltage generated:

$$V(\theta) = 2\left[\frac{\mathcal{R}L}{w}\right]\left[w\Delta K_z(\theta)\right] = \frac{\mathcal{R}LI_d}{b}\cos\theta.$$

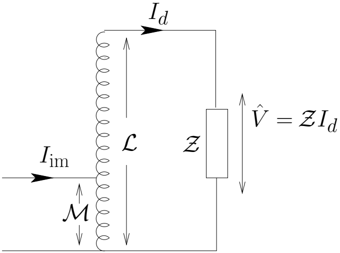

- $\dfrac{\hat{V}}{L} = \dfrac{\mathcal{R}I_d}{b} = 2\pi\dfrac{Z_0^{\parallel}\big|_{\rm RW}}{L}I_d = \mathcal{Z}I_d$.
- On pipe wall surface $\hat{E}_z = \frac{1}{2}\dfrac{\hat{V}}{L} = \frac{1}{2}\mathcal{Z}I_d$. (Note factor $\frac{1}{2}$)
- Now compute impedance: $\dfrac{F_x}{e} = E_x - vB_y = \dfrac{v}{i\omega}\dfrac{\partial E_z}{\partial x} = \dfrac{v\mathcal{Z}I_d}{i2\omega b}$.

$$\frac{Z_1^H\big|_{\rm RW}}{L} = \frac{F_x/e}{i\beta I\Delta} = -\frac{c\mathcal{Z}I_d}{2\omega bI\Delta} = -\frac{c\pi}{\omega b}\frac{I_d}{I\Delta}\frac{Z_0^{\parallel}\big|_{\rm RW}}{L}.$$

- What is left is to compute the ratio I_d/I in presence of resistivity.

Although $\dfrac{\mathcal{M}}{\mathcal{L}} = \dfrac{2\Delta}{\pi b}$ is unchanged, $\dfrac{I_d}{I}$ has changed and $\neq -\dfrac{2\Delta}{\pi b}$.

$$-i\omega\mathcal{M}(I_{\rm im}-I_d) = \left[-i\omega(\mathcal{L}-\mathcal{M})+\mathcal{Z}\right] I_d .$$

obtain

$$\frac{I_d}{I_{\rm im}}=\frac{2\Delta}{\pi b}\,\frac{-i\omega\mathcal{L}}{-i\omega\mathcal{L}+\mathcal{Z}}$$

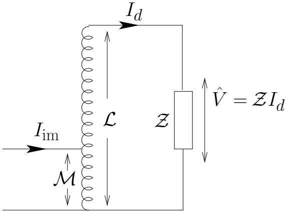

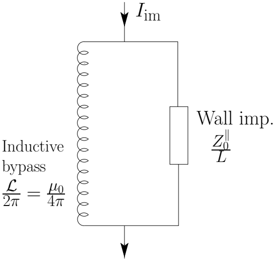

$$-i\omega\mathcal{M}(I_{\rm im}-I_d) = \left[-i\omega(\mathcal{L}-\mathcal{M})+\mathcal{Z}\right] I_d .$$

obtain

$$\frac{I_d}{I_{\rm im}}=\frac{2\Delta}{\pi b}\,\frac{-i\omega\mathcal{L}}{-i\omega\mathcal{L}+\mathcal{Z}}$$

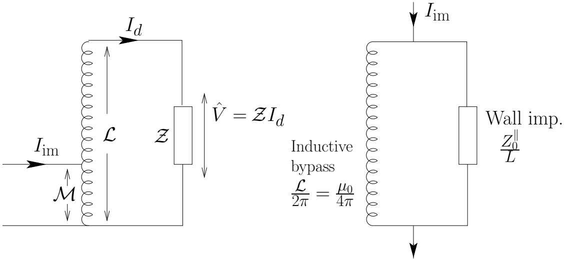

- Finally the imp. $\displaystyle \frac{Z_1^H\big|_{\rm RW}}{L}=\frac{2c}{\omega b^2}\,\frac{\dfrac{-i\omega\mathcal{L}}{2\pi}\,\dfrac{Z_0^{\parallel}\big|_{\rm RW}}{L}}{\dfrac{-i\omega\mathcal{L}}{2\pi}+\dfrac{Z_0^{\parallel}\big|_{\rm RW}}{L}}.$ $\longleftarrow$ 2 imp. in parallel

- Thus Z_1^H is just 2 impedances in parallel: $\dfrac{-i\omega\mathcal{L}}{2\pi}$ and $\dfrac{Z_0^{\parallel}\big|_{\rm RW}}{L}$.

$$-i\omega\mathcal{M}(I_{\rm im}-I_d) = \left[-i\omega(\mathcal{L}-\mathcal{M})+\mathcal{Z}\right] I_d .$$

obtain

$$\frac{I_d}{I_{\rm im}} = \frac{2\Delta}{\pi b}\,\frac{-i\omega\mathcal{L}}{-i\omega\mathcal{L}+\mathcal{Z}}$$

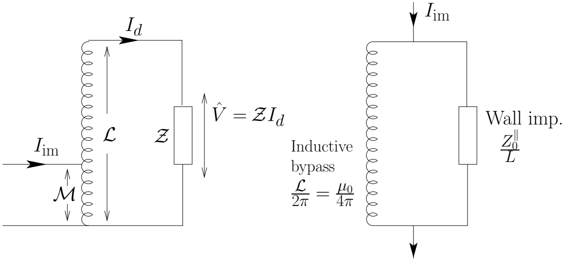

- Finally the imp. $\displaystyle \frac{Z_1^H\big|_{\rm RW}}{L} = \frac{2c}{\omega b^2}\,\frac{\dfrac{-i\omega\mathcal{L}}{2\pi}\,\dfrac{Z_0^\parallel\big|_{\rm RW}}{L}}{\dfrac{-i\omega\mathcal{L}}{2\pi}+\dfrac{Z_0^\parallel\big|_{\rm RW}}{L}}.$ $\leftarrow$ 2 imp. in parallel

- Thus Z_1^H is just 2 impedances in parallel: $\dfrac{-i\omega\mathcal{L}}{2\pi}$ and $\dfrac{Z_0^\parallel\big|_{\rm RW}}{L}$.

- Large ω, go thru $\dfrac{Z_0^\parallel\big|_{\rm RW}}{L}$ and $\dfrac{Z_1^H\big|_{\rm RW}}{L} \to \dfrac{2c}{b^2}\,\dfrac{Z_0^\parallel\big|_{\rm RW}}{\omega L}$. $\leftarrow$ classical region

- Small ω, go thru $\dfrac{-i\omega\mathcal{L}}{2\pi}$ and $\dfrac{Z_1^H\big|_{\rm RW}}{L} \to \dfrac{-ic\mathcal{L}}{\pi b^2} = \dfrac{-iZ_0}{2\pi b^2}$. $\leftarrow$ inductive bypass

Results of Maxwell Equations [11]

- Tevatron: $R = 1$ km, pipe radius $b = 3$ cm, wall thickness $t = 1.5$ mm. s.s. wall $\sigma_c = 1.35 \times 10^6\ (\Omega\text{-m})^{-1}$.
- Skin depth fills pipe wall at $f_c = 83.4$ Hz ($kb = 5.24 \times 10^{-5}$).

Results of Maxwell Equations [11]

- Tevatron: $R = 1$ km, pipe radius $b = 3$ cm, wall thickness $t = 1.5$ mm. s.s. wall $\sigma_c = 1.35 \times 10^6$ $(\Omega\text{-m})^{-1}$.
- Skin depth fills pipe wall at $f_c = 83.4$ Hz ($kb = 5.24 \times 10^{-5}$).
- Bend-around between $kb \sim \dfrac{4}{Z_0\sigma_c b} = 2.6\times 10^{-7}$ ($f \sim 0.4$ kHz)

  and $kb \sim \dfrac{2}{Z_0\sigma_c t} = 2.6\times 10^{-6}$ ($f \sim 4.2$ kHz)
- $\nu_y = 19.6$ and $(1-Q)$ line at 19.1 kHz ($kb = 1.2$).

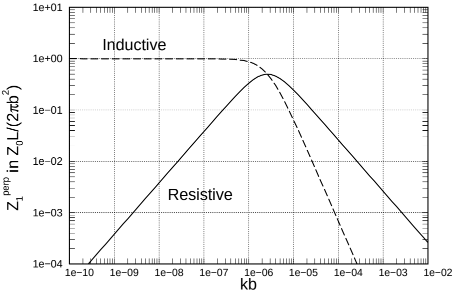

thin-wall model ($t \ll \delta_c$)

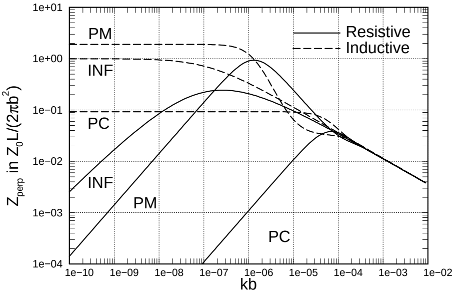

thick-wall model

Comments

- It appears that $f_{\rm bend}$ depends on σ_c, b, and t only, and not on size and energy of ring.

  $f_{\rm bend} \sim 0.4$ to 4 kHz.

- Unless $f_{\rm bend} \sim f_0$, low ω region is of no importance at all.

Comments

- It appears that $f_{\rm bend}$ depends on σ_c, b, and t only, and not on size and energy of ring.

  $f_{\rm bend} \sim 0.4 \text{ to } 4 \text{ kHz}$.

- Unless $f_{\rm bend} \sim f_0$, low ω region is of no importance at all.

- Tevatron: $f_0 = 47.7 \text{ kHz} \gg f_{\rm bend}$.

  LHC: $f_0 = 11.3$ kHz, may start to see effect of the bend-around region.

  VLHC: $f_0 = 1.3$ kHz $\Longrightarrow$ $(1-Q)$ driving sideband will be inside low-ω region.

Comments

- It appears that $f_{\rm bend}$ depends on σ_c, b, and t only, and not on size and energy of ring.
  $f_{\rm bend} \sim 0.4 \text{ to } 4 \text{ kHz}$.
- Unless $f_{\rm bend} \sim f_0$, low ω region is of no importance at all.
- Tevatron: $f_0 = 47.7 \text{ kHz} \gg f_{\rm bend}$.
  LHC: $f_0 = 11.3$ kHz, may start to see effect of the bend-around region.
  VLHC: $f_0 = 1.3$ kHz $\Longrightarrow (1 - Q)$ driving sideband will be inside low-ω region.
- Will show later that low-ω region is important to Booster.
- First let us review some measurement of $Z_1^\perp$ at low ω by Mostacci *et al*. Measurement was performed to understand low ω effect to LHC.

Direct Measurement of $Z_1^\perp(\omega)$ [12]

- Current I was passed into a N-turn loop $L_w = 1.25$ m long and $\Delta = 2.25$ cm wide, inside a s.s. beam pipe of length $L = 50$ cm and radius $b = 5$ cm, wall thickness $t = 1.5$ mm.

Direct Measurement of $Z_1^\perp(\omega)$ [12]

- Current I was passed into a N-turn loop $L_w = 1.25$ m long and $\Delta = 2.25$ cm wide, inside a s.s. beam pipe of length $L = 50$ cm and radius $b = 5$ cm, wall thickness $t = 1.5$ mm.
- $I_{\rm im} \to B \to V$ on loop thru imp. $Z_{\rm pipe}$ of pipe.

  Then $Z_1^\perp\Big|_{\rm RW} = \dfrac{c}{\omega}\dfrac{Z_{\rm pipe} - Z_{\rm PC}}{N^2\Delta^2}$, where $Z_{\rm PC}$ is same as $Z_{\rm pipe}$ but with a perfectly conducting pipe instead.

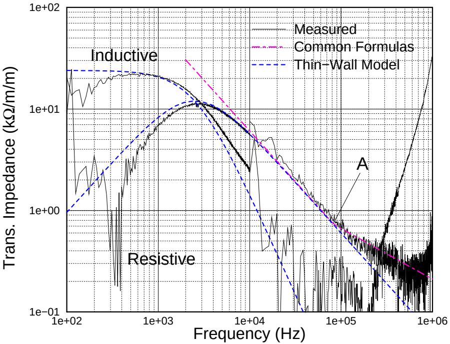

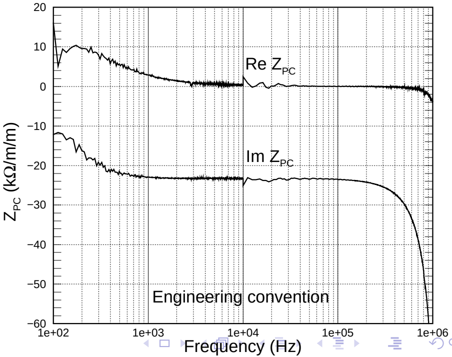

Comments on Measurement

- $N = 10$ was chosen as a compromise to improve signal and to keep lowest self-resonance above 1 MHz.

Comments on Measurement

- $N = 10$ was chosen as a compromise to improve signal and to keep lowest self-resonance above 1 MHz.
- A dipole particle beam sees both magnetic and electric images in wall. The two cancelled when $\gamma \to \infty$.
- The dipole current loop sees only magnetic image but not electric. This magnetic contribution must be subtracted, leaving us with the $Z_1^\perp$ we are after.

Comments on Measurement

- $N = 10$ was chosen as a compromise to improve signal and to keep lowest self-resonance above 1 MHz.
- A dipole particle beam sees both magnetic and electric images in wall. The two cancelled when $\gamma \to \infty$.
- The dipole current loop sees only magnetic image but not electric. This magnetic contribution must be subtracted, leaving us with the $Z_1^\perp$ we are after.
- A perfectly (PC) conducting pipe will just produce this magnetic contribution. So such a subtraction is necessary.
- Actually a copper pipe was used as PC.
  $\sigma_{c\,\mathrm{Cu}} = 5.88 \times 10^7\ (\Omega\mathrm{m})^{-1}$
  $\sigma_{c\,\mathrm{SS}} = 1.35 \times 10^5\ (\Omega\mathrm{m})^{-1}$ $\qquad (\sigma_{c\,\mathrm{Cu}}/\sigma_{c\,\mathrm{SS}} = 44)$
- Measured impedance for copper pipe:
  $\mathcal{R}e\, Z_1^\perp$ almost zero because of small resistivity.
  $$\frac{\mathcal{I}m\, Z_1^\perp}{L} = \frac{iZ_0}{2\pi b^2} = i23\ \Omega/\mathrm{m}/\mathrm{m}. \qquad \text{(capacitive)}$$

Laminations [13, 14]

- The beam sometimes sees a laminated surface rather than a smooth one, like Lambertson magnets and laminated combined-fcn magnets.
- These surfaces can be approximated as

  2 parallel laminated plates

  or

  a laminated annular ring.

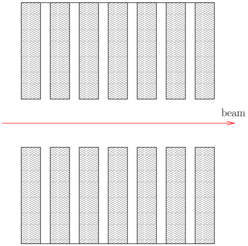

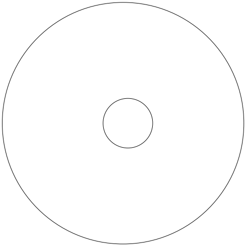

- Want to compute the impedance seen by the beam.

	crack	lamination
Width or thickness	$h=0.000375''$	$\tau=0.025''$
Relative mag. suseptibility	$\mu_{1r}=1$	$\mu_{2r}=100$
Relative dielectric	$\epsilon_{1r}=4.75$	$\epsilon_{2r}=1$
Conductivity	$\sigma_{c1}=1.0\times10^{-3}$ $(\Omega\text{-m})^{-1}$	$\sigma_{c2}=0.5\times10^{7}$ $(\Omega\text{-m})^{-1}$

Crack Impedance

- Solve Maxwell eq.
  $$\frac{1}{r}\frac{\partial}{\partial r}\left(r\frac{\partial E_z}{\partial r}\right)+q^2E_z=0$$
  to get E_z across crack
  and then surface imp. $\mathcal{R}_c$.

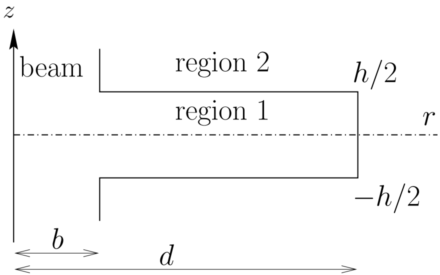

Crack Impedance

- Solve Maxwell eq.
  $$\frac{1}{r}\frac{\partial}{\partial r}\left(r\frac{\partial E_z}{\partial r}\right)+q^2E_z=0$$
  to get E_z across crack
  and then surface imp. $\mathcal{R}_c$.

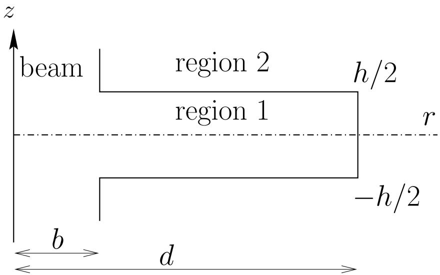

- Solution for annular-ring model
  $$\frac{\mathcal{R}_c}{Z_0}=-\frac{E_z(b)}{Z_0H_\theta(b)}=\frac{-iqc}{\epsilon_{1r}\omega}\frac{J_0(qb)N_0(qd)-N_0(qb)J_0(qd)}{J_1(qb)N_0(qd)-N_1(qb)J_0(qd)}\,,$$
  with $q^2=k_\ell^2+g_\ell^2,\quad \ell=1,2,$ and $\epsilon_\ell\rightarrow\epsilon_0\left(\epsilon_{\ell r}+\dfrac{\sigma_{\ell c}}{i\omega\mu_\ell\epsilon_0}\right)$.

- q is trans. wave numbers, $k_1^2=\omega^2\mu_1\epsilon_1,\quad k_2^2=\omega^2\mu_2\epsilon_2=\dfrac{2i}{\delta_{2c}^2}$.

- Longitudinal decrement: $g_1=(1+i)k_1^2\dfrac{\mu_2}{\mu_1}\dfrac{\delta_{2c}}{h},\quad g_2\sim\dfrac{1-i}{\delta_{2c}}$.

Low-Frequency Behavior

- At low $\omega > 0$, use small-argument expansion to get
$$\frac{\mathcal{R}_c}{Z_0} \to (1-i)\frac{\omega\delta_{2c}b}{ch}\mu_{2r}\ln\frac{d}{b}$$
- This can be shown to be imp. seen by $I_{\rm im}$ going in and out of crack penetrating δ_{2c} into laminations.
- The model is therefore good when lamination thickness $\tau > \delta_{2c}$, or when $f \ge \dfrac{c}{\pi Z_0\sigma_{2c}\mu_{2r}\tau^2} = 1.26$ kHz.

Low-Frequency Behavior

- At low $\omega > 0$, use small-argument expansion to get
  $$\frac{\mathcal{R}_c}{Z_0} \to (1-i)\frac{\omega\delta_{2c}b}{ch}\mu_{2r}\ln\frac{d}{b}$$
- This can be shown to be imp. seen by $I_{\rm im}$ going in and out of crack penetrating δ_{2c} into laminations.
- The model is therefore good when lamination thickness $\tau > \delta_{2c}$, or when $f \ge \dfrac{c}{\pi Z_0\sigma_{2c}\mu_{2r}\tau^2} = 1.26$ kHz.
- For bend-around of $Z_1^\perp$, compare with bypass ind. $Z_{\rm bypass} = \dfrac{\omega Z_0}{4\pi c}$, or $\left|(1-i)\dfrac{2\delta_{2c}\mu_{2r}}{\tau}\ln\dfrac{d}{b}\right| \sim 1.$
- For $b = 1.25''$ and $d = 6''$, get $f_{\rm bend} \sim 250$ MHz. (~ 100 MHz in actual computation).
- Small-argument expansion good for $f \ll 5\ MHz$.

High-Freqency Behavior

At high ω, large-argument expansions of $H_0^{(1),(2)}$ and $H_1^{(1),(2)}$ give

$$\frac{\mathcal{R}_c}{Z_0} = \frac{jqc}{\epsilon_{1r}\omega}\tan q(d-b).$$

Like a cavity, but filled with dissipative medium.

Resonances will be damped, except maybe the first one.

The crack also acts like a capacitance in parallel with surface impedance.

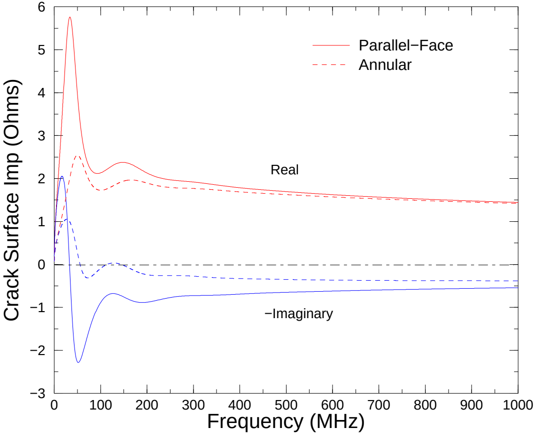

High ω, $I_{\rm im}$ flows across crack as displacement current more easily.

But at low ω, $I_{\rm im}$ has to flow thru surfaces of each crack; expect large imp.

Application to Booster

- Booster consists of 48 F and 48 D laminated magnets.
  Vertical gap: $2b = 1.64''$ (F) and $2b = 2.25''$ (D).
  Magnet height: $2d = 12''$.
- Calculation and Measurement [15] of $Z_0^{\parallel}$ of 96 Booster magnets:
  ($ImZ > 0$ implies inductive)

Theory

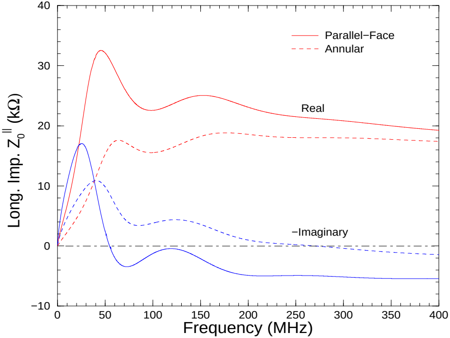

Crisp's Measurement

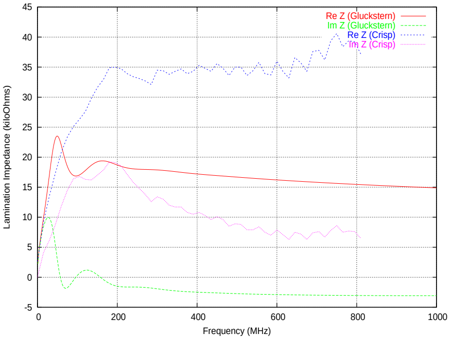

- Measurement was made by Crisp using a current in a wire.

Z_1^V of Booster Lamination Magnets

- See inductive bypass at low freq.
- $\mathcal{R}e\, Z_1^V$ bends around $\sim$ 70 MHz
- No $\omega^{-1/2}$ behavior at low freq.
  Broad-band from 70 MHz to 200 MHz.

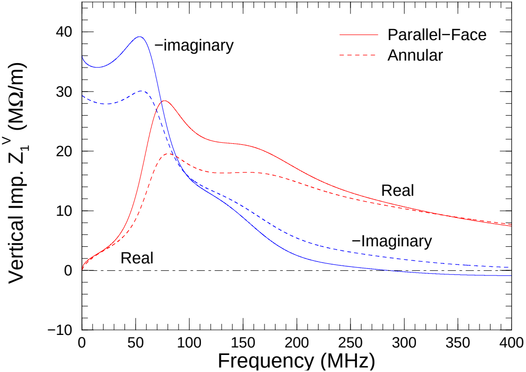

- Relatively high bend-around freq. is result of high lamination imp.
- Will not drive trans. coupled bunch instabilities.
- Since $|Z_1^V|$ is large ($\sim 20\ \mathrm{M}\Omega/\mathrm{m}$), will drive head-tail instabilities.

Beam Pipe Contribution

- Lamination magnets cover $\sim 60\%$ of the Booster ring, leaving $\sim 40\%$ with beam pipes.
- These s.s. beam pipes will exhibit $\omega^{-1/2}$ behavior near revolution frequency, and will drive coupled-bunch instabilities.

Beam Pipe Contribution

- Lamination magnets cover $\sim 60\%$ of the Booster ring, leaving $\sim 40\%$ with beam pipes.
- These s.s. beam pipes will exhibit $\omega^{-1/2}$ behavior near revolution frequency, and will drive coupled-bunch instabilities.
- 6-m long straight section joining 2 D-magnets: 2.25" s.s. pipe
  1.2-m short straight section joining 2 F-magnets: 4.25" s.s. pipe
  0.5-m straight joining D- and F-magnets: 2.25" s.s. pipe.
- These pipes amount to $Z_1^V\Big|_{\rm RW} = (1-i)\dfrac{0.20}{\sqrt{n}}\ \mathrm{M\Omega/m}$.

Beam Pipe Contribution

- Lamination magnets cover $\sim 60\%$ of the Booster ring, leaving $\sim 40\%$ with beam pipes.
- These s.s. beam pipes will exhibit $\omega^{-1/2}$ behavior near revolution frequency, and will drive coupled-bunch instabilities.
- 6-m long straight section joining 2 D-magnets: 2.25" s.s. pipe
  1.2-m short straight section joining 2 F-magnets: 4.25" s.s. pipe
  0.5-m straight joining D- and F-magnets: 2.25" s.s. pipe.
- These pipes amount to $Z_1^V\Big|_{\rm RW} = (1-i)\dfrac{0.20}{\sqrt{n}}\ \mathrm{M\Omega/m}$.
- For $\nu_y = 6.7$, they can drive the $(1-Q)$ mode with growth rate 337 s^{-1} ($\tau = 3.0$ ms) at injection energy (400 MeV).

Beam Pipe Contribution

- Lamination magnets cover $\sim 60\%$ of the Booster ring, leaving $\sim 40\%$ with beam pipes.
- These s.s. beam pipes will exhibit $\omega^{-1/2}$ behavior near revolution frequency, and will drive coupled-bunch instabilities.
- 6-m long straight section joining 2 D-magnets: 2.25" s.s. pipe
  1.2-m short straight section joining 2 F-magnets: 4.25" s.s. pipe
  0.5-m straight joining D- and F-magnets: 2.25" s.s. pipe.
- These pipes amount to $Z_1^{\rm V}\big|_{\rm RW} = (1-i)\dfrac{0.20}{\sqrt{n}}\ \mathrm{M\Omega/m}$.
- For $\nu_y = 6.7$, they can drive the $(1-Q)$ mode with growth rate $337\ \mathrm{s}^{-1}$ ($\tau = 3.0$ ms) at injection energy (400 MeV).
- Chromaticity is ineffective in shifting power spectrum because of large $\eta = -0.458$.
- However, during the ramp, growth rate decreases (with E^{-1}) $|\eta|$ becomes smaller, making chromaticity more effective.
- Thus transverse coupled-bunch instabilities can only be appreciable near injection.

Lambertson Magnets in Tevatron

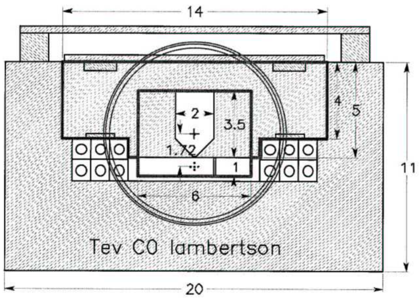

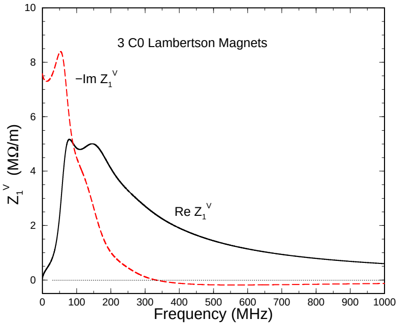

- During 2003 shutdown, 3 C0 Lambertsons for fixed target beam extractions were removed.
- These magnets served as dipoles with beam passing thru the narrow 1" gap.
- They will not drive transverse coupled-bunch instabilities, but head-tail instabilities.

Lambertson Magnets F0 in Tevatron

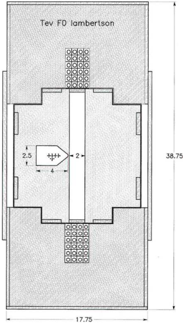

- There are 4 F0 Lambertsons in Tevatron.
- Unlike the C0's, beam is in field-free region during storage (vertical gap$\sim 2.5''$).
- Can compute Z_1^V by approx. as annular magnet.
- Result is an order of mag. less than the C0's.
- Z_1^V had been measured by Crisp and Fellenz. [16]

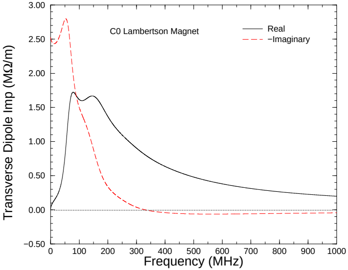

- Attenuation S_{21} was measured along 2 parallel wires driven differentially.
- The wires, $\Delta = 1.0$ cm apart, form a TEM balanced transmission line, matched to 100 Ω with resistive L-pads and driven with a 100 Ω broadband 180° hybrid splitter.
- Imp. computed from $Z_1^V = -\dfrac{c}{\omega\Delta^2} 2Z_c \ln S_{21}$
- Agreement of $\mathcal{I}m\, Z_1^V$ are good, but much smaller for the plateau region.

Betatron Tune Shift in Booster

- Betatron tune shifts were measured in Booster by X. Huang in 2008, at 2, 4, 6, 8, 20-turn injection. [17]
- A pinger was turned on every 0.5 ms with 2-μs width for whole cycle.
- Each segment of data, $\sim$ 0.5 ms long (225 to 200 turns), are analyzed for coherent motion.

Betatron Tune Shift in Booster

- Betatron tune shifts were measured in Booster by X. Huang in 2008, at 2, 4, 6, 8, 20-turn injection. [17]
- A pinger was turned on every 0.5 ms with 2-μs width for whole cycle.
- Each segment of data, $\sim$ 0.5 ms long (225 to 200 turns), are analyzed for coherent motion.
- Betatron oscillation modes were solved using ICA, and ν_y was computed from FFT.
- ICA routine increases accuracy of measurement because all BPM data are used.
- Only data up to transition are used, because of lack of H-V coupling while pinger kicks horizontally.

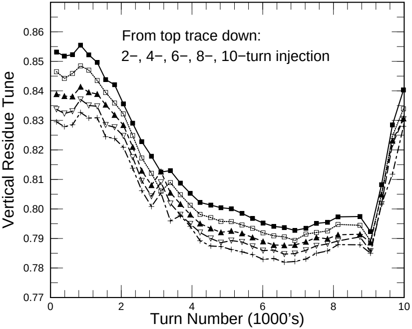

What Should be Included in $\mathcal{I}m\, Z_1^V$?

- Assuming Gaussian distribution, $\Delta\nu_y\Big|_{\rm dyn} = \dfrac{e^2 N_b R}{8\pi^{3/2}\beta E_0 \nu_y \sigma_\tau}\, \mathcal{I}m\, Z_1^V\Big|_{\rm eff}$.
- Effective imp.: $\mathcal{I}m\, Z_1^V\Big|_{\rm eff} = \dfrac{\displaystyle\int_{-\infty}^{\infty}\frac{d\omega}{2\pi} Z_1^V(\omega) e^{-\omega^2\sigma_\tau^2}}{\displaystyle\int_{-\infty}^{\infty}\frac{d\omega}{2\pi} e^{-\omega^2\sigma_\tau^2}}$.

What Should be Included in $\mathcal{I}m\, Z_1^V$?

- Assuming Gaussian distribution, $\Delta\nu_y\Big|_{\rm dyn} = \dfrac{e^2 N_b R}{8\pi^{3/2}\beta E_0 \nu_y \sigma_\tau}\,\mathcal{I}m\, Z_1^V\Big|_{\rm eff}$.
- Effective imp.: $\mathcal{I}m\, Z_1^V\Big|_{\rm eff} = \dfrac{\displaystyle\int_{-\infty}^{\infty}\frac{d\omega}{2\pi} Z_1^V(\omega) e^{-\omega^2\sigma_\tau^2}}{\displaystyle\int_{-\infty}^{\infty}\frac{d\omega}{2\pi} e^{-\omega^2\sigma_\tau^2}}$.
- To compare with experiment, we must compute $\Delta\nu_y\Big|_{\rm coh} = \Delta\nu_y\Big|_{\rm dyn} + \Delta\nu_y\Big|_{\rm incoh}$
- What should be included in $\mathcal{I}m\, Z_1^V\Big|_{\rm eff}$?

What Should be Included in $\mathcal{I}m\, Z_1^V$?

- Assuming Gaussian distribution, $\Delta\nu_y\big|_{\rm dyn} = \dfrac{e^2 N_b R}{8\pi^{3/2}\beta E_0 \nu_y \sigma_\tau}\, \mathcal{I}m\, Z_1^V\Big|_{\rm eff}$.
- Effective imp.: $\mathcal{I}m\, Z_1^V\Big|_{\rm eff} = \dfrac{\displaystyle\int_{-\infty}^{\infty} \frac{d\omega}{2\pi} Z_1^V(\omega) e^{-\omega^2\sigma_\tau^2}}{\displaystyle\int_{-\infty}^{\infty} \frac{d\omega}{2\pi} e^{-\omega^2\sigma_\tau^2}}$.
- To compare with experiment, we must compute $\Delta\nu_y\big|_{\rm coh} = \Delta\nu_y\big|_{\rm dyn} + \Delta\nu_y\big|_{\rm incoh}$
- What should be included in $\mathcal{I}m\, Z_1^V\Big|_{\rm eff}$?
- Consider $\mathcal{I}m\, Z_1^V\Big|_{\rm SC} = \dfrac{Z_0}{\pi\beta^2\gamma^2} \displaystyle\sum_i L_i \left[\frac{\epsilon_{sc}^V}{a_{vi}^2} - \frac{\xi_1^V - \epsilon_1^V}{h_i^2}\right]$.
- Self-field part is cancelled by adding $\Delta\nu_y\big|_{\rm incoh}^{\rm self}$.
  ϵ_1^V-part is cancelled by adding the incoherent part.
- So only ξ_1^V-part should be included.
  This is the coherent wall image contribution.

The Coherent Wall Image Contribution

- Coherent wall-image consists of $\dfrac{\xi_1^v}{h_i^2\gamma^2} = \dfrac{\xi_1^v}{h_i^2} - \beta^2\dfrac{\xi_1^v}{h_i^2}$ the electric and magnetic contributions.
- Beam pipe will contribute $\mathcal{I}m\, Z_1^v \sim 24\ \mathrm{M\Omega/m}$.

The Coherent Wall Image Contribution

- Coherent wall-image consists of $\dfrac{\xi_1^v}{h_i^2\gamma^2} = \dfrac{\xi_1^v}{h_i^2} - \beta^2 \dfrac{\xi_1^v}{h_i^2}$
  the electric and magnetic contributions.
- Beam pipe will contribute $\mathcal{I}m\, Z_1^v \sim 24\ \mathrm{M\Omega/m}$.
- Lamination surface is not perfect conductor, electric image may form at back of laminations $\bar{h}_i \sim 8'' \gg h_{i\,\mathrm{gap}}$.
- We write $\dfrac{\xi_1^v}{h_i^2\gamma^2} \to \dfrac{\xi_1^v}{\bar{h}_i^2} + \beta^2 \dfrac{\xi_2^v}{h_i^2}$.
- $\xi_1^v \to \xi_2^v, \ -\beta^2 \to +\beta^2$ because of image in magnetic surface.
- We have then $Z_1^v\Big|_{\mathrm{mag}} = \dfrac{Z_0 \xi_2^v}{\pi} \displaystyle\sum_i \dfrac{L_i}{h_i^2}$.

The Coherent Wall Image Contribution

- Coherent wall-image consists of $\dfrac{\xi_1^v}{h_i^2\gamma^2} = \dfrac{\xi_1^v}{h_i^2} - \beta^2\dfrac{\xi_1^v}{h_i^2}$ the electric and magnetic contributions.
- Beam pipe will contribute $\mathcal{I}m\, Z_1^v \sim 24\ \mathrm{M\Omega/m}$.
- Lamination surface is not perfect conductor, electric image may form at back of laminations $\bar{h}_i \sim 8'' \gg h_{i\mathrm{gap}}$.
- We write $\dfrac{\xi_1^v}{h_i^2\gamma^2} \to \dfrac{\xi_1^v}{\bar{h}_i^2} + \beta^2\dfrac{\xi_2^v}{h_i^2}$.
- $\xi_1^v \to \xi_2^v, \ -\beta^2 \to +\beta^2$ because of image in magnetic surface.
- We have then $Z_1^v\big|_{\mathrm{mag}} = \dfrac{Z_0\xi_2^v}{\pi}\sum_i \dfrac{L_i}{h_i^2}$.
- This still has problems, since laminated surface is not perfect magnetic surface. Cracks and laminations become more apparent at high freq.
- More appropriate representation is what we have computed of Z_1^V for laminated surface. When $\omega \to 0$, beam sees bypass inductance. Higher frequency, beam sees laminations.

Compare with Measurement [18]

- Other contributions including BPM's, bellows,steps, etc. are small.
  E.g., they contribute to only ~ 0.4 MΩ/m in Tevatron up to 200 MHz.

Compare with Measurement [18]

- Other contributions including BPM's, bellows,steps, etc. are small. E.g., they contribute to only ~ 0.4 MΩ/m in Tevatron up to 200 MHz.
- $\mathcal{I}m\, Z_1^V$ is computed from tune-shift measurement and compared with calculated dipole imp.

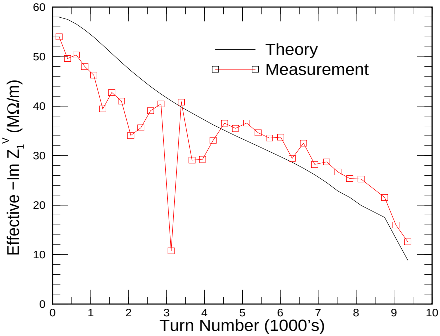

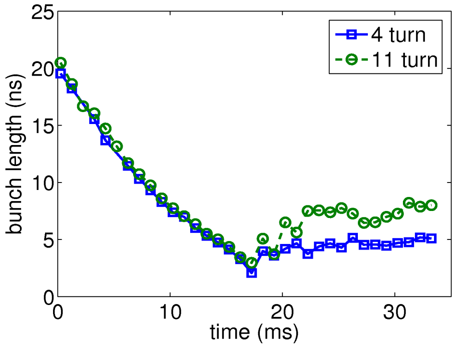

- Data point near 3000 turns involves error and should be excluded.
- Agreement is satisfactory, although not perfect.

Strip-Line BPM [19]

- Tevatron is equipped with strip-line BPM's terminated at both ends.
- Strip line and extruded beam pipe forms a transmission line of $Z_s = 50\ \Omega$.
- 2 terminations are also of Z_s.
- We will see, for a short pulse ($\ll \ell$),
  - front termination registers a positive pulse followed by by a negative pulse
  - rear termination registers nothing

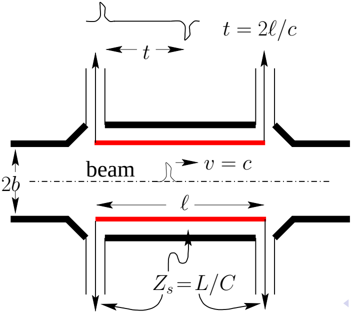

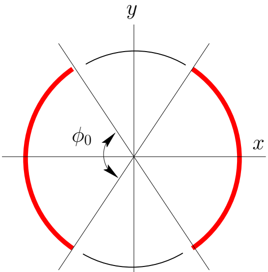

- Then $Z_0^{\parallel}$ and $Z_1^{\perp}$ are derived.

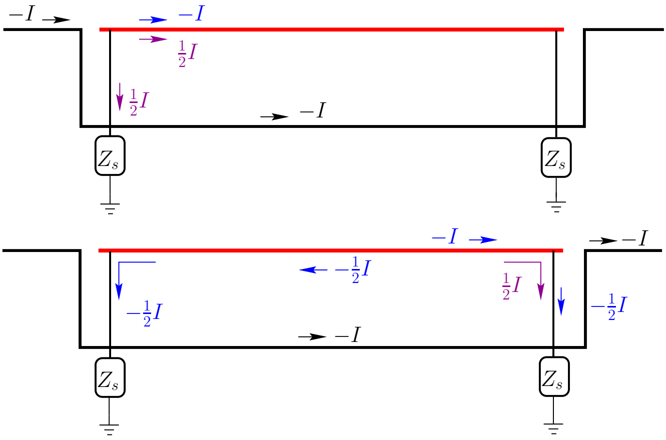

$$V_u(t) = \frac{Z_s}{2}\left(\frac{\phi_0}{2\pi}\right)\left[I(t) - I\left(t - \frac{\ell}{\beta c} - \frac{\ell}{\beta_s c}\right)\right]$$

$$V_d(t) = \frac{Z_s}{2}\left(\frac{\phi_0}{2\pi}\right)\left[I\left(t - \frac{\ell}{\beta_s c}\right) - I\left(t - \frac{\ell}{\beta c}\right)\right]$$

β is particle velocity
β_s is transmission line velocity

Strip-Line Longitudinal Impedances

- For a beam current $I(t) = I_0 e^{-i\omega t}$, $V_u(\omega) = \frac{Z_s}{2}\left(\frac{\phi_0}{2\pi}\right) I_0 \left(1 - e^{i2\omega\ell/\beta c}\right)$.

Strip-Line Longitudinal Impedances

- For a beam current $I(t) = I_0 e^{-i\omega t}$, $V_u(\omega) = \dfrac{Z_s}{2}\left(\dfrac{\phi_0}{2\pi}\right) I_0 \left(1 - e^{i2\omega\ell/\beta c}\right)$.
- Voltage seen by beam is $V_b(\omega) = \left(\dfrac{\phi_0}{2\pi}\right) V_u(\omega)$,

  since only a fraction of beam sees the gap.

Strip-Line Longitudinal Impedances

- For a beam current $I(t) = I_0 e^{-i\omega t}$, $V_u(\omega) = \dfrac{Z_s}{2}\left(\dfrac{\phi_0}{2\pi}\right) I_0 \left(1 - e^{i2\omega\ell/\beta c}\right)$.
- Voltage seen by beam is $V_b(\omega) = \left(\dfrac{\phi_0}{2\pi}\right) V_u(\omega)$,

  since only a fraction of beam sees the gap.
- Long. imp.: $Z_0^{\parallel}\Big|_{BPM} = \dfrac{V_b(\omega)}{I_0} = Z_s\left(\dfrac{\phi_0}{2\pi}\right)^2 \left(\sin^2\dfrac{\omega\ell}{\beta c} - i\sin\dfrac{\omega\ell}{\beta c}\cos\dfrac{\omega\ell}{\beta c}\right)$.

Strip-Line Longitudinal Impedances

- For a beam current $I(t) = I_0 e^{-i\omega t}$, $V_u(\omega) = \dfrac{Z_s}{2}\left(\dfrac{\phi_0}{2\pi}\right) I_0 \left(1 - e^{i2\omega\ell/\beta c}\right)$.
- Voltage seen by beam is $V_b(\omega) = \left(\dfrac{\phi_0}{2\pi}\right) V_u(\omega)$,
  since only a fraction of beam sees the gap.
- Long. imp.: $Z_0^{\parallel}\Big|_{BPM} = \dfrac{V_b(\omega)}{I_0} = Z_s \left(\dfrac{\phi_0}{2\pi}\right)^2 \left(\sin^2\dfrac{\omega\ell}{\beta c} - i\sin\dfrac{\omega\ell}{\beta c}\cos\dfrac{\omega\ell}{\beta c}\right)$.
- Low freq.: purely inductive $\quad Z_0^{\parallel}\Big|_{BPM} \longrightarrow -iZ_s\left(\dfrac{\phi_0}{2\pi}\right)^2\dfrac{\omega\ell}{\beta c}$.
- After $\omega > \dfrac{\pi\beta c}{2\ell}$, $\; Z_0^{\parallel}\big|_{BPM}$ alternates between capacitive and inductive.
- There is no resonance at all, which is the merit of this BPM.
  However, this BPM is not so linear as the diagonal-cut one.
- Power dissipated is $P(\omega) = \dfrac{|V_u(\omega)|^2}{2Z_s}$.

Strip-Line Transverse Impedance

- When beam I_0 is offset by Δ horizontally, surface current density on beam pipe is $J(\theta; x_0) = -\dfrac{I_0 \Delta \cos\theta}{\pi b^2}$.

Strip-Line Transverse Impedance

- When beam I_0 is offset by Δ horizontally, surface current density on beam pipe is $J(\theta; x_0) = -\dfrac{I_0 \Delta \cos\theta}{\pi b^2}$.
- Total current on right/left: $I_{R/L} = \mp \displaystyle\int_{-\phi_0/2}^{\phi_0/2} \frac{I_0 \Delta \cos\theta}{\pi b^2} b d\theta = \mp \frac{2 I_0 \Delta}{\pi b} \sin\frac{\phi_0}{2}$.

Strip-Line Transverse Impedance

- When beam I_0 is offset by Δ horizontally, surface current density on beam pipe is $J(\theta;x_0) = -\dfrac{I_0\Delta\cos\theta}{\pi b^2}$.
- Total current on right/left: $I_{R/L} = \mp\displaystyle\int_{-\phi_0/2}^{\phi_0/2}\frac{I_0\Delta\cos\theta}{\pi b^2}\,bd\theta = \mp\frac{2I_0\Delta}{\pi b}\sin\frac{\phi_0}{2}$.
- Voltage at right/left gap: $V_{R/L} = \pm Z_s\dfrac{I_0\Delta}{\pi b}\sin\dfrac{\phi_0}{2}\left(1 - e^{i2\omega\ell/\beta c}\right)$.

Strip-Line Transverse Impedance

- When beam I_0 is offset by Δ horizontally, surface current density on beam pipe is $J(\theta; x_0) = -\dfrac{I_0 \Delta \cos\theta}{\pi b^2}$.
- Total current on right/left: $I_{R/L} = \mp \displaystyle\int_{-\phi_0/2}^{\phi_0/2} \frac{I_0 \Delta \cos\theta}{\pi b^2} b d\theta = \mp \frac{2 I_0 \Delta}{\pi b} \sin\frac{\phi_0}{2}$.
- Voltage at right/left gap: $V_{R/L} = \pm Z_s \dfrac{I_0 \Delta}{\pi b} \sin\dfrac{\phi_0}{2} \left(1 - e^{i2\omega\ell/\beta c}\right)$.
- Power dissipated: $P = \dfrac{1}{2Z_s}(|V_L|^2 + |V_R|^2) = 4 Z_s \left(\dfrac{|I_0|\Delta}{\pi b}\right)^2 \sin^2\dfrac{\phi_0}{2} \sin^2\dfrac{\omega\ell}{\beta c}$.

Strip-Line Transverse Impedance

- When beam I_0 is offset by Δ horizontally, surface current density on beam pipe is $J(\theta;x_0)=-\dfrac{I_0\Delta\cos\theta}{\pi b^2}$.
- Total current on right/left: $I_{R/L}=\mp\displaystyle\int_{-\phi_0/2}^{\phi_0/2}\frac{I_0\Delta\cos\theta}{\pi b^2}bd\theta=\mp\frac{2I_0\Delta}{\pi b}\sin\frac{\phi_0}{2}$.
- Voltage at right/left gap: $V_{R/L}=\pm Z_s\dfrac{I_0\Delta}{\pi b}\sin\dfrac{\phi_0}{2}\left(1-e^{i2\omega\ell/\beta c}\right)$.
- Power dissipated: $P=\dfrac{1}{2Z_s}(|V_L|^2+|V_R|^2)=4Z_s\left(\dfrac{|I_0|\Delta}{\pi b}\right)^2\sin^2\dfrac{\phi_0}{2}\sin^2\dfrac{\omega\ell}{\beta c}$.
- This power loss is also $P=\dfrac{1}{2}(|I_0|\Delta)^2\,\mathcal{R}e\,Z_1^{\parallel}\Big|_{BPM}$.

Strip-Line Transverse Impedance

- When beam I_0 is offset by Δ horizontally, surface current density on beam pipe is $J(\theta; x_0) = -\dfrac{I_0 \Delta \cos\theta}{\pi b^2}$.
- Total current on right/left: $I_{R/L} = \mp \displaystyle\int_{-\phi_0/2}^{\phi_0/2} \frac{I_0 \Delta \cos\theta}{\pi b^2} b d\theta = \mp \frac{2 I_0 \Delta}{\pi b} \sin\frac{\phi_0}{2}$.
- Voltage at right/left gap: $V_{R/L} = \pm Z_s \dfrac{I_0 \Delta}{\pi b} \sin\dfrac{\phi_0}{2} \left(1 - e^{i2\omega\ell/\beta c}\right)$.
- Power dissipated: $P = \dfrac{1}{2Z_s}(|V_L|^2 + |V_R|^2) = 4 Z_s \left(\dfrac{|I_0|\Delta}{\pi b}\right)^2 \sin^2\dfrac{\phi_0}{2} \sin^2\dfrac{\omega\ell}{\beta c}$.
- This power loss is also $P = \dfrac{1}{2}(|I_0|\Delta)^2 \mathcal{R}e\, Z_1^{\parallel}\Big|_{BPM}$.
- Panofsky-Wenzel $\longrightarrow$ $\mathcal{R}e\, Z_1^{H}\Big|_{BPM} = \dfrac{8 Z_s}{\pi^2 b^2} \dfrac{c}{\omega} \sin^2\dfrac{\phi_0}{2} \sin^2\dfrac{\omega\ell}{\beta c}$.

Strip-Line Transverse Impedance

- When beam I_0 is offset by Δ horizontally, surface current density on beam pipe is $J(\theta;x_0) = -\dfrac{I_0\Delta\cos\theta}{\pi b^2}$.
- Total current on right/left: $I_{R/L} = \mp\displaystyle\int_{-\phi_0/2}^{\phi_0/2}\frac{I_0\Delta\cos\theta}{\pi b^2}b\,d\theta = \mp\frac{2I_0\Delta}{\pi b}\sin\frac{\phi_0}{2}$.
- Voltage at right/left gap: $V_{R/L} = \pm Z_s\dfrac{I_0\Delta}{\pi b}\sin\dfrac{\phi_0}{2}\left(1-e^{i2\omega\ell/\beta c}\right)$.
- Power dissipated: $P = \dfrac{1}{2Z_s}(|V_L|^2+|V_R|^2) = 4Z_s\left(\dfrac{|I_0|\Delta}{\pi b}\right)^2\sin^2\dfrac{\phi_0}{2}\sin^2\dfrac{\omega\ell}{\beta c}$.
- This power loss is also $P = \dfrac{1}{2}(|I_0|\Delta)^2\,\mathcal{R}e\,Z_1^{\parallel}\Big|_{BPM}$.
- Panofsky-Wenzel $\longrightarrow$ $\mathcal{R}e\,Z_1^H\Big|_{BPM} = \dfrac{8Z_s}{\pi^2b^2}\dfrac{c}{\omega}\sin^2\dfrac{\phi_0}{2}\sin^2\dfrac{\omega\ell}{\beta c}$.
- Hilbert transform $\longrightarrow$ $Z_1^H\Big|_{BPM} = \dfrac{c}{b^2}\left(\dfrac{4}{\phi_0}\right)^2\sin^2\dfrac{\phi_0}{2}\dfrac{Z_0^{\parallel}\Big|_{BPM}}{\omega}$.

- Some may have doubt about derivation via $Z_1^{\|}$ because
  1. cylindrical symmetry is broken by strip-lines
  2. P-W relation requires cylindrical symmetry.

- Some may have doubt about derivation via $Z_1^{\parallel}$ because

  1. cylindrical symmetry is broken by strip-lines
  2. P-W relation requires cylindrical symmetry.

- The dipole current loop $I_0\Delta$ links mag. flux and I_0 sees an imp. $\mathcal{Z}$.

  Faraday Law: $i\omega B_y L\Delta = \mathcal{Z} I_0$. ($L =$ length of loop)

- Some may have doubt about derivation via $Z_1^{\|}$ because
  1. cylindrical symmetry is broken by strip-lines
  2. P-W relation requires cylindrical symmetry.
- The dipole current loop $I_0\Delta$ links mag. flux and I_0 sees an imp. $\mathcal{Z}$.
  Faraday Law: $i\omega B_y L\Delta = \mathcal{Z} I_0$. ($L =$ length of loop)
- Trans. imp. is $Z_1^H = \dfrac{LvB_y}{iI_0\Delta\beta} = \dfrac{c\mathcal{Z}}{\omega\Delta^2}$.

- Some may have doubt about derivation via $Z_1^{\|}$ because
  1. cylindrical symmetry is broken by strip-lines
  2. P-W relation requires cylindrical symmetry.
- The dipole current loop $I_0\Delta$ links mag. flux and I_0 sees an imp. $\mathcal{Z}$.
  Faraday Law: $i\omega B_y L\Delta = \mathcal{Z} I_0$. ($L =$ length of loop)
- Trans. imp. is $Z_1^H = \dfrac{LvB_y}{iI_0\Delta\beta} = \dfrac{c\mathcal{Z}}{\omega\Delta^2}$.
- $\mathcal{Z}$ can be evaluated from

$$P = \frac{1}{2}|I_0|^2\mathcal{Z} = 4Z_s\left(\frac{|I_0|\Delta}{\pi b}\right)^2 \sin^2\frac{\phi_0}{2}\sin^2\frac{\omega\ell}{\beta c}.$$

- Get $\mathcal{R}e\, Z_1^H\Big|_{BPM} = \dfrac{8Z_s}{\pi^2 b^2}\dfrac{c}{\omega}\sin^2\dfrac{\phi_0}{2}\sin^2\dfrac{\omega\ell}{\beta c}$. $\longleftarrow$ same result as before

- Some may have doubt about derivation via $Z_1^{\|}$ because
  1. cylindrical symmetry is broken by strip-lines
  2. P-W relation requires cylindrical symmetry.
- The dipole current loop $I_0\Delta$ links mag. flux and I_0 sees an imp. $\mathcal{Z}$.
  Faraday Law: $i\omega B_y L\Delta = \mathcal{Z} I_0$. ($L =$ length of loop)
- Trans. imp. is $Z_1^H = \dfrac{LvB_y}{iI_0\Delta\beta} = \dfrac{c\mathcal{Z}}{\omega\Delta^2}$.
- $\mathcal{Z}$ can be evaluated from
  $$P = \frac{1}{2}|I_0|^2\mathcal{Z} = 4Z_s\left(\frac{|I_0|\Delta}{\pi b}\right)^2 \sin^2\frac{\phi_0}{2}\sin^2\frac{\omega\ell}{\beta c}.$$
- Get $\mathcal{R}e\, Z_1^H\Big|_{BPM} = \dfrac{8Z_s}{\pi^2 b^2}\dfrac{c}{\omega}\sin^2\dfrac{\phi_0}{2}\sin^2\dfrac{\omega\ell}{\beta c}$. $\longleftarrow$ same result as before
- For vertical impedance, offset current in y-direction.
  There is not net dipole image current on horizontal strip-lines.
  No dissipation, therefore $Z_1^V = 0$.

- There are $M = 216$ sets of BPM's in the Tevatron.

  Radius $b = 3.5$ cm, $\ell = 18$ cm, and $\phi_0 = 110^\circ$, $Z_s = 50\ \Omega$.

  Total imp. at $f \ll 180$ Hz, $\dfrac{Z_0^{\parallel}\Big|_{BPM}}{n} = -i0.36\ \Omega$, $Z_1^{H/V}\Big|_{BPM} = -i0.43\ \mathrm{M\Omega/m}$.

- There are $M = 216$ sets of BPM's in the Tevatron.

  Radius $b = 3.5$ cm, $\ell = 18$ cm, and $\phi_0 = 110^\circ$, $Z_s = 50\ \Omega$.

  Total imp. at $f \ll 180$ Hz, $\dfrac{Z_0^\parallel\Big|_{BPM}}{n} = -i0.36\ \Omega$, $Z_1^{H/V}\Big|_{BPM} = -i0.43\ \mathrm{M\Omega/m}$.
- One terminal monitors p beam and the other monitor $\bar{p}$ beam.
- In MI, there is only one beam, so there is only the upstream terminal but not the downstream one.

- There are $M = 216$ sets of BPM's in the Tevatron.

  Radius $b = 3.5$ cm, $\ell = 18$ cm, and $\phi_0 = 110^\circ$, $Z_s = 50\ \Omega$.

  Total imp. at $f \ll 180$ Hz, $\left.\dfrac{Z_0^\parallel\Big|_{BPM}}{n} = -i0.36\ \Omega,\ Z_1^{H/V}\right|_{BPM} = -i0.43\ \mathrm{M\Omega/m}.$

- One terminal monitors p beam and the other monitor $\bar{p}$ beam.
- In MI, there is only one beam, so there is only the upstream terminal but not the downstream one.

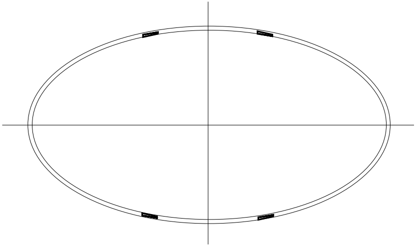

- Fraction covered by each strip-line is $f_\parallel = 0.055$ using POISSON. [20]
- With $M = 208$ sets of BPMs,

  $$Z_0^\parallel\Big|_{BPM} = 2Mf_\parallel^2\left(1 - \cos\frac{2\omega\ell}{\beta c} - i\sin\frac{2\omega\ell}{\beta c}\right)$$

- Note: $f_\parallel$ takes the place of $\dfrac{\phi_0}{2\pi}$.

- There are $M = 216$ sets of BPM's in the Tevatron.

  Radius $b = 3.5$ cm, $\ell = 18$ cm, and $\phi_0 = 110^\circ$, $Z_s = 50\ \Omega$.

  Total imp. at $f \ll 180$ Hz, $\dfrac{Z_0^{\parallel}\big|_{BPM}}{n} = -i0.36\ \Omega$, $Z_1^{H/V}\Big|_{BPM} = -i0.43\ \mathrm{M\Omega/m}$.
- One terminal monitors p beam and the other monitor $\bar{p}$ beam.
- In MI, there is only one beam, so there is only the upstream terminal but not the downstream one.
- Fraction covered by each strip-line is $f_{\parallel} = 0.055$ using POISSON. [20]
- With $M = 208$ sets of BPMs,

$$Z_0^{\parallel}\Big|_{BPM} = 2Mf_{\parallel}^2\left(1 - \cos\frac{2\omega\ell}{\beta c} - i\sin\frac{2\omega\ell}{\beta c}\right)$$

- Note: $f_{\parallel}$ takes the place of $\dfrac{\phi_0}{2\pi}$.

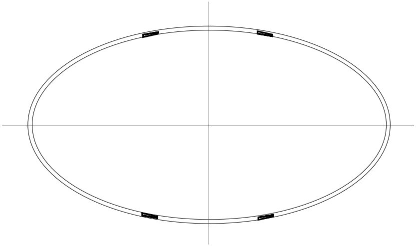

- Low freq. ($\ll 190$ MHz), $Z_0^{\parallel}\Big|_{BPM} = -i\dfrac{4Mf^2 Z_s \ell}{R} = 0.030\ \Omega \quad (\ell = 12.5 \text{ cm})$

$Z_1^{H,V}\Big|_{BPM}$ for MI

- To derive Z_1^H, first determine image current I_x flows in a stripline for a dipole current at beam pipe center.
- i.e., determine the transfer function f_x where $I_x = f_x I_0 \Delta$.

$Z_1^{H,V}\Big|_{BPM}$ for MI

- To derive Z_1^H, first determine image current I_x flows in a stripline for a dipole current at beam pipe center.
- i.e., determine the transfer function f_x where $I_x = f_x I_0 \Delta$.
- Voltage drop in strip line: $V_1 = Z_s I_x = Z_s f_x I_0 \Delta$.
- Power lost in 4 strip-lines: $P = \dfrac{4|V_1|^2}{2Z_s} = Z_s \left(f_x I_0 \Delta\right)^2 \sin^2 \dfrac{\omega\ell}{\beta c}$.

$Z_1^{H,V}\Big|_{BPM}$ for MI

- To derive Z_1^H, first determine image current I_x flows in a stripline for a dipole current at beam pipe center.
- i.e., determine the transfer function f_x where $I_x = f_x I_0 \Delta$.
- Voltage drop in strip line: $V_1 = Z_s I_x = Z_s f_x I_0 \Delta$.
- Power lost in 4 strip-lines: $P = \dfrac{4|V_1|^2}{2Z_s} = Z_s\,(f_x I_0 \Delta)^2 \sin^2 \dfrac{\omega\ell}{\beta c}$.
- This power loss is also $P = \dfrac{1}{2}(|I_0|\Delta)^2\,\mathcal{R}e\,Z_1^{\parallel}\Big|_{BPM}$.

$Z_1^{H,V}\Big|_{BPM}$ for MI

- To derive Z_1^H, first determine image current I_x flows in a stripline for a dipole current at beam pipe center.
- i.e., determine the transfer function f_x where $I_x = f_x I_0 \Delta$.
- Voltage drop in strip line: $V_1 = Z_s I_x = Z_s f_x I_0 \Delta$.
- Power lost in 4 strip-lines: $P = \dfrac{4|V_1|^2}{2Z_s} = Z_s\left(f_x I_0 \Delta\right)^2 \sin^2 \dfrac{\omega \ell}{\beta c}$.
- This power loss is also $P = \dfrac{1}{2}(|I_0|\Delta)^2\, \mathcal{R}e\, Z_1^{\parallel}\Big|_{BPM}$.
- Panofsky-Wenzel $\longrightarrow$ $\mathcal{R}e\, Z_1^H\Big|_{BPM} = \dfrac{2Z_s c f_x^2}{\omega} \sin^2 \dfrac{\omega \ell}{\beta c}$.

$Z_1^{H,V}\Big|_{BPM}$ for MI

- To derive Z_1^H, first determine image current I_x flows in a stripline for a dipole current at beam pipe center.
- i.e., determine the transfer function f_x where $I_x = f_x I_0 \Delta$.
- Voltage drop in strip line: $V_1 = Z_s I_x = Z_s f_x I_0 \Delta$.
- Power lost in 4 strip-lines: $P = \dfrac{4|V_1|^2}{2Z_s} = Z_s \left(f_x I_0 \Delta\right)^2 \sin^2 \dfrac{\omega\ell}{\beta c}$.
- This power loss is also $P = \dfrac{1}{2}(|I_0|\Delta)^2\, \mathcal{R}e\, Z_1^{\parallel}\Big|_{BPM}$.
- Panofsky-Wenzel $\longrightarrow$ $\mathcal{R}e\, Z_1^H\Big|_{BPM} = \dfrac{2Z_s c f_x^2}{\omega} \sin^2 \dfrac{\omega\ell}{\beta c}$.
- Hilbert transform $\longrightarrow$ $Z_1^H\Big|_{BPM} = \dfrac{2Z_s c f_x^2}{\omega}\left(1 - \cos^2 \dfrac{2\omega\ell}{\beta c} - i \sin^2 \dfrac{2\omega\ell}{\beta c}\right)$.

$Z_1^{H,V}\Big|_{BPM}$ for MI

- To derive Z_1^H, first determine image current I_x flows in a stripline for a dipole current at beam pipe center.
- i.e., determine the transfer function f_x where $I_x = f_x I_0 \Delta$.
- Voltage drop in strip line: $V_1 = Z_s I_x = Z_s f_x I_0 \Delta$.
- Power lost in 4 strip-lines: $P = \dfrac{4|V_1|^2}{2Z_s} = Z_s \left(f_x I_0 \Delta\right)^2 \sin^2 \dfrac{\omega \ell}{\beta c}$.
- This power loss is also $P = \dfrac{1}{2}(|I_0|\Delta)^2\, \mathcal{R}e\, Z_1^{\parallel}\Big|_{BPM}$.
- Panofsky-Wenzel $\longrightarrow$ $\mathcal{R}e\, Z_1^H\Big|_{BPM} = \dfrac{2Z_s c f_x^2}{\omega} \sin^2 \dfrac{\omega \ell}{\beta c}$.
- Hilbert transform $\longrightarrow$ $Z_1^H\Big|_{BPM} = \dfrac{2Z_s c f_x^2}{\omega} \left(1 - \cos^2 \dfrac{2\omega \ell}{\beta c} - i \sin^2 \dfrac{2\omega \ell}{\beta c}\right)$.
- f_x and f_y can be computed via POISSON or directly measured.
- For all BPM's at low freq., $Z_1^H\Big|_{BPM} = -i2.66\ \mathrm{k}\Omega/\mathrm{m}$, $Z_1^V\Big|_{BPM} = -i5.15\ \mathrm{k}\Omega/\mathrm{m}$.

Impedances of Cavities

- Cavity-like structures are high-Q discontinuities in the vacuum chamber.
- The simplest characterization is by 3 variables:

  resonant freq. $k_r = \dfrac{\omega_r}{c}$, shunt impedance R_s and quality factor Q.

Impedances of Cavities

- Cavity-like structures are high-Q discontinuities in the vacuum chamber.
- The simplest characterization is by 3 variables:

  resonant freq. $k_r = \dfrac{\omega_r}{c}$, shunt impedance R_s and quality factor Q.

- Near resonant freq. a cavity is best modeled by a RLC-circuit.

$$Z_m^{\parallel} = \frac{R_s^{(m)}}{1 + iQ\left(k_r/k - k/k_r\right)}, \qquad Z_m^{\perp} = \frac{R_s^{(m)}/k}{1 + iQ\left(k_r/k - k/k_r\right)}.$$

- The above gives $Z_0^{\parallel} \to k^{-1}$ as $k = \omega/c \to \infty$.

Impedances of Cavities

- Cavity-like structures are high-Q discontinuities in the vacuum chamber.
- The simplest characterization is by 3 variables:

  resonant freq. $k_r = \dfrac{\omega_r}{c}$, shunt impedance R_s and quality factor Q.
- Near resonant freq. a cavity is best modeled by a RLC-circuit.

$$Z_m^{\parallel} = \frac{R_s^{(m)}}{1 + iQ\left(k_r/k - k/k_r\right)}, \qquad Z_m^{\perp} = \frac{R_s^{(m)}/k}{1 + iQ\left(k_r/k - k/k_r\right)}.$$

- The above gives $Z_0^{\parallel} \to k^{-1}$ as $k = \omega/c \to \infty$.
- But the correct behavior given by optical diffraction model is [21]

  $Z_0^{\parallel} \to k^{-1/2}$ for non-periodic cavities

  $Z_0^{\parallel} \to k^{-3/2}$ for an infinite array of cavities.

Impedances of Cavities

- Cavity-like structures are high-Q discontinuities in the vacuum chamber.
- The simplest characterization is by 3 variables:

  resonant freq. $k_r = \dfrac{\omega_r}{c}$, shunt impedance R_s and quality factor Q.

- Near resonant freq. a cavity is best modeled by a RLC-circuit.

$$Z_m^{\parallel} = \frac{R_s^{(m)}}{1 + iQ\,(k_r/k - k/k_r)}, \qquad Z_m^{\perp} = \frac{R_s^{(m)}/k}{1 + iQ\,(k_r/k - k/k_r)}.$$

- The above gives $Z_0^{\parallel} \to k^{-1}$ as $k = \omega/c \to \infty$.
- But the correct behavior given by optical diffraction model is [21]

  $Z_0^{\parallel} \to k^{-1/2}$ for non-periodic cavities

  $Z_0^{\parallel} \to k^{-3/2}$ for an infinite array of cavities.

- Shunt impedance is responsible to resistive loss and beam loading.
- High shunt impedance and high Q are responsible for coupled-bunch instabilities.

Closed Pill-Box Cavities

- If cavity is pill-box like with relatively small beam pipe,
  it can be approximated by a closed pill-box of radius d and width g.

Closed Pill-Box Cavities

- If cavity is pill-box like with relatively small beam pipe, it can be approximated by a closed pill-box of radius d and width g.
- From Jackson, for example,

resonant freq.: $k_{mnp}^2 = \dfrac{x_{mn}^2}{d^2} + \dfrac{p^2\pi^2}{g^2}$.

shunt impedance:

$$\left[\frac{R_s}{Q}\right]_{0np} = \frac{Z_0}{x_{0n}^2 J_0'^2(x_{0n})} \frac{8}{\pi g k_{0np}} \begin{cases} \sin^2 \dfrac{gk_{0np}}{2\beta} \times \dfrac{1}{1+\delta_{0p}} & p \text{ even} \\ \cos^2 \dfrac{gk_{0np}}{2\beta} & p \text{ odd} \end{cases}$$

$$\left[\frac{R_s}{Q}\right]_{1np} = \frac{Z_0}{J_1'^2(x_{1n})} \frac{2}{\pi g d^2 k_{1np}^2} \begin{cases} \sin^2 \dfrac{gk_{1np}}{2\beta} & p \neq 0 \text{ and even} \\ \cos^2 \dfrac{gk_{1np}}{2\beta} & p \text{ odd} \end{cases}$$

- Resonant freq. $\omega_{mnp} = k_{mnp} c$.
x_{mn} is nth zero of Bessel function $J_m(x)$.

Numerical Computation and Measurement

- Only impedances of cavities of simplest shape, like the pill-box, can be computed analytically.
- For the actual cavities, numerically computation is necessary, using codes like SUPERFISH, URMEL, etc.
- Calculation gives resonant freq. f_r, R/Q and R and $\vec{E}$ and $\vec{H}$ for the lower modes.

Numerical Computation and Measurement

- Only impedances of cavities of simplest shape, like the pill-box, can be computed analytically.
- For the actual cavities, numerically computation is necessary, using codes like SUPERFISH, URMEL, etc.
- Calculation gives resonant freq. f_r, R/Q and R and $\vec{E}$ and $\vec{H}$ for the lower modes.
- Here is a URMEL modeling of Tevatron rf cavity

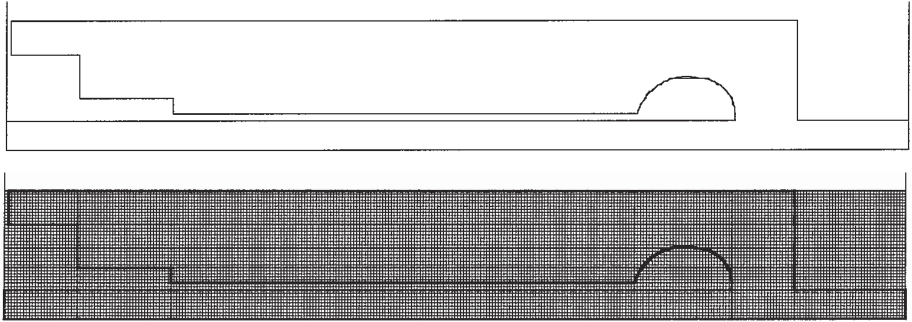

- Only half of cavity is modeled.
- Need to specify boundary at left. Either $E_\perp = 0$ or $H_\perp = 0$.

- Only half of cavity is modeled.
- Need to specify boundary at left. Either $E_\perp = 0$ or $H_\perp = 0$.

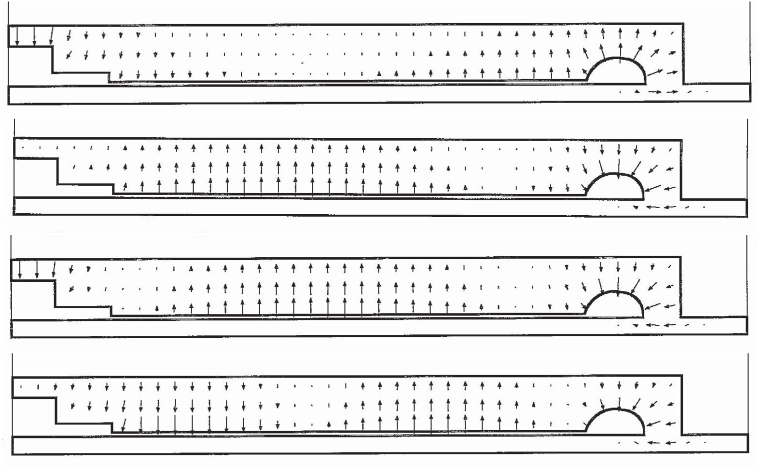

Mode 2: $H_\perp = 0$
$f_{\rm res} = 84.1$ MHz

Mode 3: $E_\perp = 0$
$f_{\rm res} = 166.6$ MHz

Mode 4: $H_\perp = 0$
$f_{\rm res} = 188.9$ MHz

Mode 5: $E_\perp = 0$
$f_{\rm res} = 286.0$ MHz

- Only half of cavity is modeled.
- Need to specify boundary at left. Either $E_\perp = 0$ or $H_\perp = 0$.

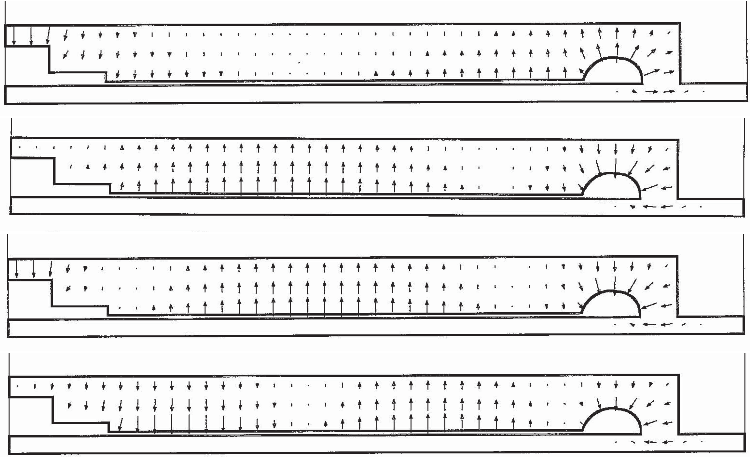

Mode 2: $H_\perp = 0$
$f_{\rm res} = 84.1$ MHz

Mode 3: $E_\perp = 0$
$f_{\rm res} = 166.6$ MHz

Mode 4: $H_\perp = 0$
$f_{\rm res} = 188.9$ MHz

Mode 5: $E_\perp = 0$
$f_{\rm res} = 286.0$ MHz

- Tevatron cavity has also been measured by Sun and Colestock using method of dielectric bead-pull and wire measurement.

Longitudinal Modes of Tevatron Cavity

	URMEL Results			Sun's Measurements		
Mode Type	Frequency (MHz)	R/Q (Ω)	Q	Frequency (MHz)	R/Q (Ω)	Q
TM0-EE-1	53.49	87.65	9537	53.11	109.60	6523
TM0-ME-1	84.10	22.61	12819	56.51	18.81	3620
TM0-EE-2	166.56	18.47	16250	158.23	11.68	6060
TM0-ME-2	188.94	10.83	18235			
TM0-EE-3	285.94	7.53	20524	310.68	7.97	15923
TM0-ME-3	308.46	4.07	22660			
TM0-EE-4	402.69	4.93	25486	439.77	5.23	13728
TM0-ME-4	431.34	1.72	26407	424.25	1.28	6394
TM0-EE-5	511.69	5.57	25486	559.48	6.73	13928
TM0-ME-5	549.57	1.36	29453			
				748.18	10.90	13356
				768.03	2.47	16191

Transverse Modes of Tevatron Cavity

- Agreement is not bad except for quality factors Q, which are much higher in URMEL computation.
- There are many de-Q structures not taken into account in URMEL.

Transverse Modes of Tevatron Cavity

- Agreement is not bad except for quality factors Q, which are much higher in URMEL computation.
- There are many de-Q structures not taken into account in URMEL.
- The transverse of dipole modes have never been measured. Below are the URMEL results:

Mode Type	Frequency (MHz)	R/Q (Ω/m)	Q
1-EE-1	486.488	229.80	31605
1-ME-2	486.864	148.95	31487
1-EE-2	513.370	117.38	33262
1-ME-3	518.317	117.93	34008
1-EE-3	561.727	81.62	33029
1-ME-4	575.298	3.84	35810
1-EE-4	625.123	61.00	32598
1-ME-5	650.853	35.21	37592
1-EE-5	699.723	54.76	33407

Bellows

- Bellows are flexible joints between 2 elements.
- They also provide significant stretching in temperature change. especially when the ring cools down to super-conducting temperature.

Bellows

- Bellows are flexible joints between 2 elements.
- They also provide significant stretching in temperature change. especially when the ring cools down to super-conducting temperature.
- There are essentially 2 types of bellows.
- Inner Bellows: just a combination of many small ripples. Example: MI
- Outer Bellows: Consist of a large can with only a few ripples.
- Example: former Fermilab Main Ring.

  Can be treated as a big cavity with ripples neglected.

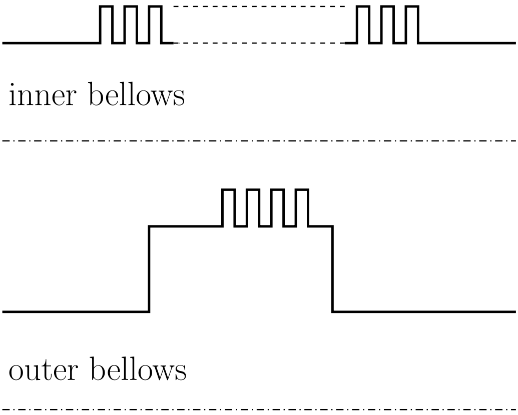

Analytic Solution of One Ripple [22, 25]

- The imp. of one single cavity has been worked out by Henke via field matching.
- Essentially, infinite length of beam pipe is assumed.
- The imp. is much simplied when $g \ll b$,

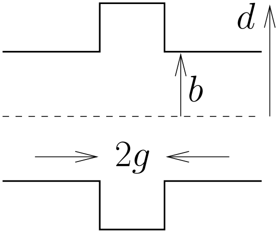

Analytic Solution of One Ripple [22, 25]

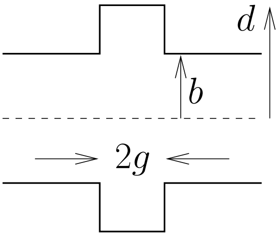

- The imp. of one single cavity has been worked out by Henke via field matching.
- Essentially, infinite length of beam pipe is assumed.
- The imp. is much simplied when $g \ll b$,

$$Z_\parallel(\omega) = \frac{-igZ_0}{\pi b I_0^2(kb/\beta\gamma)D}$$

$$D = -i\frac{R_0'(kb)}{R_0(kb)} + 2ik\left[\sum_{s=1}^{S}\frac{1}{\beta_s^2 b}\left(1 - e^{i\beta_s g}\frac{\sin\beta_s g}{\beta_s g}\right) - \sum_{s=S+1}^{\infty}\frac{1}{\alpha_s^2 b}\left(1 - e^{-\alpha_s g}\frac{\sinh\alpha_s g}{\alpha_s g}\right)\right].$$

$$\beta_s b = \sqrt{k^2b^2 - j_{0s}^2}, \qquad \alpha_s b = \sqrt{j_{0s}^2 - k^2b^2},$$

j_{0s} is sth zero of the Bessel function J_0

j_{0S} is the zero that is just larger than or equal to kb.

$R_0(kb) = J_0(kb)N_0(kd) - J_0(kd)N_0(kb)$, with $d = b + \Delta$.

- As an example, consider a bellow ripple with $\Delta/b = 0.1, \quad g/b = 0.025$

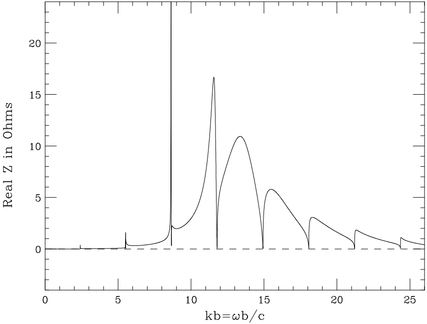

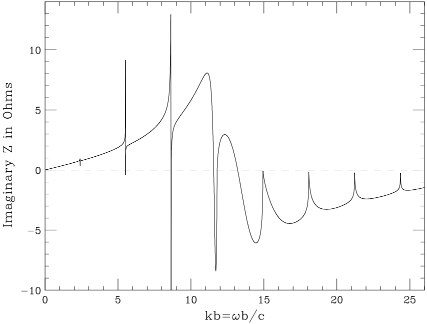

- For pipe radius $b = 3.5$ cm, $\Delta = 3.5$ mm and $2g = 1.75$ mm.
  Main peak at $f_r \approx 1.64$ GHz above cutoff, broadband with $Q \sim 12$.
- At Tevatron rev. freq., $Z_{\rm sh}/n \sim 3.8 \times 10^{-5}\ \Omega$.
- Res. freq. is given by $\mathcal{I}m\, D = 0$.
- Here since $kb \gg 1$, D can further be simplified by letting $g/b \to 0$.

- $D = i \cot k\Delta + 2kg \left(\sum_{s=1}^{S} \frac{1}{\sqrt{k^2 b^2 - j_{0s}^2}} - \sum_{s=S+1}^{\infty} \frac{i}{\sqrt{j_{0s}^2 - k^2 b^2}} \right).$
- If we neglect summations, res. freq. are just given by $\cot k_r \Delta = 0,$ condition for radial waveguide of depth Δ.

  Res. occur at $k_r \Delta = \frac{\pi}{2}, \; \frac{3\pi}{2}, \; \cdots,$ and are very sharp and narrow.

- $D = i \cot k\Delta + 2kg \left(\sum_{s=1}^{S} \frac{1}{\sqrt{k^2 b^2 - j_{0s}^2}} - \sum_{s=S+1}^{\infty} \frac{i}{\sqrt{j_{0s}^2 - k^2 b^2}} \right).$
- If we neglect summations, res. freq. are just given by $\cot k_r \Delta = 0$, condition for radial waveguide of depth Δ.

  Res. occur at $k_r \Delta = \frac{\pi}{2},\ \frac{3\pi}{2},\ \cdots,$ and are very sharp and narrow.
- 1st summation: all waves above cut-offs, which contribute to heavy damping of the resonances, contributing to Q.

- $D = i\cot k\Delta + 2kg\left(\sum_{s=1}^{S}\frac{1}{\sqrt{k^2b^2-j_{0s}^2}} - \sum_{s=S+1}^{\infty}\frac{i}{\sqrt{j_{0s}^2-k^2b^2}}\right).$
- If we neglect summations, res. freq. are just given by $\cot k_r\Delta = 0$, condition for radial waveguide of depth Δ.

  Res. occur at $k_r\Delta = \frac{\pi}{2}, \frac{3\pi}{2}, \cdots$, and are very sharp and narrow.
- 1st summation: all waves above cut-offs, which contribute to heavy damping of the resonances, contributing to Q.
- 2nd summation: all below-cutoff waves that are trapped near cavity opening.

  They increases the effective depth of ripple and thus lowers the resonant freq., — detuning
- Here, res. freq. is reduced from $k_rb = (k_r\Delta)\left(\frac{b}{\Delta}\right) = \frac{\pi b}{2\Delta} = 15.7$ to ~ 12.

- $D = i\cot k\Delta + 2kg\left(\sum_{s=1}^{S}\frac{1}{\sqrt{k^2b^2 - j_{0s}^2}} - \sum_{s=S+1}^{\infty}\frac{i}{\sqrt{j_{0s}^2 - k^2b^2}}\right).$
- If we neglect summations, res. freq. are just given by $\cot k_r\Delta = 0$, condition for radial waveguide of depth Δ.

  Res. occur at $k_r\Delta = \frac{\pi}{2},\ \frac{3\pi}{2},\ \cdots,$ and are very sharp and narrow.
- 1st summation: all waves above cut-offs, which contribute to heavy damping of the resonances, contributing to Q.
- 2nd summation: all below-cutoff waves that are trapped near cavity opening.

  They increases the effective depth of ripple and thus lowers the resonant freq., — detuning
- Here, res. freq. is reduced from $k_r b = (k_r\Delta)\left(\frac{b}{\Delta}\right) = \frac{\pi b}{2\Delta} = 15.7$ to ~ 12.
- Quality factor: $Q \sim \frac{kb}{2\,\mathcal{R}e\,D}\frac{d\,\mathcal{I}m\,D}{d(kb)}\bigg|_{kb=k_r b}$, get typically $Q \sim 3$ to 8.

- For N ripples in bellows system, a rough estimate is to assume f_r and Q same as one ripple, while $Z_{\rm shunt}$ becomes N-fold.
- Bellow convolutions are closed to each other and therefore talk to each other. Resonance freq. will be lower.

- For N ripples in bellows system, a rough estimate is to assume f_r and Q same as one ripple, while $Z_{\rm shunt}$ becomes N-fold.
- Bellow convolutions are closed to each other and therefore talk to each other. Resonance freq. will be lower.
- Codes TBCI [23] or ABCI [24] computes the wake behind a Gaussian bunch passing thru a cylindrical symmetric structure.
- TBCI example:
  5 consecutive ripples
  $b = 4.5$ cm
  $\Delta = 5$ mm
  $2g = 1.5$ mm
  bunch $\sigma_\ell = 4$ mm
  cell width 0.375 mm
  wake length 80 cm

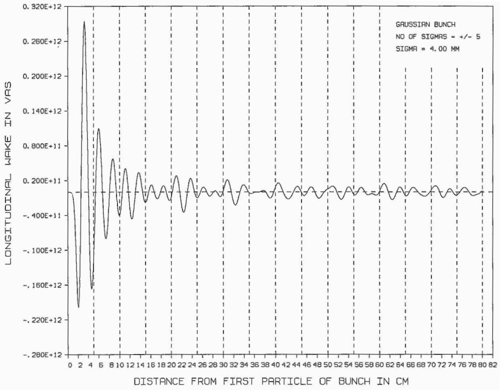

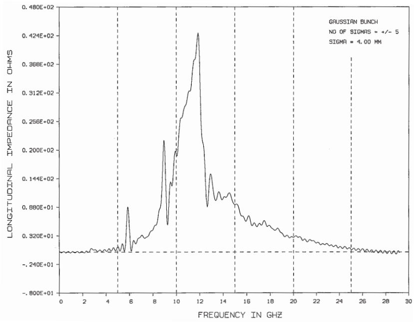

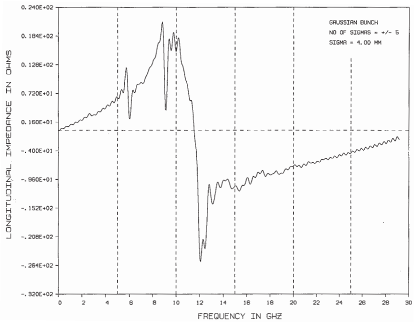

- TBCI solves Maxwell equation in time domain.
  The wake for the bunch distribtuion $\lambda(z) = e^{-z^2/2\sigma_\ell^2}$ is
  $\hat{W}_0(z) = \int dz' \lambda(z') W_0(z-z')$ $\qquad$ $\left[W_0(z)\text{: wake for point charge}\right]$
- Imp. $\hat{Z}(\omega)$ seen by bunch is computed from $\hat{W}_0(z)$ by Fourier transform. It is related to the true imp. by $\hat{Z}(\omega) = Z(\omega)e^{-\frac{1}{2}(\omega\sigma_\ell/c)^2}$.
- Thus $Z(\omega)$ can be recovered from $\hat{Z}(\omega)$, but error is large for large ω
  Recovery has been made in above imp. plots.

Comparison with Henke's Formula [25]

Case No.	b cm	Δ cm	$2g$ cm	f_r in GHz Henke	TBCI($\parallel$)	TBCI($\perp$)
1	1.50	0.50	0.15	13.3	12.3	12.3
2	2.00	0.50	0.15	12.2	11.5	12.2
3	2.75	0.50	0.15	12.9	11.8	11.6
4	3.25	0.50	0.15	12.2	11.6	11.9
5	3.50	0.50	0.15	13.1	11.7	11.8
6	4.50	0.50	0.15	12.1	11.6	11.8
7	6.15	0.50	0.15	13.1	11.4	11.6
8	6.50	0.50	0.15	12.6	11.4	11.6
9	8.00	0.50	0.15	12.3	11.6	11.3
10	2.00	0.50	0.20	11.9	11.2	11.5
11	2.00	0.25	0.15	24.1	21.0	21.0
12	2.00	0.75	0.15	9.4	8.3	8.3
13	2.00	1.00	0.15	7.4	7.0	7.0
14	6.50	0.50	0.20	12.3	10.8	10.9
15	6.50	0.50	0.30	12.0	10.2	10.3

$f_{r\parallel}$, $f_{r\perp}$ are lowered as expected.
But Henke's estimate is good within 10% except for Case 11.

Empirical Formula for Resonant Frequency

- We fit TBCI results and obtain
  $$k_r b = 1.37\left(\frac{\Delta}{b}\right)^{-0.948}.$$
- No dependence on ripple width g. Doubling g lowers $f_r^{\parallel}$ by only 9%.
- Empirical formula can also be written as $k_r\Delta = 1.37\left(\frac{\Delta}{b}\right)^{0.052}$, implying that $k_r\Delta$ is lowered from $\frac{\pi}{2} = 1.57$ to 1.37.
- Trans. res. freq. roughly given by
  $$f_r^{\perp} \sim c\sqrt{\left(\frac{1}{4\Delta}\right)^2 + \left(\frac{1}{2\pi b}\right)^2} \sim \frac{c}{4\Delta},$$
  since $(2\Delta/\pi b)^2 \ll 1$.
  This explains why $f_{r\perp} \approx f_{r\parallel}$.

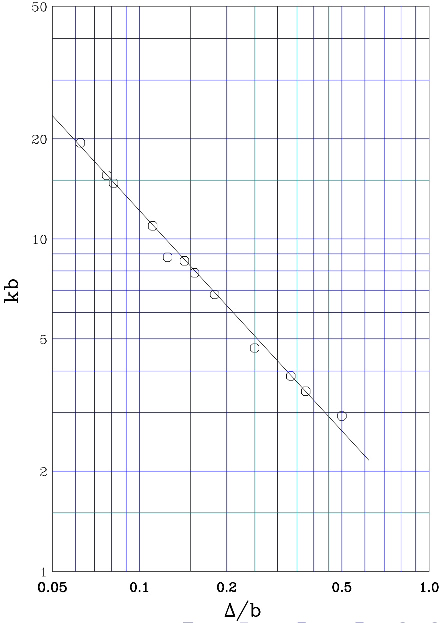

Low-Freq. Behaviors

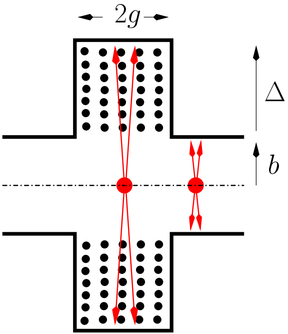

- After particle passage, EM fields are trapped inside ripples.
- High-freq. fields contribute to resonances and are heavily damped.
- For low-freq., only $\vec{B}$ are trapped, but not $\vec{E}$, because boundary condition cannot be satisfied when $\ell = 2g \ll b$.
- $\Phi = \dfrac{\mu_0 I_0 \ell}{2\pi} \ln \dfrac{b+\Delta}{b}$, $\quad \dfrac{Z_0^{\parallel}}{n} = -i \dfrac{Z_0 \beta \ell}{2\pi R} \ln \dfrac{b+\Delta}{b}$,
- For trans., consider $Z_1^{\perp}\Big|_{\rm spch} = i Z_0 R \left(\dfrac{1}{\beta^2} - 1\right)\left(\dfrac{1}{a^2} - \dfrac{1}{b^2}\right)$,
- $Z_1^{\perp} = i \dfrac{Z_0 \ell}{2\pi}\left[\dfrac{1}{b^2} - \dfrac{1}{(b+\Delta)^2}\right] = -i \dfrac{Z_0 \ell}{\pi b^2} \dfrac{S^2-1}{2S^2}$,
- From $Z_0^{\parallel}(\omega) = \dfrac{R_{\parallel}}{1 + iQ\left(\frac{\omega_{r\parallel}}{\omega} - \frac{\omega}{\omega_{r\parallel}}\right)}$, get $\displaystyle\lim_{\omega\to 0} \frac{\mathcal{I}m\, Z_0^{\parallel}}{\omega} = -\frac{R_{\parallel}}{\omega_r Q}$.

- From $Z_1^{\perp}(\omega) = \dfrac{\omega}{\omega_{r\perp}} \dfrac{R_{\perp}}{1 + iQ\left(\frac{\omega_{r\perp}}{\omega} - \frac{\omega}{\omega_{r\perp}}\right)}$, get $\lim_{\omega\to 0} \mathcal{I}m\, Z_1^{\perp} = -\dfrac{R_{\perp}}{Q}$.

Case	b	Δ	$2g$	$-\mathcal{I}m\, Z_0^{\parallel}/f$ (Ω/GHz)		$-\mathcal{I}m\, Z_1^{\perp}$ (Ω/m)	
	cm	cm	cm	formula	TBCI	formula	TBCI
1	1.50	0.50	0.15	0.542	0.540	224	199
2	2.00	0.50	0.15	0.410	0.410	98.8	89.6
3	2.75	0.50	0.15	0.315	0.310	39.4	36.0
4	3.25	0.50	0.15	0.269	0.270	24.2	22.4
5	3.50	0.50	0.15	0.252	0.256	19.5	18.4
6	4.50	0.50	0.15	0.199	0.202	9.33	8.88
7	6.15	0.50	0.15	0.150	0.147	3.71	3.54
8	6.50	0.50	0.15	0.140	0.140	3.15	3.7
9	8.00	0.50	0.15	0.117	0.117	1.70	1.64
10	2.00	0.50	0.20	0.561	0.556	132	116
11	2.00	0.25	0.15	0.222	0.221	52.8	46.7
12	2.00	0.75	0.15	0.600	0.600	139	124
13	2.00	1.00	0.15	0.764	0.720	173	155
14	6.50	0.50	0.20	0.186	0.190	4.20	3.94
15	6.50	0.50	0.30	0.280	0.277	6.30	5.70

Effects of Many Ripples

- We concentrate on Case 2 with $b = 2$ cm, $\Delta = 5$ mm, and $2g = 1.5$ mm for various number of ripples.

n	$f_{r\|}$ GHz	$f_{r\perp}$ GHz	$-\mathcal{I}m\, Z_0^{\|}/f$ Ω/GHz	$-\mathcal{I}m\, Z_1^{\perp}$ Ω/m	$k_{\|}$ $10^{11}\Omega$/sec	$k_{\perp}$ $10^{11}\Omega$/m/sec
1	12.1	13.2	0.413	85.8	0.561	22.3
5	11.5	12.2	0.410	89.6	0.534	19.9
20	10.0	10.3	0.407	83.4	0.520	16.7
40	9.0	9.7	0.414	86.5	0.530	16.0

- Both $f_{r\|}$ and $f_{r\perp}$ continued lowered with more ripples.
- However, $\mathcal{I}m\, Z_0^{\|}/f$, $\mathcal{I}m\, Z_1^{\perp}$ and $k_{\|}$ are almost n-independent. These are quantities used in the study of single-bunch and coupled-bunch instabilities as well as parasitic heating.
- Conclusion: we can safely use formulae developed to compute these quantities per ripple, multiply them by ripple number, and use results in stability criteria and parasitic energy loss formula.

Loss Factors $k_\parallel$ and $k_\perp$

- Monopole energy loss: $\dfrac{d\mathcal{E}}{dt} = \dfrac{c^3}{R}\displaystyle\int_{-\infty}^{\infty} d\omega |\tilde{\rho}(\omega)|^2 Z_0^\parallel(\omega)$

  Defn.: $\dfrac{d\mathcal{E}}{dt} = e^2 N^2 f_0 k_\parallel$
- Then $k_\parallel = \dfrac{1}{\pi}\displaystyle\int_0^\infty d\omega\, e^{-(\omega\sigma_\ell/c)^2}\, \mathcal{R}e\, Z_0^\parallel(\omega)$
- A similar definition for the transverse,
  $$k_\perp = \frac{i}{2\pi}\int_{-\infty}^{\infty} d\omega\, Z_1^\perp(\omega) e^{-(\omega\sigma_\ell/c)^2} = -\frac{1}{\pi}\int_0^\infty d\omega\, e^{-(\omega\sigma_\ell/c)^2}\, \mathcal{I}m\, Z_1^\perp(\omega)$$
- For a Gaussian bunch and using RLC-parallel-circuit formulas for $Z_0^\parallel$ and $Z_1^\perp$,
  $$k_\parallel = \frac{R_\parallel \omega_r}{2Q\alpha}\left(1 - \frac{1}{4Q^2}\right)^{-1/2} \mathcal{R}e\left[zw(z)\right]$$
  $$k_\perp = \frac{R_\perp \omega_r}{2Q}\left(1 - \frac{1}{4Q^2}\right)^{-1/2} \mathcal{I}m\, w(z)$$
  $w(z)$ is complex error function.

Numerical Computation

- All we discussed above are for inner bellows.
  Most bellows are in between inner and outer bellows.
- Tevatron bellows system is an example,
  and we need to resort to numerical computation.

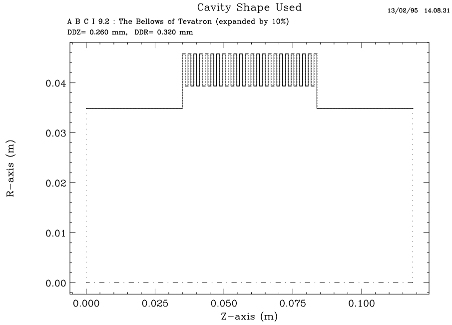

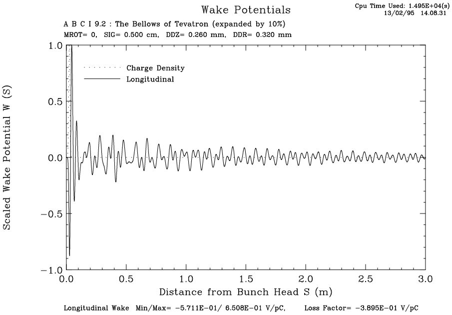

-

- Fourier transform is performed to the wake to obtain the impedance.

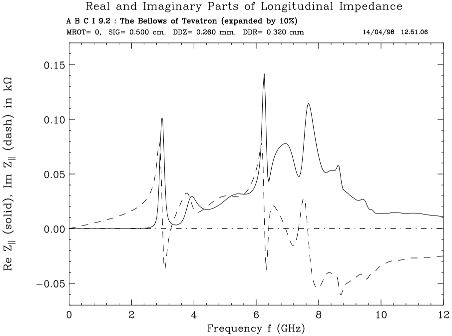

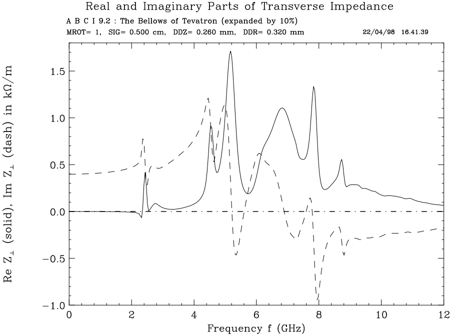

- The broadband res. is at ~ 7 GHz for both $Z_0^{\|}$ and $Z_1^{\perp}$ lower than what Henke's prediction, and more broadband ($Q \sim 1$).
- We see more structure in imp. spectrum. Here even without ripples, the bellows structure acts as a cavity.
- Result: $Z_{\rm sh}^{\|}/n \sim 0.68\ \Omega$ and low freq. $\mathcal{I}m\, Z_{\rm sh}^{\|}/n \sim -i0.34\ \Omega$.

  $Z_{\rm sh}^{\perp} \sim 1.1\ {\rm M}\Omega/{\rm m}$ and low freq. $\mathcal{I}m\, Z_{\rm sh}^{\perp} \sim -i0.40\ {\rm M}\Omega/{\rm m}$.

Comments on Bellows Numerical Computations

- Exit pipe length is an issue, since all fields are assumed to drop to zero on both sides.
- Need to extend pipe length until results do not change by much. It is best to have exit pipe length $>$ pipe radius.
- Time step has to be much less than width of ripple.
- Incident beam is a short Gaussian bunch instead of point charge. Reduction to point-particle wake fcn. is possible, but error increases rapidly when $\omega > \sigma_\omega$.
- Wake must terminate at a certain length in calculation. Fourier transform will exhibit $\dfrac{\sin x}{x}$-behavior. This can be minimized by ending the wake at a point where wake is zero. Or add a filter to Fourier transform.
- A 2D code is always faster and easier to use than 3D code like MAFIA.

Separators [26]

- There are 27 separators in Tevatron to separate p and $\bar{p}$ bunches.
- Simplified model:

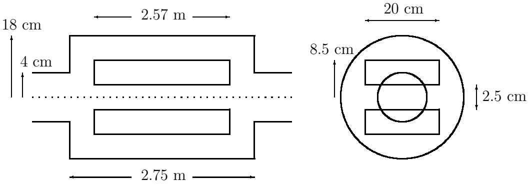

- Each separator consists of 2 thick plates, 2.57 m long.

Separators [26]

- There are 27 separators in Tevatron to separate p and $\bar{p}$ bunches.
- Simplified model:

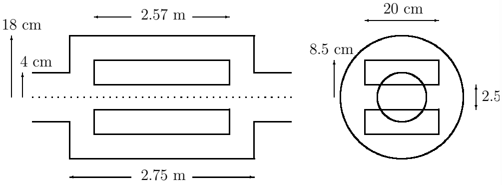

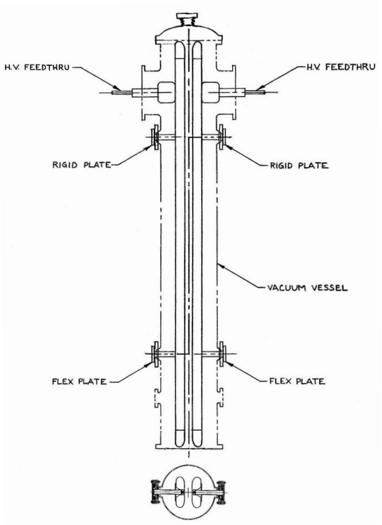

- Each separator consists of 2 thick plates, 2.57 m long.
- A beam particle can excite resonances at the upstream and downstream gaps.
- Space between plate and enclosure forms a transmission line.
- Use MAFIA to compute wakes and FFT to obtain imp.

MAFIA Results

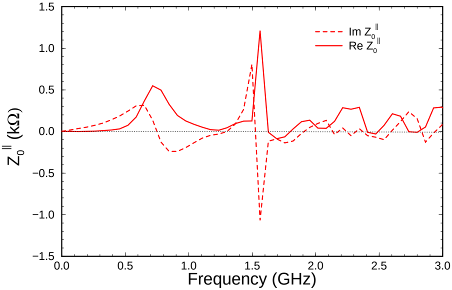

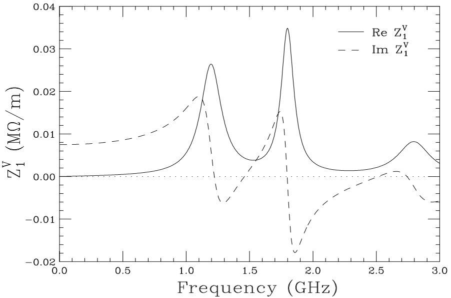

- At low freq., for each separator, $Z_0^{\|}/n \sim -i0.019\ \Omega$, $Z_1^V \sim -i0.0075\ \mathrm{M\Omega/m}$.
- For 27 separators, $Z_0^{\|}/n \sim -i0.51\ \Omega$, $Z_1^V \sim -i0.20\ \mathrm{M\Omega/m}$.
- These are very small.
- We would like to understand more about the impedances.
- Instead of MAFIA, which is a 3D code, we use the 2D code URMEL in the frequency domain.

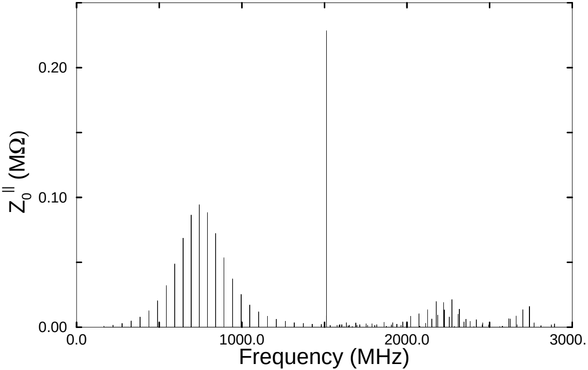

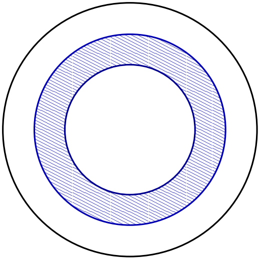

- First 50 resonant modes are shown.

  They are narrow because well below $f_{\rm cutoff} = 4.59$ GHz.

- In 2D representation, upstream and downstream gaps can be viewed as 2 cavities, connected by a coaxial waveguide.

- Waveguide resonates when $\ell = \frac{1}{2}n\lambda$, with lowest mode $f = c/2\ell = 54.5$ MHz. Successive modes are also separated by 54.5 MHz.

- These modes will be excited most when cavities are excited, with 1st pill-box (18-cm-deep) mode at $\sim$ 637 MHz.

  We see coaxial transmission line mode peaks there.

- 2nd pill-box mode at 1463 MHz with radial node at 7.84 cm, at the side edge of separator plate.

- Since it is not perturbed by coaxial guide.

  This mode is very strong.

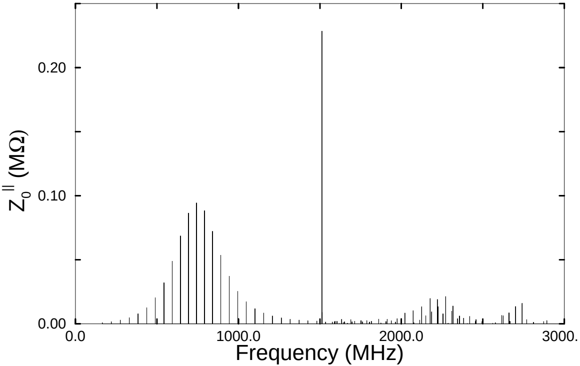

- Similar analysis applies to the trans. dipole modes.
- The lowest 50 dipole modes are shown.
- First 2 pill-box dipole modes: 1016, 1860 MHz.
- There is a special mode when one wavelength wraps around "cylindrical plates" at $r = 8.5$ to 18 cm. Or freq. between 265 and 562 MHz.
- This is seen in URMEL result (1st cluster).
- This is not seen in MAFIA result, because there is no cylindrical symmetry.

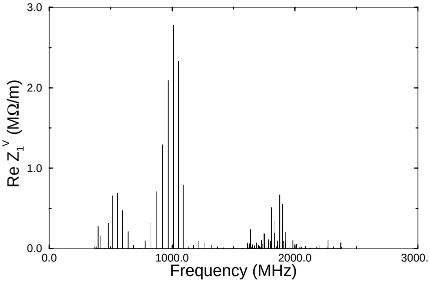

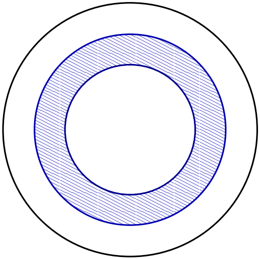

- Impedances of separator has been measured by Crisp and Fellenz, using a current-carrying wire for $Z_0^{\parallel}$ and a current loop pad for $Z_1^{\perp}$. [27]
- Attenuation S_{21} was measured and the imp. calculated according to
$$Z_0^{\parallel} = 2Z_s\left(\frac{1}{S_{21}} - 1\right), \quad Z_1^{V} = \frac{2Z_s c \ln S_{21}}{\omega\Delta^2},$$
$\Delta = 1$ cm is current loop separation.
- We do see similar imp. structures as predicted by MAFIA and URMEL, except for a resonance near 22.5 MHz.
- The resonance is due to the absorption of 1st waveguide mode by power cables, connected to plates thru a 50 Ω resistor.

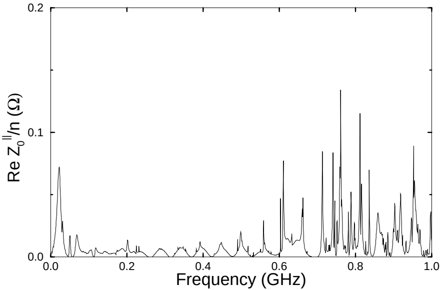

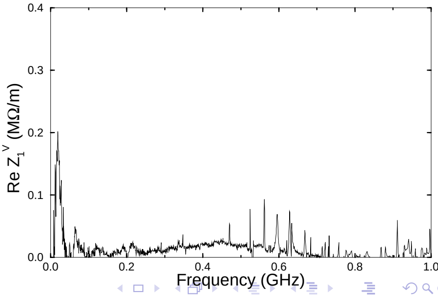

Comments on Separators

- The 2-m power cables increases the effective length of plates and shifts 1st resonant mode down from 54.5 to 22.5 MHz.
- This resonance contribute $\frac{\mathcal{R}e\, Z_0^{\parallel}}{n} = 0.82\ \Omega, \quad \mathcal{R}e\, Z_1^{\perp} = 2.1\ \mathrm{M}\Omega/\mathrm{m},$ which are appreciable.
- There are several ways to alleviate the effect:
  - Smooth out the resonance by increasing the 50 Ω damping resistor to 500 Ω.
  - Increase length of power cables to further lower resonant freq.
  - Maintain short Tevatron bunches to $\sigma_\ell = 37$ cm, so as to increase lowest head-tail mode to 82.8 MHz.

Separators vs. Strip-line BPM's

- Separator resembles stripline BPM.
  Why is separator imp. so much lower?
- In BPM, image current created at strip-lines eventually flows into terminations, which carry 50 Ω.
- But image currents created on upper and lower sides
  of separator plate at upstream gap,
  annihilate each other at downstream gap.
- Since no terminations to collect and dissipate image currents,
  the loss is small.
- Strip-line BPM does not exhibit resonances.
  But there will be resonances at separator assembly,
  which can contribute impedances.
- So we must de-Q these resonances or shift them to frequencies
  not harmful to the beam.

Asymptotic Behavior of $\mathcal{R}e\, Z_0^{\parallel}(\omega)$ [28]

- There is an experiment at CERN ISR to demonstrate asymptotic behavior of $\mathcal{R}e\, Z_0^{\parallel}(\omega)$.
- A coasting beam is circling ISR for many hours.
  From inward movement of beam, energy loss is inferred.
- Loss due to synchrotron radiating and collision with residual gas can be separated, leaving parasitic loss due to impedance.

$$\Delta\mathcal{E} = \int_{-\infty}^{\infty} \left|I(\omega)\right|^2 \mathcal{R}e\, Z_0^{\parallel}(\omega) d\omega, \qquad I(\omega) = \sum_{n=1}^{N} i_n(\omega).$$

- $\left|I(\omega)\right|^2$ consist of 2 parts: coherent $\propto N^2$, incoherent $\propto N$.
- Coherent part is equivalent to $\left|I(\omega)\right|^2 \to \left|I_{\rm av}(\omega)\right|^2$.
- But $I_{\rm av}(\omega)$ consists of only $\omega = 0$ component, and does not contribute because $\mathcal{R}e\, Z_0^{\parallel}(0) = 0$.
- what we measure here is incoherent loss, or energy loss of each individual particle.

- For each particle, image on beam pipe has rms length $\sigma_\tau = \dfrac{b}{\sqrt{2}\gamma\beta c}$.
- Spectrum is $i_n(\omega) = -\dfrac{qe^{i\omega t_n}}{2\pi I_0(\sqrt{2}\sigma_\tau\omega)}$.
- Av. energy loss per particle per turn: $\overline{\Delta\mathcal{E}} = \dfrac{q^2}{\pi}\displaystyle\int_0^\infty \dfrac{\mathcal{R}e\, Z_0^\parallel(\omega)}{I_0^2(\sqrt{2}\sigma_\tau\omega)}$.

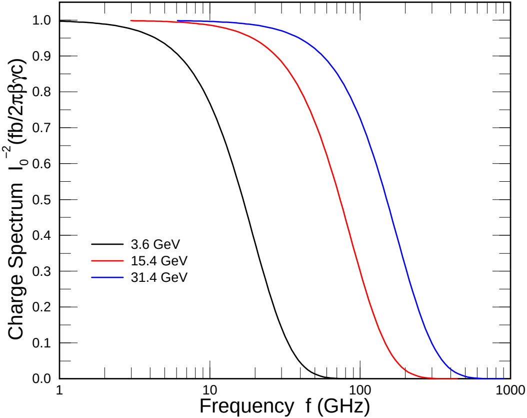

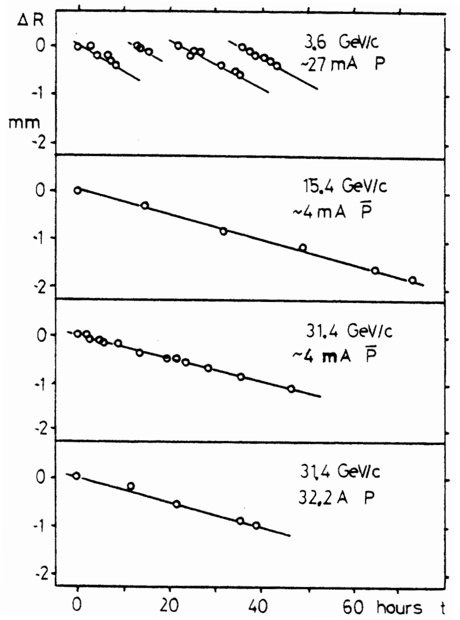

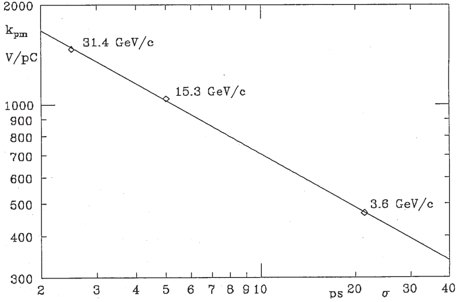

- $k_{pm} \propto \sigma_\tau^{-0.533}$
- Results show that parasitic loss of coasting beam is individual point particle loss.

p GeV/c	U μeV	k_{pm} V/pc	σ ps	$\omega_t/2\pi$ GHz	$\langle\omega\rangle/2\pi$ GHz	$\langle Z\rangle$ kΩ	$\langle Z/n\rangle$ Ω
3.6	75	470	21.4	6			
					16	14.4	0.29
15.3	167	1040	5.0	26			
					44	6	0.04
31.4	235	1470	2.5	62			

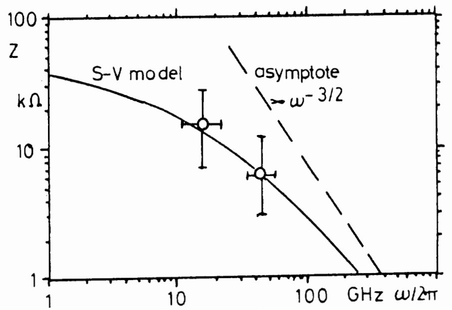

- If only 2 points are fit with a straight line, result consistent with $Z_0^{\parallel} \to \omega^{-1/2}$.
- It is nice that the experiment can be repeated at Tevatron.

Slides can be downloaded at

www-ap.fnal.gov/ng/lecture09.pdf

References

[1] A.W. Chao, *Physics of Collective Beam Instabilities in High Energy Accelerators*, John Wiley & Sons, 1993.

[2] W.K.H. Panofsky and W.A. Wenzel, Rev. Sci. Instrum. **27**, 961 (1956).

[3] J. E. Griffin, K. Y. Ng, Z. B. Qian and D. Wildman, *Experimental Study of Passive Compensation of Space Charge Potential Well Distortion at the Los Alamos National laboratory Proton Storage Ring*, Fermilab Report FN-661, 1997; M. A. Plum, D. H. Fitzgerald, J. Langenbrunner, R. J. Macek, F. E. Merrill, F. Neri, H. A. Thiessen, P. L. Walstrom, J. E. Griffin, K. Y. Ng, Z. B. Qian, D. Wildman and B. A. Jr. Prichard, *Phys. Rev. ST Accel. Beams* **2**, 064201 (1999).

[4] K.Y. Ng, *Space-Charge Impedances of Beams with Non-uniform Transverse Distribution*, Fermilab Report FN-0756, 2004.

[5] J. Gareyte, *Impedances: Measurements and Calculations for Non-symmetric Structures*, Proc. EPAC 2002 (Paris, June 3–7, 2002), p. 89.

[6] K. Y. Ng, *Space-Charge Impedances of Beams with Non-uniform Transverse Distributions*, Fermilab Report FN-0756, 2004.

[7] Fermilab Report FN-0760-AD, 2004; K.Y. Ng, *Resistive-Wall Instability at Fermilab Recycler Ring*, AIP Conf. Proc. **77**, 365 (2004).

[8] J. Crisp and M. Hu, *Recycler Ring Instabilities Measured on 6/9/04*, 2004 (unpublished); M. Hu and J. Crisp, *Recycler Instability Observed with Protons*, 2004 (unpublished).

[9] W. Chou and J. Griffin, *Impedance Scaling and Impedance Control*, PAC'97 1724 (1997).

[10] L. Vos, *The Transverse Impedance of a Cylindrical Pipe with Arbitrary Surface Impedance*, CERN Report CERN-AB-2003-005 ABP, 2003.

[11] B. Zotter, *New Results on the Impedance of Metal Walls of Finite Thickness*, CERN Report CERN-AB-2005-043, 2005.

[12] A. Mostacci, La Sapienza, F. Casper, *Bench Measurement of Low Frequency Transverse Impedance*, PAC'03 1801 (2003).

[13] K.Y. Ng, *Coupling Impedances of Laminated Magnets*, Fermilab Report FN-0744, 2004.

[14] S.C. Snowdon, *Wave Propagation Between Booster Laminations Induced by Longitudinal Motion of Beam*, Fermilab Report TM-2770, 1970.

[15] J. Crisp and B. Fellenz, *Measured Longitudinal Beam Impedances of Booster Magnets*, Fermilab Report TM-2145, 2001.

[16] J. Crisp and B. Fellenz, *Comparison of Tevatron C0 and F0 Lambertson beam impedance*, Fermilab Report TM-2205, 2003.

[17] X. Huang, *Beam Diagnosis and Lattice Modeling of the Fermilab Booster*, PhD thesis, Indiana University, 2005; X. Huang, *The Coherent Detuning of Vertical Betatron Tunes*, 2005 (unpublished).

[18] K.Y. Ng, *Physics of Intensity Dependent Beam Instabilities*, World Scientific, 2006, p.432.

[19] K.Y. Ng, *Impedances of Beam Position Monitors*, Fermilab Report FN-444, 1986; Particle Acc. **23**, 93 (1988).

[20] M.A. Martens and K.Y. Ng, *Impedance Budget and Beam Stability Analysis of the Fermilab Main Injector*, Fermilab Report TM-1880, 1994; PAC'83, 3300 (1993).

[21] D. Brandt and B. Zotter, *Calculation of the Wakefiled with the Optical Resonator Model*, CERN Report CERN-ISR/TH/82-13, (LEP Note 388), 1982; L.A. Vainshtein, Soviet Phys. JETP **17** (1969); S.A. Heifets and S.A. Kheifets, *High-Frequency Limit of the Longitudinal Impedance*, Particle Accelerators **25**, 61 (1990).

[22] H. Henke, *Point Charge Passing a Resonator with Beam Tubes*, CERN Report CERN-LEP-RF/85-41, 1985.

[23] T. Weiland, DESY Report 82-015 (1982) and Nucl. Inst. and Meth. **212**, 13 (1983).

[24] Y.H. Chin, ABCI User's Guide, CERN Report CERN/LEP-TH/88-3, 1988.

[25] King-Yuen Ng, *Impedances of Bellows Corrugations*, Fermilab Report FN-449, 1987; PAC'87, 1051 (1987).

[26] K.Y. Ng, *Impedances of the Tevatron Separators*, Fermilab Report TM-2199, 2003; PAC'03, 3065 (2003).

[27] James L. Crisp and Brian J. Fellenz. *Tevatron separator beam impedance*, Fermilab Report TM-2202, 2003.

[28] A. Hofmann and T. Risselada, *Measuring the ISR Impedance at Very High Frequencies by Observing the Energy Loss of a Coasting Beam*, IEEE Trans. Nucl. Sc. **NS-30**, No. 4, 2400, 1983; A. Hofmann, T. Risselada, and B. Zotter, *Measurement of the Asymptotic Behavior of the High Frequency Impedance*, 4th Advanced ICFA Beam Dynamics Workshop on Collective Effects in Short Bunches, Ed. K. Hirata and T. Suzuki, KEK, Japan, 1990, p.138 (KEK Report 90-21).